

**Role of the nonsense-mediated mRNA decay
pathway in cerebellar granule neuron progenitors
and medulloblastoma progression**

Sushmetha Ananthanarayanan Mohan

Integrated Program in Neuroscience,

McGill University, Montreal

November 2023

A thesis submitted to McGill University in partial fulfillment of the
requirements of the degree of Doctor of Philosophy

© Sushmetha Ananthanarayanan Mohan 2023

Dedication

This thesis is dedicated to my beloved family- my loving parents, Mohan and Jaya

Mohan and my most supportive brother Shreekanth.

This PhD journey and work would not have been possible without their constant encouragement and unconditional support.

Table of contents

Abstract.....	8
Résumé.....	10
Acknowledgements.....	13
List of Abbreviations.....	16
List of Figures and Tables.....	19
Preface and Contribution of Authors.....	21
Chapter 1. Introduction.....	23
1.1.Cerebellar development.....	24
1.1.1. Development of cerebellum during neurogenesis	24
1.1.2. Postnatal cerebellar development.....	27
1.1.3. Canonical Sonic Hedgehog (Shh) signaling in the developing cerebellum.....	29
1.1.4. GCPs are the cell of origin of SHH-MB.....	32
1.1.5. Additional extracellular players in MB progression.....	33
1.2. Medulloblastoma (MB).....	35
1.2.1. Molecular subgroups of MB.....	35
<i>SHH-MB</i>	35
<i>WNT-MB</i>	38
<i>Group 3 and Group 4 MB</i>	39
1.2.2. Shh signaling-based MB mouse model.....	43
<i>Ptch1 +/- mouse model</i>	43
<i>Overactivated Smo mouse model</i>	44
1.2.3. Events in Shh-MB progression using <i>Ptch1</i> model of medulloblastoma.....	45

1.2.4. Candidate collaborators of <i>Ptch1</i> in Shh-MB.....	48
1.3. Nonsense-mediated mRNA decay (NMD) Pathway.....	48
1.3.1. Classic NMD/ EJC-dependent NMD.....	48
1.3.2. EJC-independent NMD.....	50
1.3.3. Key NMD effectors.....	54
<i>Up-frameshift proteins (UPF)</i>	54
<i>Suppressor with Morphological effects on Genitalia (SMG) proteins</i>	56
<i>Exon Junction complex (EJC) components</i>	59
1.3.4. Degradation mechanisms of NMD target.....	60
1.4. Regulators of NMD.....	63
1.4.1. Autoregulation of NMD.....	63
1.4.2. microRNA-mediated regulation of NMD.....	64
1.4.3. PABP as a human NMD antagonizing factor.....	65
1.5. NMD as a critical regulator of the transcriptome.....	68
1.5.1. Essentiality of NMD in mammalian viability and development.....	70
1.5.2. Alternative Splicing coupled NMD in homeostatic regulation of splicing factors.....	71
1.5.3. Physiological response of NMD to stress.....	73
1.5.4. Role of NMD in neural development and function.....	75
1.6. NMD in disease.....	78
1.6.1. NMD associated neural disease.....	78
1.6.2. NMD and cancer.....	80
Chapter 2. Rationale and contribution to original knowledge	82

Chapter 3. Methodology.....	86
3.1. Mouse lines.....	87
3.2. GCP isolation and culture.....	87
3.3. Cell culture.....	88
3.4. siRNA transfection.....	88
3.5. Lentivirus preparation.....	89
3.6. Western blotting.....	89
3.7. Immunostainings.....	90
3.7.1. Dissociated GCP IF.....	90
3.7.2. Mouse MB tissue section IF.....	90
3.8. Luciferase assays.....	91
3.9. NMD efficiency measurement.....	92
3.10. p-UPF1 RNA Immunoprecipitation -qPCR.....	92
3.11. qRT-PCR.....	93
3.12. In utero electroporation.....	93
3.13. Orthotopic transplantation.....	94
3.14. Statistical Methods.....	94
3.15. Bioinformatics.....	95
3.15.1. NMD feature prediction.....	95
3.15.2. NMD target signature generation and human MB data analysis.....	95
3.16. Supplemental information.....	95
3.16.1. Reagents.....	95
3.16.2. Plasmids.....	96

3.16.3. Antibodies.....	96
Table 3.16.4: sgRNA sequences.....	97
Table 3.16.5: siRNA duplex sequences.....	97
Table 3.16.6: Primer sequences used for quantitative RT-PCR.....	97
Chapter 4. Results.....	99
4.1. The NMD pathway is functional in cerebellar granule cell precursors (GCPs).....	100
4.2. NMD regulates Shh pathway activity, expression of proliferation-regulating genes, and GCP proliferation.....	104
4.3. NMD regulates Shh signaling by direct modulation of Gli transcriptional activity.....	109
4.4. The 3'UTRs of Smo and Gli2 are targets of NMD-mediated degradation.	111
4.5. p-UPF1 binds to the 3'UTRs of Smo and Gli2 to mark and target their mRNAs for NMD.....	115
4.6. NMD inactivation cooperates with Ptch1 inactivation to enhance medulloblastoma tumorigenesis.....	118
4.7. NMD upregulation leads to a delay in MB tumor latency and significantly improved survival <i>in vivo</i>	125
4.8. NMD activity level is a determinant of prognosis in specific subgroups of human medulloblastoma.....	131
Chapter 5. General Discussion.....	135
Graphical abstract.....	138

5.1. Interdependency of NMD regulation and Shh signaling in MB.....	139
5.2. Role of NMD in maintaining the equilibrium between proliferation and differentiation.....	140
5.3. NMD, genomic instability and MB: the sisterhood.....	142
5.4. NMD activation as potential therapy for SHH-MB.....	144
Chapter 6. Conclusion	148
Chapter 7. Bibliography	151

Abstract

The development of the nervous system requires precise control of gene expression of effectors that direct various neuronal processes such as proliferation, differentiation, stemness, and migration. Dysregulation of neurodevelopmental programs such as Sonic hedgehog (SHH) and WNT pathways give rise to a broad spectrum of neurological disorders, including brain tumors such as medulloblastoma (MB). One critical mRNA surveillance pathway involved in maintaining global gene expression integrity is nonsense-mediated mRNA decay (NMD). NMD has two important roles: it degrades aberrant mRNAs harboring premature termination codons (PTC) and it regulates expression of endogenous transcripts which impacts several physiological processes including cell proliferation and differentiation, response to environmental cues and even development of disease. Thus, understanding developmental programs can provide valuable insights into the molecular mechanisms underlying tumor formation and progression.

MB is the most common malignant pediatric brain tumor and are classified into four molecular subgroups: SHH, WNT, Group 3 and Group 4. Although survival is about 70%, the current standard of care is aggressive and non-specific, leaving patients with severe life-long neurological deficits. Thus, developing targeted therapies with milder side effects is necessary. About 30% of MB cases display hyper-activated SHH signaling. In this pathway, SHH binds to its receptor Patched1 (PTCH1), causing proliferation of cerebellar granule cell precursors (GCPs), the cells of origin of SHH-MB. Hyper activation of the Shh pathway in GCPs is a critical early event that is accompanied by collaborative mutations to aid in its oncogenic transformation and tumorigenesis.

In Chapter 4 of the thesis, I utilise the developing cerebellum as a model system to study the molecular mechanisms underlying MB tumorigenesis by identifying novel molecular

regulators of the Shh pathway. Previously, our lab demonstrated that *Ptch1* loss of heterozygosity (LOH) is essential for preneoplastic lesion formation and inactivation of additional tumor suppressors collaborating with *Ptch1* LOH is required for progression to advanced tumors.

We hypothesized that NMD is a novel tumor suppressor in MB and aimed to elucidate the underlying molecular mechanisms. First, we demonstrate that NMD inactivation leads to hyperactivated Shh signaling in GCPs and the subsequent upregulation of proliferation-regulating genes, causing excessive GCP proliferation. Conversely, activation of NMD leads to downregulation of Shh pathway activity and a decrease of GCP proliferation.

We further investigated the mechanism of NMD-mediated regulation of Shh signaling. NMD selectively targets mRNA transcripts with specific features that induce its degradation, such as the presence of an upstream open reading frame (uORF) in the 5' untranslated region (5'UTR), a lengthy 3' UTR exceeding 1000 nucleotides, and introns in the 3'UTR. Genome-wide “NMD feature” prediction from *Mus musculus* Ensembl gene annotation revealed presence of such NMD-inducing features in regulators of the Shh pathway. We identify that the intron-containing long 3'UTR of mRNAs of at least two Shh signalling effectors are direct targets of the NMD machinery and are responsible for their NMD-mediated degradation. Next, using CRISPR-Cas9-mediated gene inactivation of key NMD machinery components in the *Ptch1* MB mouse model, we showed that NMD inactivation cooperates with *Ptch1* inactivation to accelerate MB progression and aggressiveness *in vivo*. Conversely, NMD activation causes a delay in MB tumor latency and improves survival in mice.

Overall, we have identified NMD as a new molecular pathway involved in regulating the proliferation of cerebellar granule neuron progenitors. Our findings might help the development of novel therapies to treat MB.

Résumé

Le développement du système nerveux nécessite un contrôle précis de l'expression génique des effecteurs qui dirigent divers processus neuronaux tels que la prolifération, la différenciation, la propriété des cellules souches et la migration. La dérégulation des programmes neurodéveloppementaux tels que les voies Sonic hedgehog (SHH) et WNT donne lieu à un large éventail de troubles neurodéveloppementaux, y compris des tumeurs cérébrales solides telles que le médulloblastome. Une voie critique de surveillance de l'ARNm impliquée dans le maintien de l'intégrité globale de l'expression génique est la dégradation des ARNm non-sens (NMD). La NMD a deux rôles importants : elle dégrade les ARNm aberrants comportant des codons de terminaison prématurés et elle régule l'expression de transcrits endogènes qui a un impact sur un large éventail de processus physiologiques, notamment la prolifération et la différenciation cellulaire, la réponse aux signaux environnementaux et même le développement de maladies. Ainsi, la compréhension des programmes de développement peut fournir des informations précieuses sur les mécanismes moléculaires sous-jacents à la formation et à la progression des tumeurs.

Le médulloblastome est la tumeur cérébrale pédiatrique maligne la plus courante et est classé en quatre sous-groupes moléculaires : SHH, WNT, groupe 3 et groupe 4. La norme de soins actuelle, qui comprend une résection chirurgicale, suivie d'une chimiothérapie et d'une radiothérapie, est agressive et non spécifique aux quatre sous-groupes. Bien que la survie soit d'environ 70 %, elle laisse les patients avec de graves déficits neurologiques à vie. Ainsi, le développement de thérapies ciblées avec des effets secondaires plus légers est nécessaire. Environ 30% des cas de médulloblastome montrent une signalisation SHH hyperactive. Dans cette voie, SHH se lie à son récepteur Patched1 (PTCH1), provoquant la prolifération des précurseurs des cellules granulaires cérébelleuses (GCP), les cellules à l'origine du médulloblastome SHH.

L'hyperactivation de la voie Shh dans les GCP est un événement précoce critique qui s'accompagne de mutations collaboratives supplémentaires pour faciliter sa transformation oncogène et sa tumorigenèse.

Dans le chapitre 4 de la thèse, j'utilise le cervelet en développement comme système modèle pour étudier au niveau moléculaire les mécanismes sous-jacents à la tumorigenèse du médulloblastome en identifiant de nouveaux régulateurs moléculaires de la voie Shh. Des travaux antérieurs dans notre laboratoire ont démontré que la perte d'hétérozygotie (LOH) de Ptch1 est essentielle à la formation de lésions préneoplasiques et que l'inactivation de suppresseurs de tumeurs supplémentaires collaborant avec Ptch1 LOH est nécessaire pour la progression vers des tumeurs avancées.

Nous avons émis l'hypothèse que la NMD est un nouveau suppresseur de tumeur dans le médulloblastome et visons à élucider les mécanismes moléculaires sous-jacents. La NMD cible sélectivement les transcrits d'ARNm avec des caractéristiques spécifiques qui induisent sa dégradation. Ces caractéristiques comprennent la présence d'un cadre de lecture ouvert en amont (uORF) dans la région 5' non traduite (5'UTR), une longue région 3' non traduite (3'UTR) dépassant 1000 nucléotides et la présence d'un ou de plusieurs introns dans le 3'UTR. Lors de la déplétion de facteurs de NMD, nous avons observé une augmentation de l'expression de cibles NMD bien établies hébergeant des caractéristiques induisant une NMD, démontrant que la voie NMD est fonctionnelle dans les GCP cérébelleux qui sont les cellules d'origine du MB-SHH. Conformément à notre hypothèse, nous démontrons que l'inactivation de NMD conduit à une signalisation Shh hyperactive dans les GCP. Cela a conduit à la régulation à la hausse ultérieure des cibles transcriptionnelles de Gli qui sont des gènes régulateurs de la prolifération, provoquant

une prolifération excessive des GCP. Inversement, l'activation de NMD entraîne une régulation négative de l'activité de la voie Shh et une diminution de la prolifération des GCP.

Dans ce chapitre, nous avons étudié plus en détail le mécanisme de régulation de la signalisation Shh médiée par NMD. La prédiction de la «caractéristique NMD» à l'échelle du génome à partir de l'annotation du gène Ensembl de *Mus musculus* a révélé la présence de caractéristiques induisant la NMD dans les régulateurs de la voie de signalisation Shh. Nous avons identifié que le 3'UTR des ARNm d'au moins deux effecteurs de la signalisation Shh (*Smo* et *Gli2*) sont responsables en tant que déclencheurs directs de la dégradation de leurs ARNm médiée par NMD. Dans la voie NMD, la phosphorylation du facteur NMD central UPF1 par la kinase SMG1 est cruciale pour marquer les cibles NMD et déclencher leur dégradation. À l'aide d'expériences p-UPF1 RIP-qPCR, nous déterminons en outre que p-UPF1 marque les transcrits *Smo* et *Gli2* pour la dégradation médiée par NMD, potentiellement par sa liaison aux longs 3'UTR contenant des introns de leurs ARNm.

Ensuite, nous avons évalué l'impact de l'inactivation de la NMD sur la tumorigenèse du médulloblastome *Ptch1 in vivo*. En utilisant l'inactivation génique médiée par CRISPR-Cas9 des principaux composants de la machinerie NMD dans le modèle murin de médulloblastome *Ptch1*, nous avons montré que l'inactivation des composants NMD coopère avec l'inactivation de *Ptch1* pour accélérer la progression et l'agressivité du médulloblastome *in vivo*. À l'inverse, l'activation de la NMD entraîne un retard de la latence tumorale du médulloblastome et améliore la survie des souris. Dans l'ensemble, nous avons identifié la NMD comme une nouvelle voie moléculaire impliquée dans la régulation de la prolifération des progéniteurs des neurones granulaires cérébelleux. Nos découvertes pourraient aider au développement de nouvelles thérapies pour traiter le médulloblastome.

“The important thing is not to stop questioning.”

- *Albert Einstein*

Acknowledgements

First, I extend my deepest gratitude to my esteemed supervisor, *Dr. Frederic Charron*, who accepted me into his lab and provided me with the exciting opportunity to carry out my PhD thesis work under his supervision. His attentive mentorship, scholarly insights during our one-on-one discussions and lab meetings, continued motivation, support, and permanent guidance have been instrumental in shaping the course of my research and critical thinking skills. He also gave me the freedom to think and work independently in the lab and provided all the necessary resources and assistance to drive the research forward. I would like to thank him for his timely and excellent reviewing of scholarship applications, presentations, manuscript, and thesis. I am also thankful to him for helping me hone my presentation and writing skills. Overall, his guidance not only fueled my scientific growth but also fostered in me a deeper appreciation for the pursuit of knowledge.

I extend my sincere thanks to *Dr. Patricia Yam* for all the meticulous work she does for the lab that makes the working in lab easier and smooth, for being so resourceful, for all the pertinent questions and discussions she has raised for my project during each lab meeting, for providing me with useful feedback on my scholarship applications, and invaluable suggestions for experiments, statistical analyses, and mouse colony management.

I would like to express my heartfelt appreciation to the members of my advisory committee, *Dr. Yasser Riazalhosseini* and *Dr. Imed Gallouzi* for their valuable feedback and constructive criticism, it has been pivotal in refining the trajectory of my research.

I am indebted to IRCM and McGill University for providing me with the resources, facilities, and academic freedom necessary to embark on this intellectual voyage. Special thanks to *Dominic Fillion* for all his microscopy training and assistance, and to the Animal Care facility including *Jessica Barthe*, *Constantin Androne*, *Manon Laprise*, *Caroline Dube*, *Karyne Deschenes*, *Mariane Canuel*, *Corine Morin*, and *Marie-Anne Riquelme Jacob*. They have been an incredibly helpful team during my time here.

I would like to thank the pioneer of the NMD pathway, *Dr. Lynne Maquat* for kindly providing us with the β -globin NMD reporter constructs used in my experiments.

I would also like to take this opportunity to thank all the agencies that funded my research in the form of scholarships, fellowships, poster, and oral presentation awards: IRCM, McGill-IPN, McGill-HBHL and FRQS. This helped to boost my confidence and stay motivated.

The Charron has always been a multi-cultural environment, and it has been enriching both academically and personally to have spent the last 5 years here. I am indebted and thankful to all the members of the Charron lab past and present.

Dr. Lukas Tamayo-Orrego: Thank you for training me on several important techniques including GCP isolation, culture and microscopy to perform my research and giving me an opportunity to contribute to your first author publication in Nature Cancer.

Dr. Chia-Lun Wu: Thank you for laying the early foundation of my project, your mentorship, raising pertinent questions, helping with experimental design, training me ever so patiently with GCP-related techniques and challenging *in vivo* techniques such as *in utero* electroporation and orthotopic transplantations.

Jean-Francois Michaud: aka “the king of cloning “- thank you for generating efficient NMD reporter constructs for my experiments. Your technical support/advice organized and efficient lab management and precise attention to details while placing orders have ensured the smooth execution of my experiments.

Dr. Sara Calabretta: Thank you for patiently training me on RNA immunoprecipitation technique, interesting brainstorming sessions, always asking relevant and tough big picture questions during lab meetings and your constant moral support. Lastly, thanks for introducing me to the exciting world of role-playing games and having intellectual discussions about anything/everything under the sun.

Dr. François Depault: Thanks for contributing to the design and validation of gRNAs for successful use in the CRISPR experiments *in vivo*, managing all the genotyping in the earlier phase of my PhD, and teaching me the technique of cryosectioning.

Dr. Amandine Bemmo: Thanks for performing genome-wide *in silico* bioinformatic analyses to predict NMD features and discussion about various bioinformatic tools for analyses.

Dr. Sabrina Schlienger: Many thanks for patiently training me with GCP-related techniques, *in vivo* mouse techniques, supervising and helping me troubleshoot biochemistry techniques in the earlier phase of my PhD. I am grateful for your insightful discussions about my

project, baking amazing French desserts, and your unflinching support throughout my time here in Montreal, inside and outside lab.

Dr. Nursen Balekoglu: Thank you for your unwavering support and encouragement always, providing necessary technical advice, being very resourceful, being my running buddy, and introducing me to the world of delicious Turkish desserts!

Rachelle Sauvé: Thanks for your technical inputs, being my French translator for mundane conversations and my thesis abstract, discussing science and cats, sharing my love for popcorn, and introducing me to the elite club of playing video games!

Dr. Vanesa Jimenez Amilburu: Thanks for your interesting and intriguing discussions regarding GCP biology, for the weekly genotyping support, being a super fun and supportive labmate, listening to me vent and encouraging me to go on hikes!

Victoria Veas Roy, Kaiyue Zhang, Dr. Hugo Ducing, Dennis Drownik and Sneha Sukumaran: Many thanks to each one of you for initiating inspiring scientific discussions, for becoming such good friends with me in a short time, and for providing the supportive, friendly, and encouraging lab environment.

I extend my gratitude to the other lab members in the past: *Dr. Shannon Swikert, Heather Anderson-Keightly, Dr. Julien Ferent, Dr. Fred Racicot, and Dr. Shirin Makihara* whose interesting discussions, exchange of ideas, and collaborative spirit created an intellectually stimulating environment that constantly motivated me. The Charron lab has been my family away from home. I will always remember and cherish the wonderful memories we made.

I am endlessly grateful to my best friends, *Supraja Ranganathan* and *Dr. Jayashree Srinivasan* for their constant support and camaraderie throughout my PhD journey, making every challenge easier to conquer and every triumph sweeter to celebrate.

Nothing I write is sufficient to convey the respect, love, admiration, and gratitude I have for my amazing family. Your belief in me has been my driving force even when I did not believe in myself, and I am ever grateful for your sacrifices, unconditional love, unwavering support, and encouragement throughout this arduous journey.

Finally, I would like to also dedicate this dissertation to my paternal and maternal grandparents whose memory and influence continue to deeply inspire me in all my endeavors. Their legacy serves as a reminder of the profound impact that individuals can have on shaping our path.

List of Abbreviations

AS	Alternative splicing
ASC	Adenosquamous carcinoma
ASO	Antisense Oligonucleotides
ATF	Activating Transcription Factor
BBB	Blood-Brain Barrier
CARM1	Coactivator Associated Arginine Methyltransferase 1
CCND1	Cyclin D1
CH	Cysteine-Histidine domain
CHOP	C/EBP homologous protein
CHX	Cycloheximide
CLIP	Cross-linking and immunoprecipitation
DDIT3	DNA damage-inducible transcript 3
DECID	Decay Inducing complex
E	Embryonic
EGL	External granule/germinal layer
eiF	eukaryotic translation initiation factor
EJC	Exon Junction Complex
ESC	Embryonic Stem Cells
FL	Full Length form
GCP	Granule cell precursor
GN	Granule Neurons
HD	Helicase Domain
HK2	Hexokinase 2
IGL	Internal granule/germinal layer
ISR	Integrated Stress Response
IUE	in utero Electroporation
KD	Knockdown
KID	Kinase Inhibitory Domain
LOH	Loss of heterozygosity

MB	Medulloblastoma
MEF	Mouse Embryonic Fibroblasts
miR	microRNA
mTOR	mammalian Target of Rapamycin
NHEJ	Non-homologous end joining
NMD	Nonsense-mediated mRNA decay
NMDi14	NMD inhibitor drug
NPC	Neural Progenitor Cells
NSC	Neural Stem Cells
nt	nucleotides
OA	Okadaic Acid
OE	Overexpression
P	Postnatal
p-UPF1	Phosphorylated-UPF1
PABPC	PolyAdenylate-Binding Protein, Cytoplasmic
PC	Purkinje Cells
PFA	Paraformaldehyde
PIKK	Phosphatidylinositol 3-kinase-related kinase
PP2A	Protein Phosphatase 2A
PTC	Premature Termination Codon
Ptch1	Patched1
qPCR	quantitative Polymerase Chain Reaction
R	Repressor form
RIP	RNA Immunoprecipitation
ROS	Reactive Oxygen Species
SHH	Sonic hedgehog
SMG	Suppressor of Morphogenesis in Genitalia
SMO	Smoothened
SQ	Serine-Glutamine
SURF	SMG1-UPF1-eRF1-eRF3 complex
SVZ	Subventricular zone

UBC	Unipolar brush cells
uORF	Upstream open reading frame
UPF	Upstream Frameshift
UPR	Unfolded Protein Response
UTR	Untranslated region
VZ	Ventricular zone
WNT	Wingless-related integration site

List of Figures and Tables

- Figure 1.1.1. Embryonic cerebellar development.
- Figure 1.1.2. Postnatal cerebellar development.
- Figure 1.1.3. Shh signaling in the developing cerebellum.
- Figure 1.2. Overview of MB subgroups.
- Figure 1.2.3. Multistep paradigm of *Ptch1*^{+/-} MB.
- Figure 1.3.1. EJC-dependent and EJC-independent NMD pathway.
- Figure 1.3.3a. Structure of UPF1 protein.
- Figure 1.3.3b. Regulation of SMG1 kinase by SMG8-SMG9 heterodimer.
- Figure 1.3.4. SMG6, SMG5/7 mediated mRNA degradation mechanisms.
- Figure 1.4.3. Interaction of cytoplasmic PABP with eIF4G suppresses NMD.
- Figure 1.5. Dual roles of NMD.
- Figure 1.5.2. Alternative splicing coupled NMD in homeostatic autoregulation of splicing factor levels.
- Figure 1.5.3. Role of NMD in Modulating the Stress Response.
- Figure 1.5.4. NMD controls neural stem cell fate.
- Figure 4.1. The NMD pathway is functional in cerebellar granule cell precursors (GCPs).
- Figure 4.2. NMD regulates Shh pathway activity, expression of proliferation-regulating genes, and GCP proliferation.
- Figure 4.3. NMD regulates Shh signaling by direct modulation of *Gli* transcriptional activity.
- Figure 4.4. The 3'UTRs of *Smo* and *Gli2* are targets of NMD-mediated degradation.
- Figure 4.5. p-UPF1 binds to the 3'UTRs of *Smo* and *Gli2* to mark and target their mRNAs for NMD.
- Figure 4.6.1. NMD inactivation cooperates with *Ptch1* inactivation to enhance medulloblastoma tumorigenesis.
- Figure 4.6.2. Shh pathway activity is upregulated in medulloblastoma tumors when Smg1 is inactivated *in vivo*
- Figure 4.7.1 NMD upregulation decreases tumor cell proliferation *in vitro*.
- Figure 4.7.2. NMD upregulation leads to a delay in MB tumor latency and significantly improved survival *in vivo*.

Figure 4.8. NMD activity level is a determinant of prognosis in specific subgroups of human medulloblastoma.

Table 3.16.4: sgRNA sequences

Table 3.16.5: siRNA duplex sequences

Table 3.16.6: Primer sequences used for quantitative RT-PCR

Preface and Contribution of Authors

This thesis was written in accordance with the “Guideline for Thesis Preparation” provided by McGill University and is written in the traditional monograph style. Chapter 3 contains the methodology for the work depicted in Chapter 4, which represents original scholarship. Specifically, the data presented in Chapter 4 are part of an ongoing manuscript. The specific contribution of individual authors is detailed below:

Initial hypothesis: S.A.Mohan, C-L.Wu, F. Charron.

Project conception and experimental design: S.A.Mohan, F. Charron.

For Figure 4.3: Experiments performed by S.A.Mohan with input from J.F. Michaud. NMD feature prediction on *Mus musculus* genome by A. Bemmo with input from S.A.Mohan and F. Charron.

For Figure 4.4: pmCMV-GI-Norm, pmCMV-GI-39Ter and phCMV-MUP constructs were shared by Dr. Lynne Maquat. β -globin Smo 3’UTR and β -globin Gli2 3’UTR chimeric constructs were generated by J.F. Michaud.

For Figure 4.5: Experimental design by S.A.Mohan, S.Calabretta and F. Charron. Experiment performed by S.A.Mohan with inputs from S.Calabretta.

For Figure 4.6.1: CRISPR experiments were designed by C-L. Wu and F. Charron. All gRNAs for CRISPR experiments were designed and validated for *in vivo* use by F. Depault. *In utero* electroporation, tissue preparation and collection of preneoplastic lesions & advanced tumor was conducted by C-L. Wu. Analysis of preneoplastic lesion size and incidence, Kaplan-meir survival curves by C-L. Wu.

For Figure 4.7.2: Experimental design by S.A.Mohan and F. Charron. Experiment performed by S.A.Mohan with input from C-L. Wu and F. Charron.

For Figure 4.8: Generation of NMD target gene signature by F. Charron with input from S.A.Mohan. Bioinformatic analysis of NMD signature expression on publicly available human MB cohort by F. Charron.

Data analysis, figure compilation, and chapter writing – S.A.Mohan with input from F. Charron

Abstract translation to French: R. Sauve

Chapter 1
Introduction

1.1 Cerebellar development

1.1.1 Development of cerebellum during neurogenesis

During cerebellar development, the cerebellar cortex and all cerebellar nuclei are generated via a highly complex, but organized events of neurogenesis and cell migrations. The isthmic organizer, roof plate, and the transcription factors expressed rostral and caudal to the isthmus produce extracellular signals that allow the cerebellar anlage map to be generated at an early stage of development, at embryonic day 8.0–8.5 (E8.0–8.5)¹. The two distinct germinal centers that give rise to neuronal populations in the cerebellum are the ventricular zone (VZ) and the rhombic lip (**Figure 1.1.1**).

Arising from the dorsomedial VZ of the emerging cerebellar anlagen along the fourth ventricle are all the GABAergic neurons. These include Purkinje cells (PC) which is the principal output neuron of the cerebellar cortex, and various classes of *Pax2*⁺ inhibitory interneurons². The progenitors of the Purkinje cell are generated between E11-E14.5 to form physically separate and molecularly distinct clusters by ~E18³. In parallel, progenitors of cerebellar nuclei neurons are produced between E10-E12.5 and those of cerebellar interneurons, including Golgi, basket, and stellate cells occur around E13.5. As the inhibitory interneuron progenitors move through the white matter, they undergo further rounds of cell divisions *en route*, and finally settle in conjunction with the PC clusters³. All these VZ-derived neuronal cell populations are generated from a common pool of progenitors, and they eventually migrate radially along the glial fiber system⁴⁻⁷. By P20, a monolayer of parasagittal stripes is produced by association of PC clusters and accompanying interneurons that diffuse longitudinally¹.

All cerebellar glutamatergic neurons such as a subpopulation of the excitatory deep cerebellar nuclei neurons (born between E10.5-E13.5)^{8,9}, the cerebellar GCPs (born between E13.5-postnatal

period)¹⁰ and neurons from many pre cerebellar regions such as unipolar brush cells (UBC) at a relatively late developmental stage between E14.5-birth¹, are produced by distinct progenitors in the secondary germinal zone that arises along the anterior aspect of the rhombic lip. Dorsal brainstem progenitors originate from the lower rhombic lip, while the upper rhombic lip gives rise to progenitors that begin to express *Math1/Atoh1*, a bHLH transcription factor which imposes a neuronal lineage restriction. Thus, different progenitor populations control specification in the rhombic lip, in contrast to the VZ, where neuronal subtypes are produced from a single pool of progenitors^{11,12}.

All the above cell populations migrate tangentially onto the cerebellar anlage surface. The specified deep cerebella nuclei neurons assemble to build the nuclear transitory zone before forming individual nuclei^{8,12,13}. The UBCs migrate dorsally through the prospective white matter and undergo final differentiation close to P28 to reside in the internal granule layer (IGL)^{13,14}. Unlike excitatory cerebellar nuclei neurons, between E12.5-E16, GCPs spread across the surface of the cerebellum dorsally to form a secondary germinal zone called the external granule layer (EGL)¹⁵.

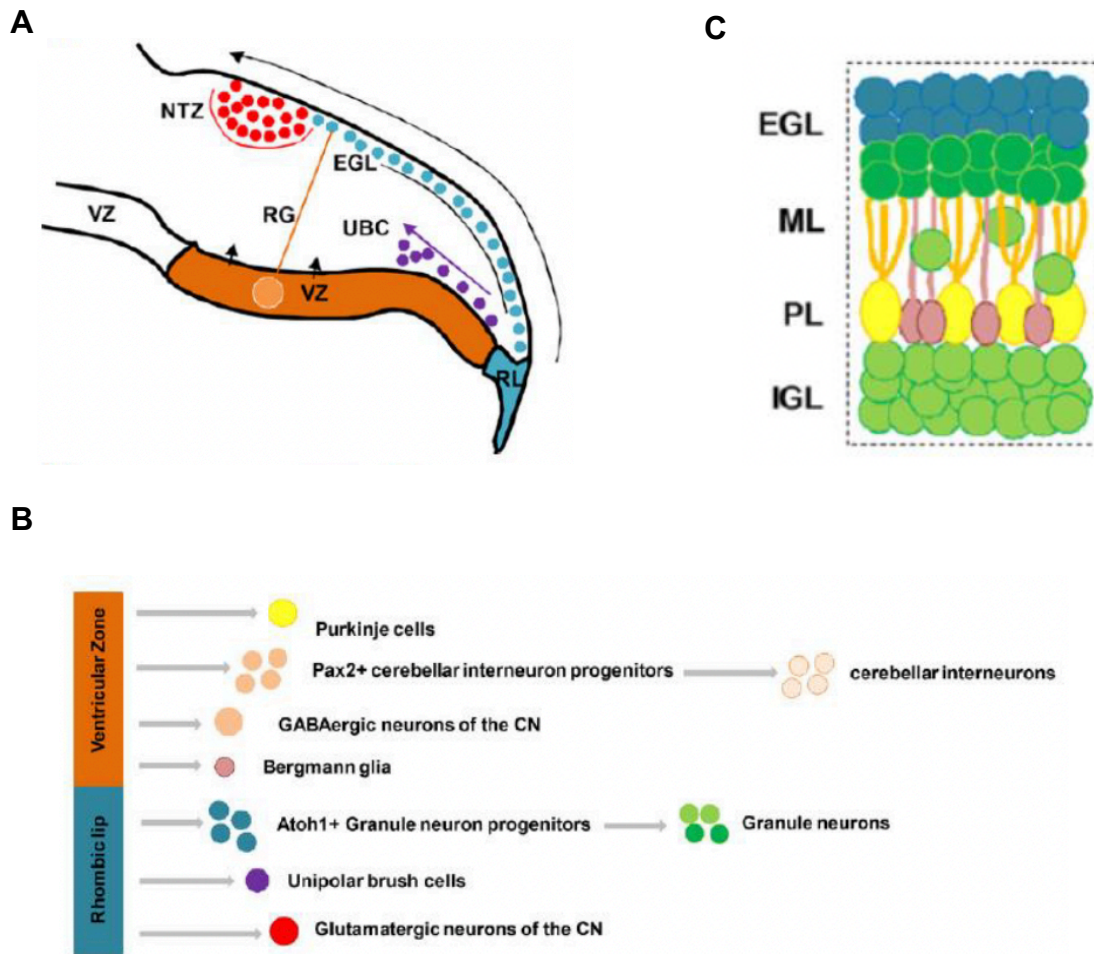


Figure 1.1.1. Embryonic cerebellar development. (A and B) Two germinal zones during embryonic neurogenesis as shown in a sagittal view: ventricular zone (VZ) and the rhombic lip (RL). From the radial glia in the VZ, all cerebellar GABAergic neurons are produced first, followed by Purkinje neurons Bergmann Glia and interneurons. From the RL arise three major glutamatergic neurons, all of which migrate tangentially into the cerebellar anlage.: first is the cerebellar nuclei projection neurons, followed by granule neurons from *Atoh1/Math1*+ granule neurons progenitors (aka GCPs), and then unipolar brush cells. (C) Lamination schematic to show the various neuronal populations organised in the P7 cerebellum that arose from progenitors in (A).

Nuclear transitory zone (NTZ); External granule layer (EGL); Radial glia (RG); Unipolar brush cell (UBC); Ventricular zone (VZ); Rhombic lip (RL); Molecular layer (ML); Purkinje layer (PL); Internal granule layer (IGL); Figure from (Haldipur and Millen, 2019)¹³.

1.1.2. Postnatal cerebellar development

Development of the cerebellum occurs in successive waves of proliferation and migration of the cerebellar GCPs throughout late embryogenesis and postnatal phase. GN arising from GCPs constitute greater than 50% of all neurons (in mouse and humans). In addition, other subpopulations of progenitors arise from the white matter postnatally that enrich the glial cell and interneuron populations¹⁶.

In mice, GCPs derived from the rostral rhombic lip undergo their first wave of proliferation at embryonic day 13.5 (E13.5) followed by migration over the surface of the cerebellum from E17.5 onwards to expand their population and form the external granule cell layer (EGL)⁴. This expansion in the EGL is stimulated by the mitogen sonic hedgehog (SHH) produced by PC as early as E17.5¹⁷⁻²⁰. Numerous signaling mechanisms boost GCP growth between postnatal days (P2-P4)¹⁸. After the SHH-dependent peak proliferation phase from P5 to P7, these progenitors move into the inner layer while they exit the cell cycle and start to differentiate into cerebellar granule neurons (GN) (**Figure 1.1.2**). There is an increase in the expression of key GCP differentiation markers, specifically NeuroD1 and p27Kip1²¹⁻²³. Following this, the differentiated cells migrate past the Purkinje layer/molecular layer to reach the internal granule cell layer (IGL), where they reside in the mature cerebellum, finally making synaptic connections with the PC^{13,24}.

In humans, from the tenth gestational week to the end of the second postnatal year, GCP expansion continues. This expansion phase concludes when the external granule layer (EGL) is no longer present¹³. In addition, human cerebellum has much higher foliation than that in mice. Altogether, the number of GN per PC is 10-fold higher in humans compared to mice¹³. A deeper understanding of human cerebellar development can be facilitated by critical analyses of animal MB models and patient-derived xenograft (PDX) models.

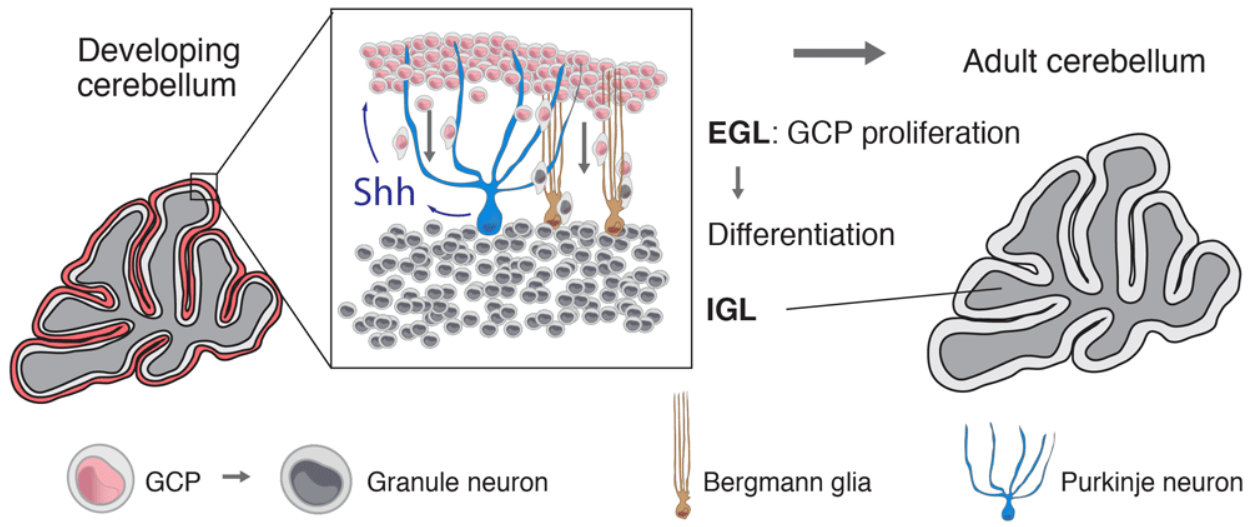


Figure 1.1.2. Postnatal cerebellar development. GCPs proliferate in response to Shh secreted by the Purkinje neurons to populate the EGL. After this Shh-dependent proliferation phase, the GCPs exit the cell cycle, start to differentiate, and migrate radially past the Purkinje layer with the help of Bergmann glia to reside as Granule neurons in the IGL of the adult cerebellum. Granule cell precursors (GCPs); External granule layer (EGL); Internal granule layer (IGL); Figure from (Tamayo-Orrero L and Charron F, 2019)²⁵.

1.1.3. Canonical Sonic Hedgehog signaling in the developing cerebellum

GCPs in the EGL continue to depend on SHH to drive their postnatal proliferation phases for generating the expanding pool of progenitor cells¹⁷⁻¹⁹. In the absence of SHH ligand, the 12-span transmembrane receptor Patched 1 (PTCH1) represses activity of the 7-pass transmembrane, G protein-coupled receptor Smoothed (SMO) keeping the intracellular signal transduction at the “OFF” state²⁶. The transcriptional activation of the pathway is prevented due to two reasons. First, full length glioma-associated oncogene family of transcription factor 2 (GLI2) is bound and sequestered by suppressor of fused (SUFU) in the cytoplasm for its proteasomal degradation²⁶. Second, full-length GLI3 is phosphorylated by Protein kinase A (PKA), Glycogen synthase kinase 3-beta (GSK3-β) and Casein kinase 1 (CK1), triggering its proteolytic cleavage to generate the truncated GLI3 repressor form (GLI3R) which blocks transcription^{27,28}. When extracellular SHH binds to PTCH1, the PTCH1-ligand complex is internalized and degraded in the endosomes, which relieves PTCH1's inhibitory effects on SMO switching the pathway to the “ON” state²⁹. Activated SMO can degrade the SUFU-GLI2 complex in the cytoplasm and trigger proteolytic cleavage of GLI2 recruitment to the nucleus where it promotes transcription of downstream Shh target genes which is required to induce GCP proliferation^{18,26,30} (**Figure 1.1.3**). Additional co-receptors of SHH that promote SHH signaling include CAM-related/downregulated by oncogenes (CDO), Brother of CDO (BOC) and Growth arrest-specific 1 (GAS1)^{20,31,32}. On the contrary, another co-receptor Hedgehog interacting protein (HHIP) can compete for PTCH1 binding, thus functioning as a negative regulator of the pathway³³.

In conclusion, activation of the canonical SHH signaling pathway ultimately leads to *Gli*-mediated transcription of genes including cell cycle regulators *cyclin D1* (*Ccnd1*), *cyclin D2* (*Ccnd2*), *cyclin E* (*Ccne*), proto-oncogene *N-myc*, *Hexokinase 2* (*Hk2*) and *Gli1*. *Ccnd1* is highly expressed in

GCPs immediately following birth³⁴⁻³⁷. Pogoriler *et al* showed that loss of *Ccnd1* in mice impaired GCP proliferation and cerebellar growth³⁸. During the peak proliferative phase of P4-P8, GCPs display high expression of both *Ccnd1* and *Ccnd2*³⁸. Shh-induced proliferation is significantly reduced by dominant-negative N-myc, proving that N-myc is necessary for the GCP proliferation³⁹. Similarly, N-myc overexpression increases GCP proliferation, and further upregulates *Ccnd1* even independently of Shh signaling³⁴. These studies demonstrate that transcription downstream of *Gli* is majorly responsible for Shh-induced GCP proliferation.

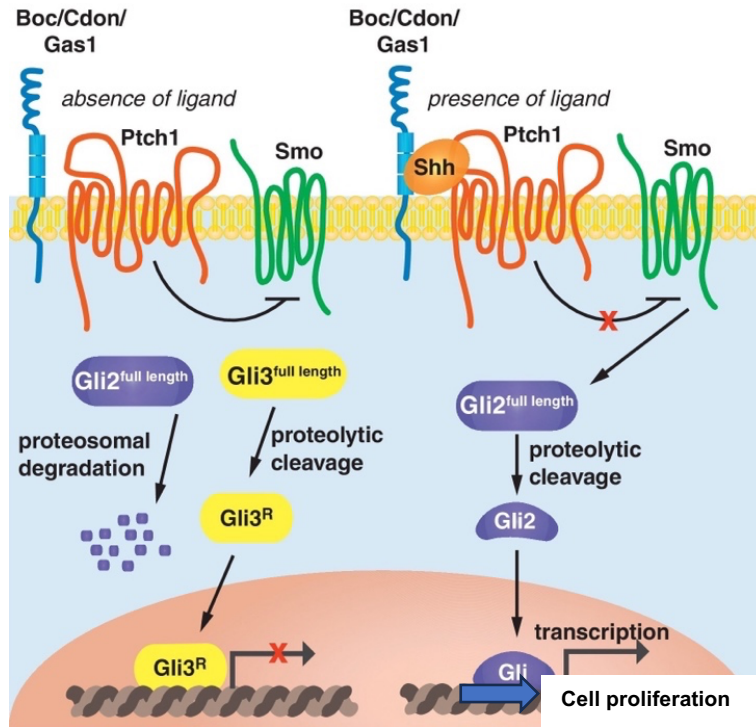


Figure 1.1.3. Shh signaling in the developing cerebellum. *Left schematic:* Ptch1 represses Smo when Shh is absent. In the OFF state, the Shh-mediated transcription remains inhibited due to the binding of the truncated repressor Gli3 in the nucleus and proteasomal degradation of the protein encoded by full length Gli2 activator. *Right schematic:* In the presence of Shh, it binds to Ptch1 along with Boc, Cdon, or Gas1, thus relieving the inhibition exerted by Ptch1 on Smo; this is the ON state of the pathway. Full length Gli2 is cleaved by proteases following Smo activation. The Gli2 activated form activates transcription of target genes in the nucleus. (Figure from Yam P.T. and Charron F, 2013)⁴⁰

1.1.4. GCPs are the cell of origin of SHH-MB

Although SHH signaling is the major driver of GCP proliferation during early postnatal period, an important consequence of hyperactivated Shh signaling in GCPs is development of cerebellar tumors called MB. Using mouse models, several individual research groups provided evidences that GCPs are the main cell of origin of SHH-MB. An early study using a mouse model with the *Math1*-driven conditional deletion of *Ptch1* in GCPs demonstrated uncontrolled GCP proliferation and MB formation with histopathologic features of desmoplastic human MBs^{41,42}. Aligned with this observation, constitutive activation of Smo also causes excessive GCP proliferation and high incidence of MB^{42,43}. Further supporting this conclusion, early progenitors or stem cells strictly committed to granule neuron lineage can be initiators of SHH-induced MB^{44,45}. In the progression of MB, there is an intermediate “preneoplasia” stage between postnatal weeks 2 and 6 in which lesions are detectable as discrete foci on the surface of the cerebellum. Tumor cells and preneoplastic lesion cells resemble GCPs in that they are *Math1* positive and express key targets of SHH-mediated Gli transcription such as *Gli1*, *Ccnd1* and *MycN*⁴⁶. Lower rhombic lip derived progenitors are also suggested as the cells of origin for non-SHH subgroups, but Swartling et al shows GCP lineage is required for Shh-MB specifically⁴⁷. For instance, Shh-MB tumors were formed in mice transplanted with N-mycT58A-transduced E16 cerebellar GFAP⁺ NSCs (which can still form GCPs *in vivo*), but Group 4 tumors developed in mice upon transplantation of N-mycT58A-transduced P0 cerebellar NSCs, which are incapable of producing GCPs *in vivo*⁴⁸. Altogether, these lines of evidence demonstrate that GCP specification is absolutely essential to drive Shh-MB tumorigenesis. Interestingly, consistent with GCP originating regions, location of human SHH MBs detected by MRI studies was in cerebellar hemispheres^{49,50}.

Over the last decade, our lab has also provided key insights highlighting that hyperactivation of the SHH signaling in GCPs render them susceptible to oncogenic transformation. First, high levels of the SHH receptor BOC in GCPs triggered *Ccnd1*-dependent DNA damage and *Ptch1* loss of heterozygosity (LOH), a critical early event that leads to advanced tumor progression⁵¹. Replication stress can induce DNA damage, and Tamayo-Orrego *et al* showed that Shh stimulation in GCPs triggered replication stress through increased origin firing and consequently hyper recombination events such as *Ptch1* LOH which initiates tumor formation⁵².

Furthermore, modulation of genes involved in GCP proliferation can directly impact Shh-mediated MB formation, as shown by use of transgenic mouse models. For example, in two separate studies using a *Ptch1* heterozygous mutant mice, (1) loss of *Ccnd1* was sufficient to suppress MB formation³⁸ and (2) inactivation of *Gli1* significantly reduced spontaneous MB formation⁵³. In another transgenic mouse MB model driven by SmoM2, cre-mediated ablation of *Hk2* minimised the aggressiveness of MB and improved survival⁵⁴.

1.1.5. Additional extracellular players in MB progression

Most of what is known about Shh-MB arises from research focused on GCPs, the cell of origin of this subgroup. Although Shh signaling is a central pathway in the tumor initiation and progression of Shh-MB, it is important to keep in mind that additional extracellular ligands in the developing cerebellum also influence Shh-MB tumorigenesis. I briefly describe the contribution of two extracellular signaling pathways: IGF2 signaling and Norrin/Frizzled signaling.

IGF signaling pathway:

The Shh pathway is primarily responsible for GCP proliferation, however Insulin-like Growth Factors (IGFs) also aid in their survival and expansion during cerebellar development⁵⁵. In

addition, Tanori and colleagues showed that increased *Igf1* expression in the *Ptch1* heterozygous mutant mouse model potently increased GCP proliferation, delayed differentiation and dampened their apoptosis⁵⁶. In addition, preneoplastic lesions form *de novo* when *Igf1* is highly expressed, but this does not alter how quickly those lesions progress to become complete tumors⁵⁶. On the other hand, Corcoran et al demonstrated in the *Ptch1* heterozygous mutant mouse model that expression of *Igf2* which is a growth promoting factor is required for the progression of preneoplastic lesions to advanced tumors by promoting tumor cell proliferation, but *Igf2* is not sufficient for *de novo* preneoplastic lesions at the initiation stage⁵⁷.

Norrin/Frizzled signaling:

There exists multiple tumor stromal cells and resident immune cells in both preneoplastic lesions and advanced medulloblastoma, suggesting their contribution to the tumorigenesis⁵⁸. The blood-brain barrier (BBB), which is made up of astrocyte processes, pericytes, and endothelial cells, protects the brain parenchyma by tightly regulating the movement of molecules, ions and even foreign substances such as chemotherapy drugs⁵⁸. The vascular development in the cerebellum is maintained via the interaction of the vascular endothelial cell with the neural cells. A key endogenous signalling axis that is involved in this process is the Norrin/Frizzled pathway, wherein Norrin, which is an atypical Wnt ligand, specifically interacts with Frizzled to activate β -catenin-dependent canonical Wnt signaling⁵⁹⁻⁶¹. The regulation of Wnt signaling in the endothelial cells aids in maintaining an intact BBB in SHH-MB⁶². During the early stages of tumorigenesis, Norrin/Frizzled signaling functions as a tumor-suppressive mechanism by the restoration of normal vasculature and inhibition of angiogenesis mediated by tumor-cell derived Wnt signaling⁶³. Conversely, loss of Frizzled signaling causes the activation of angiogenesis and stromal remodelling

leading to a decrease in apoptosis, more tumor cell proliferation and higher rates of *Ptch1* LOH and progression to advanced MB tumors in the *Ptch1* heterozygous mutant mouse model⁶³.

1.2 Medulloblastoma (MB)

Medulloblastoma (MB) is the most common malignant pediatric brain tumor and is one of the leading causes of cancer-related deaths in children, but it is also diagnosed in adults. These tumors originate from the posterior fossa but can spread to various parts in the brain and to the spinal cord. MB is classified into four molecular subgroups: Wingless Int-1 (WNT), Sonic Hedgehog (SHH), Group 3 (G3), and Group 4 (G4) (**Figure 1.2**). This classification is based on a comprehensive list of parameters including genetic alterations, transcriptomic gene expression analyses, methylation pattern analyses, and clinical characteristics such as age of onset, histology, prognosis, or metastatic risk⁶⁴⁻⁷¹. The current standard therapy which consists of maximal safe surgical removal of the tumor, risk adapted radiation therapy, and chemotherapy, is non-specific to the subgroups.

Recent large scale “-omics” screening of human MB tumors, combined with several lines of data gathered from candidate gene approaches in mouse models demonstrate that (1) these tumor subgroups display deregulation of specific developmental pathways that are critical for normal cerebellar development such as SHH and WNT, (2) the cells of origin for each of these subgroups are temporally and spatially distinct cerebellar progenitors and finally (3) these larger tumor subgroups are further subdivided into 12 biologically distinct and clinically relevant MB subtypes to address molecular and clinical intra-subgroup heterogeneity^{1,68,72-74}.

1.2.1 Molecular subgroups of MB

SHH-MB

Of all MBs, about 30 % belongs to the SHH subgroup, characterized by mutations in different components of the SHH pathway. SHH tumors are further subdivided into four subtypes based on age as a top criterion: SHH α (29 % in adolescent children between 3-10 years), SHH β (16 % in infants <3 years having poor prognosis), SHH γ (21 % in infants <3 years having good prognosis), and SHH δ (34 % in adults).

SHH tumors occur mostly in infants (pediatric) and adults and are molecularly and clinically distinct⁷⁵. In adults, the male to female ratio is 2:1 and the SHH δ subtype are mostly found in the cerebellar hemispheres and are rarely metastatic⁷⁵. In infants belonging to the SHH β and SHH γ subtypes, the male to female ratio is 1:1. These pediatric tumors are detected in the hemispheres (rarely midline) and are more frequently metastatic⁷⁵. SHH-MB can display different histology types, though the most frequent is nodular desmoplastic and second frequent is the classic histology⁷⁶.

Germline mutations in SHH pathway components drive MB tumorigenesis. For instance, Gorlin syndrome patients who have *PTCH1* germline mutations^{77,78} are predisposed to MB and basal cell carcinoma (BCC). Likewise, individuals with *SUFU* germline mutations^{79,80} and Li-Fraumeni syndrome patients who have *TP53* germline mutations are all susceptible to MB⁸¹. Somatic mutations in *PTCH1* are prevalent in infants, adolescents, and adults^{73,82,83}. Activating mutations in *SMO* are found in adult and infantile SHH MBs, whereas *SUFU* mutations mostly occur in infants^{75,80}. In adolescent patients belonging to the SHH α subtype, the genetic aberrations include amplification of *MYCN*, *SHH*, *GLI1*, *GLI2* transcription factors as well as somatic mutations in *TP53*⁷⁵. *TP53* mutation status has high prognostic impact. Whole genome sequencing has identified other recurring mutations in sporadic MBs that are genes known to either interact with

or amplify SHH signaling such as *KMT2D* (12%), *DDX3X*, *GSE1*, *GNAS*, *CREBBP* and *RKARIA*⁸⁴.

The following chromosomal aberrations have been detected to date in the SHH subgroup till date: Loss of 17p (19.8 % in adult SHH vs 12.7 % in pediatric SHH), 10q loss (19.8 % in adult SHH vs 54.5 % in pediatric SHH) and 3q gain (27 % overall)⁷⁵. However, the most frequently detected was the deletion of chromosome 9q (37.5 % in adult SHH vs 56.4 % in pediatric) which, not surprisingly, is the location of *PTCH1* (9q22)⁷⁵.

The 5-year overall survival for SHH subgroup is about 77 % in infants, about 69 % in children and about 75 % in adults⁸⁵. Despite many patients with SHH MB having favourable outcomes with current treatments, we require specialized and targeted therapeutic approaches due to the debilitating long term neurological side effects. Following surgical resection, treatment with high dose craniospinal radiation and adjuvant chemotherapy still leaves certain subtypes like SHH α patients with poor outcome. On the other hand, some MBs can be cured without radiotherapy by using postoperative chemotherapy⁸⁶. As with most chemotherapeutics, it aids in controlling tumor locally, and has more global cytotoxic effects in patients. The gold standard chemotherapy regimen includes 7 weeks of vincristine, a gap of 30 days, followed by alternating cisplatin and cyclophosphamide every 5th week starting at 11th week.⁸⁷

The most popular therapy for SHH-MBs that has been successful in preclinical studies is the inhibition of SMO using small molecule inhibitors such as vismodegib and sonidegib⁸⁸. Although vismodegib has been approved for BCC treatment, it is still not for adult SHH MBs. This could be due to the acquired resistance in SMO resulting from a mutation in its extracellular domain preventing vismodegib binding⁸⁹. Another reason could arise from the drug's inability to exert its effects due to the loss of primary cilia (the primary location of SMO-mediated SHH signaling),

which would allow basal constitutive activation of the pathway^{90,91}. For the treatment of patients with standard and high risk newly diagnosed SHH MB, a Phase II clinical trial of vismodegib in combination with chemotherapy (cisplatin, vincristine, and cyclophosphamide) is active currently. In case of Sonidegib, pediatric patients showed permanent bone growth defects in Phase I/II studies.

WNT MB

This subgroup only accounts for about 10 % of all MBs. The 5-year overall survival is higher than 90 %, meaning patients with WNT MB have the best prognosis. These tumors are rare in infants and are prevalent in children between 6-12 years of age (WNT- α) and are evenly diagnosed in males and females⁹². The tumors in adults >17 years belong to the WNT- β subtype. At the diagnosis, these tumors are located in the fourth ventricle, along the brainstem with very rare metastatic presentation⁹³.

It is well known that Turcot syndrome patients who have germline mutations in the WNT pathway repressor, *Adenomatous polyposis coli (APC)*, are predisposed to WNT MB^{85,94,95}. The Mutations in *β -catenin (CTNNB1)*, which is the transcriptional activator of the WNT pathway is the other major driver for WNT MBs⁹⁵⁻⁹⁷. More than 97% of WNT MBs are caused by mutations in these two driver genes. Some other recurring mutations found in these tumors are in genes encoding DDX3X, TP53, SMARCA4. Loss of chromosome 6 is the only cytogenic alteration in WNT MBs. Such genetic aberrations occurring in lower rhombic lip progenitor cells of the embryonic dorsal brainstem are responsible for formation of WNT MBs⁴⁹.

The aim for the ongoing clinical trials for WNT MB is to retain high cure rates and minimizing adverse side effects of treatment. Therefore, it focuses on developing de-escalation of treatment

options including reduction of craniospinal radiation dosage and/or chemotherapy regimens (NCT01878617, NCT02724579).

Group 3 (G3) and Group 4 (G4) MBs

Group 3 (G3) accounts for about 25 % of all MB cases and have the worst prognosis and highest rate of metastasis^{76,85}. The male to female ratio of occurrence is 2:1 and is prevalent in young children (3-10 years) mainly, with rare occurrence in teenagers and infants⁷⁶. The three G3 subtypes are: G3- α (chromosomes 8, 10 and 11 loss, chromosome 7 gain, and i17q, MYC amplification), G3- β (OTX1 gain and DDX31 loss on chromosome 9 and a high expression of GFI1/GFI1B) and G3- γ (i17q and MYC amplification)⁷². Metastatic presentation is observed in about 40% of all G3 cases⁹⁸.

Group 4 (G4) MBs make up around 40 % of the total cases and have an intermediate prognosis like that of SHH MBs⁸⁵. For G4, male to female ratio is 3:1, and is prevalent across all age groups with rare occurrence in infants^{64,76,85}. The three subtypes are: G4- α (MYCN and CDKNA amplifications, as well as 8p loss and 7q gain), G4- β (synuclein, α interacting protein (SNCAIP) duplications) and G4- γ (8p loss, 7q gain and CDKNA amplifications)⁷². They are detected along the midline occupying the fourth ventricle, and about 40 % of all G4 tumors are metastatic^{76,85}.

Recent multi-omics studies have revealed that G3 and G4 MB tumours originate mostly from progenitors in the subventricular zone (SVZ) of the human rhombic lip, which is internalised in the nodulus region of the cerebellum. From the rhombic lip SVZ pool, cells in the undifferentiated state give rise to G3 tumors, and the more differentiated glutamatergic cerebellar nuclei and UBCs give rise to G4 tumors.

At the molecular level, Group 3 and Group 4 tumors are the least well understood. Although not well studied sparing certain MB cell line establishment, there are also few MB tumors that share characteristics with both groups, leaving them with an ambiguous subgroup identity^{72,73,99}. What is quite evident is that 1) MYC amplifications are largely confined to G3 tumors and 2) G3 tumors possess well-defined photoreceptor identity gene expression similar to the signature identified in the human fetal rhombic lip. On the other hand, G4 tumors is suggested to resemble a typical UBC gene signature. However, it is imperative to keep in mind that G3 and G4 tumors share a continual differentiation pat. The current model suggests that the rhombic lip SVZ progenitors are the central lineage of origin for G3 and G4 tumors and are defined by the extent of their differentiation along a proliferative glutamatergic trajectory towards the UBC lineage. There is also a frequent overlap in the genetic alterations found in Group 3 and Group 4, such as DDX31 deletions, OTX2 and GFI1/GFI1B amplifications, CHD7, KMT2D and KMT2C mutations^{71,93,100}.

Current standard of care for Group 3 is associated with considerable morbidity, and new strategies need to be developed. Chemotherapy drugs such as pemetrexed and gemcitabine are currently being tested in a clinical trial for Group 3 patients¹⁰¹. Treatments against TGF- β signaling, such as targeting MYC-driven transcriptional activity and cell growth could also be more effective possibility, since Group 3 tumors are mainly associated with TGF- β signaling^{68,102,103}.

For Group 4, there is no ongoing preclinical or clinical studies. Group 4 MBs appear to have an enrichment of genes involved in neural differentiation and neuronal development based on some studies, however the clinical significance and genetic basis of this has not yet been demonstrated to move forward with therapeutic possibilities^{65,104}. Owing to growing research in subtype distinction in G4 tumors, we can anticipate improvement in therapeutic strategies and survival rates in the future.

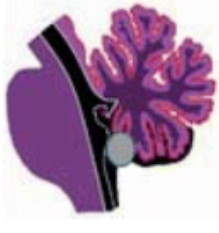
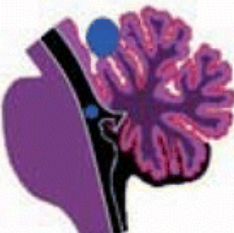
Subgroup	WNT	SHH	G3	G4
				
Frequency	10–15%	28–30%	25–28%	40–45%
Age range (years)	6–12 (peaks at 10–12), >17 (β subgroup)	Bimodal (<4, >16)	Infants and young children	All age groups (median 9)
Histology	Mostly classic, rarely LCA, never ND	Mostly ND, classic & LCA (less common)	Classic (most common), LCA	Classic and LCA (less common)
Cell of origin	Lower rhombic lip progenitor cells of the dorsal midbrain	Cerebellar GCP of the EGC	Cerebellar GCP of the EGC (prominin 1+/lineage–neural stem cells)	Unknown
Subgroups	α & β	α, β, γ & δ	α, β & γ	α, β & γ
Anatomic location	Central, frequently abutting brainstem and infiltrating foramen of Lushcka	Hemispheric (rarely midline)	Midline (filling fourth ventricle), hemispheric cases reported	Midline (filling fourth ventricle)
Metastatic disease at diagnosis	8.6% (α) 21.4% (β)	20% (α) 33% (β) 8.9% (γ) 9.4% (δ)	43.4% (α) 20% (β) 39.4% (γ)	40% (α) 40.7% (β) 38.7% (γ)
IHC	Nuclear β-catenin	Filamin A, YAP1, SFRP1, GAB1	NPR3 (suggested, needs validation)	KCNA1 (suggested, needs validation)
Chromosomal abnormalities	Monosomy of chromosome 6 (diploid in older patients)	9q deletion, loss of 10q and 17p, gains of 3q and 9p	i17q, 1q gain, loss of 5q and 10q	i17q, loss of 8, 10, 11 and gain of 4, 7, 17, and 18
Genetics	<i>CTNNB1</i> , <i>DDX3X</i> , <i>SMARCA4</i> , <i>TP53</i> and <i>KMT2D</i>	<i>PTCH1</i> , <i>TP53</i> (high prognostic impact), <i>KMT2D</i> , <i>DDX3X</i> , <i>MYCN</i> , <i>BCOR</i> , <i>LDB1</i> , <i>GLI</i>	<i>MYC</i> , <i>OTX2</i> , <i>SMARCA4</i> , <i>NOTCH</i> , <i>TGF-β</i>	<i>MYCN</i> , <i>CDKNA</i> , <i>SNCAIP</i> duplications
Epigenetics	SRFP family (inhibitors of WNT signaling pathway)	MLL2/KMT2D & MLL3/KMT2C (promote H3K4me2/3), <i>SMARCA4</i>	H3K27, H3K4, BRD/BRD	H3K27, H3K4, KDM family
Diagnosis	Exon 3 sequencing for <i>CTNNB1</i> or both nuclear β-catenin (IHC) and monosomy 6 (FISH)	Gene expression/methylation profiling and/or IHC for filamin A and YAP1 +/- GAB1	Genome wide methylation, expression array	Genome wide methylation, expression array
Prognosis (5-year survival)	97% (α) 100% (β)	69.8% (α) 67.3% (β) 88% (γ) 98.5% (δ)	66.2% (α) 55.8% (β) 41.8% (γ)	66.8% (α) 75.4% (β) 82.5% (γ)
Possible targeted therapies	Trichostatin A (HDAC inhibitor), other small molecules to inhibit WNT pathway in preclinical studies	Vismodegib, arsenic trioxide, bromodomain inhibitors, aurora kinase inhibitors	Bromodomain inhibitors, HDAC inhibitors, PI3K inhibitors	None
Genetic predisposition	APC (germline), most tumors lack <i>CTNNB1</i> mutation	<i>SUFU</i> , <i>PTCH1</i> , <i>TP53</i> , <i>PALB2</i> , and <i>BRCA2</i>	<i>PALB2</i> and <i>BRCA2</i> (rare)	<i>PALB2</i> and <i>BRCA2</i> (rare)
Other	Increased permeability of BBB, excellent outcome even with residual tumors			

Figure 1.2. Overview of MB subgroups. This table has details on patient demographics and molecular features of each subgroup and their subtypes.

LCA: Large cell/anaplastic; ND: Nodular Desmoplastic; GCP: Granule cell progenitor; EGC: External granule layer; BBB: Blood–brain barrier; G3: Group 3; G4: Group 4; HDAC: Histone deacetylases; IHC: Immunohistochemistry; FISH: Fluorescence In Situ Hybridization; SHH: Sonic Hedgehog; WNT: Wingless. Figure from (Doussouki ME and Chamdine O, 2019)¹⁰⁵.

1.2.2 Shh signaling-based MB mouse models

Numerous genetic mouse models that replicate each of the four MB subgroups have been developed^{106,107}. Understanding the molecular mechanisms underlying SHH-MB has been the focus of my thesis, and I have used two well established and widely accepted SHH-MB mouse models for this research.

***Ptch1* +/- mouse model:**

Ptch1 heterozygous mice is a model that recapitulates the histological features of human MB caused by the most frequent MB driver mutation (*PTCH1*). In this mouse model, part of *Ptch1* exon 1 (including the putative start codon) and all of exon 2 were replaced with *lacZ* and a neomycin resistance gene; the resultant protein made from any alternative start codon would lack the transmembrane domain, thus affecting its orientation on the membrane leading to pathway activation⁴². Two distinct groups developed genetically engineered *Ptch1*^{+/-} mouse models that could generate MB tumors with a low 14% incidence, and latency between 5-25 weeks^{42,108}. Further, our lab has demonstrated that these *Ptch1*^{+/-} tumors are representative of the Shh α subtype specifically⁵². Goodrich *et al* also observed that full activation of the Shh pathway, as in the case of homozygous germline deletion of *Ptch1* (*Ptch1*^{-/-}) led to embryonic lethality⁴². Strikingly, *Ptch1*^{+/-} mice crossed with a *p53*-null mice dramatically increased the MB incidence to 100% and reduced the latency to 12 weeks¹⁰⁹. Several researchers utilize the *Ptch1*^{+/-} mice as a pre-clinical model in combination with genetic alterations of candidate genes that may serve as potential drivers of Shh-MB.

In addition to homozygous deletion of *Ptch1* (*Ptch1*^{-/-}), GCP-specific hyperactivation of Shh signaling achieved with over-activating point mutation of Smo (W539L: SmoA1/M2 or S537N:

SmoA2) or *Gli* overexpression can also result in Shh-MB tumors with a high penetrance. This is because GCPs, which is the cell of origin of Shh-MB retain their tumorigenic potential until P10.

Overactivated Smo mouse model

Since the *Ptch1*^{+/-} transgenic line displayed low tumor incidence, another mouse model capable of resulting in higher tumor incidence was developed. Widespread upregulation of Shh signaling ensuing from the embryonic stage achieved by homozygous mutations in components of the Shh pathway mainly caused embryonic or early postnatal death. So, an essential and cell-autonomous positive effector of the Shh pathway, *Smo* was chosen for this improved Shh-MB model. *ND2-SmoA* hemizygous mouse model was created by Hallahan *et al* in which a constitutively active Smo was exclusively produced in GCPs under the control of the *NeuroD2* promoter⁴³. Following this, the same group developed a homozygous *ND2-SmoA* mouse model (*Smo/Smo*)⁹⁸. The MB incidence went from 48% in hemizygous model to 94% in the homozygous model.

Furthermore, mutant forms of SMO were previously identified in human BCC and MB^{110,111}. Consequently, point mutations such as W539L (designated as SmoA1/M2) or S537N (designated as SmoA2) in a conditionally activated allele of Smo was targeted into the ubiquitously expressed *Rosa26*¹¹⁰⁻¹¹³. When crossed with a *Math1-Cre* driver mice, the SmoM2 mutant results in the ligand-independent constitutive activation of the Shh signaling specifically in GCPs until P7-P10^{9,12}. *Math1-Cre*⁺; *Smo*^{+/M2} mice is an aggressive MB mouse model that developed diffuse MB with 100% penetrance and had an average survival of about 35 days⁴⁵.

1.2.3. Events in Shh-MB progression using *Ptch1*^{+/-} mouse model

The first indication that hyperactive SHH signaling due to mutations in components of the SHH pathway are responsible for MB tumorigenesis was from the finding that Gorlin syndrome patients, who inherit germ line mutations in the *PTCH1* gene, are predisposed to SHH-MB, basal cell carcinoma and rarely, rhabdomyosarcomas¹¹⁴⁻¹¹⁷. The most commonly occurring mutations in human SHH-MBs are mutations in *PTCH1*, *SUFU* and *SMO*, or amplifications in *GLI* family of transcription factor (*GLI1*, *GLI2*) and *N-MYC*⁸⁵. As a result, clinically relevant mouse models such as those with *Ptch1* heterozygosity and activating mutations in *Smo* have been developed to study Shh-MB, as described in the previous section⁴². The "one-hit model" of activated *Smo* (*SmoM2*) is sufficient for constant activation of the Shh pathway to lead to MB tumor formation with 100% incidence and very short latency, thus making it a very aggressive MB model¹¹³. Mice with *Ptch1* heterozygosity, on the other hand, develop MB tumors with lower penetrance and longer latency⁴².

In the past, researchers claimed *Ptch1* heterozygosity to be the initiating event which led to the formation of precancerous lesions (also called preneoplastic lesions) which are discrete cancerous foci preceding advanced tumor development on the cerebellar surface between P14-P40 in *Ptch1*^{+/-} mouse model^{118,119}. This was thought to be followed by a second step of *Ptch1* LOH for advanced tumor formation¹¹⁸.

Two important observations from previous studies facilitated further understanding of tumor progression: (1) the incidence of preneoplastic lesions in this model is much higher than that of advanced tumor^{46,57}, and (2) all advanced MB exhibit *Ptch1* LOH¹¹⁸. This raises the possibility of a tumor suppressive mechanism after acquisition of *Ptch1* LOH to prevent advanced

tumor progression and work from our lab identified oncogene-induced senescence as this rate limiting rate-limiting step in the progression of MB.

Altogether, the current paradigm is a three-step process of tumorigenesis in this mouse model (**Figure 1.2.3**). First is the presence of *Ptch1* heterozygosity. Second, acquisition of *Ptch1* LOH which leads to the formation of preneoplastic lesions, and induction of oncogene-induced senescence, a mechanism of tumor suppression, the reason attributed to why certain tumors do not advance to MB. Third, progression from a preneoplastic lesion to an advanced MB tumor requires evasion of senescence. Tamayo-Orrego *et al* identified cellular senescence occurred due to mutations in p53 and/or p16ink4a (a cyclin-dependent kinase inhibitor) inactivation through increased promoter methylation¹²⁰.

Additional data from our lab delineates the mechanism of MB initiation, that is, the acquisition of *Ptch1* mutation such as *Ptch1* LOH is the result of genomic instability through replication stress induced by the mitogen Shh⁵².

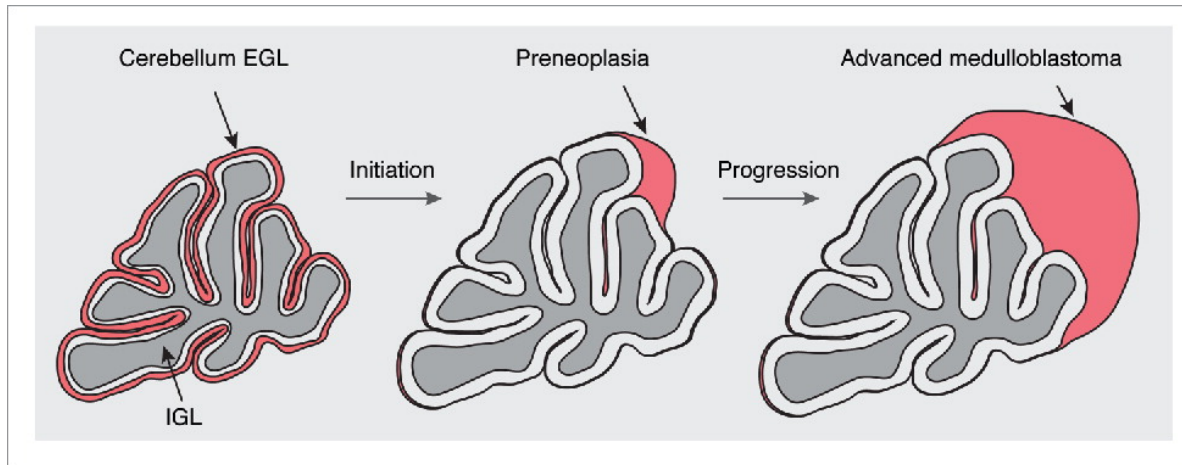


Figure 1.2.3. Multistep paradigm of *Ptch1*^{+/-} MB. In addition to functioning as a mitogen, Shh induces replication stress and a subsequent increase in recombination events in the cell of origin of MB (GCPs) such as *Ptch1* LOH, which is indispensable for preneoplastic formation. Additional genetic co-drivers are necessary for the transition to an advanced tumour from the preneoplastic stage to overcome tumor suppressive mechanisms such as senescence. Figure from (Tamayo-Orrigo et al., 2016)¹²¹.

1.2.4. Candidate collaborators of *Ptch1* LOH in Shh-MB

To understand the molecular mechanism of tumor formation and progression from a pre-cancerous lesion to an advanced MB tumor, we performed deep sequencing of RNA and identified potential somatic mutations in *Ptch1*^{+/-} MB that aid in tumor progression. Our lab has shown that cellular senescence is a tumor suppressive mechanism following *Ptch1* loss of heterozygosity in preneoplastic MB lesions, whereby the cells select for *p53* mutations or *p16ink4a* inactivation, which will lead to evasion of senescence and thus progression to advanced MB tumors¹²⁰. In addition, deep sequencing of RNA from *Ptch1*^{+/-} MB tumors revealed mutations in certain genes known to be implicated in various pathways ranging from mitochondrial metabolism, proteasomal regulation, RNA regulation and cell proliferation. Of interest, mutations in two genes, *SMG1* and *SMG5* were identified. SMG1 and SMG5 are important components of a mRNA surveillance mechanism called nonsense-mediated mRNA decay (NMD).

1.3. Nonsense-mediated mRNA decay (NMD) pathway

1.3.1. Classic NMD/ EJC-dependent NMD

DNA is transcribed to pre-mRNA, which undergoes processing steps such as 5' capping, 3' poly-adenylation and splicing, to form a processed mRNA. Eukaryotic cells are subject to a variety of environmental stress, genetic insults, and errors in pre-mRNA splicing, and these can alter the protein-coding potential of the DNA/mRNA, thus affecting both the quality and quantity of mRNA being produced. To maintain the integrity of gene expression, cells employ surveillance mechanisms that scans mRNAs for any errors that may eventually lead to the excessive production of deleterious proteins¹²²⁻¹²⁴. NMD is a translation-dependent mechanism involving degradation of faulty transcripts through a highly orchestrated sequence of protein-protein interactions

involving core NMD factors such as UPF1, UPF2, UPF3B, SMG1, SMG5, SMG6 and SMG7¹²⁵. Intron splicing results in the deposition of tetrameric complexes known as Exon junction complexes (EJC) approximately 20–24 nucleotides upstream of exon–exon junctions. EJC recruits UPF3B, followed by association with UPF2. During translation, the ribosome along with the release factors, eRF1 and eRF3 scans along the mRNA and displaces every EJC until it reaches the canonical termination codon, where translation terminates. This is the case for a normal transcript with no premature termination codon (PTC). However, when an mRNA has NMD sensitive features in the canonical ORF such as the presence of a PTC located >55 nucleotides (nt) upstream of an exon-exon junction, then the ribosome halts followed by EJC retention resulting in translation termination¹²⁶. This triggers the most well studied branch of NMD called the 3' UTR EJC-dependent NMD, with the RNA helicase UPF1 being the central effector in the pathway¹²⁴ (**Figure 1.3.1**). A close encounter with the PTC during the pioneer round of translation causes the interaction of UPF1 with the cap binding protein on the 5' cap to facilitate association of UPF1 with the kinase SMG1 and to release factors bound to the ribosome to form the SURF complex (SMG1-UPF1-eRF1-eRF3). The SURF complex interacts with the UPF2/UPF3B bound EJC, resulting in the formation of a decay inducing complex (DECID)¹²⁷⁻¹²⁹. Transition to the DECID complex initiates the remodelling and translocation of NMD complexes from 5' end of the EJC toward its 3' end, which has three consequences on the pathway. First, the ribosome along with the release factors are dissociated and this is thought to link the surveillance machinery to translation termination. Second, it triggers the phosphorylation of UPF1 by SMG1 kinase, which is the most critical step of NMD pathway¹²⁷. Third, UPF1 undergoes conformational changes due to its interaction with UPF2 to adopt an active helicase form. UPF1 unwinds the RNA and removes the

proteins bound to the mRNA when its helicase activity is initiated, allowing recruitment of nucleases to the mRNA to initiate the final degradation phase in the pathway.

Degradation of the faulty mRNA can occur either via the exonucleolytic or endonucleolytic RNA degradation pathways. Phospho-binding proteins SMG5 and SMG7 are recruited to phosphorylated UPF1 (p-UPF1) by forming a stable heterodimer to promote mRNA deadenylation, decapping and 5'–3' or 3'–5' exonucleolytic degradation¹³⁰⁻¹³². Alternatively, SMG6 is an endonuclease that can be recruited to cleave the mRNA in the vicinity of the PTC into free 5' and 3' fragment ends for exoribonucleases to further degrade them¹³³⁻¹³⁵. In addition, SMG5, SMG6, SMG7 along with protein phosphatase 2A (PP2A) also mediate dephosphorylation of UPF1¹³⁶⁻¹³⁸. Overall, UPF1 undergoing cycles of phosphorylation and dephosphorylation by complexing with various NMD effectors is essential for NMD-mediated degradation of the mRNA target.

1.3.2. EJC-independent NMD

In mammalian cells, there are at least two different branches of NMD, and NMD target discrimination dictates the choice of the NMD mechanism. Studies using knockdown of EJC components, and experiments using artificial tethering of UPF1 to 3' UTRs, revealed evidence for cellular transcripts undergoing EJC-independent NMD (**Figure 1.3.1**)^{139,140}.

In a normal scenario, to ensure prompt and effective termination of translation, the cytoplasmic polyadenylate-binding protein 1 (PABPC1) binds to the polyA tail and causes eRF1 and eRF3 to be recruited to the terminating ribosome¹⁴¹. However, if UPF1, which is known to compete with PABPC1 located on the polyA tail, recruits the translation termination complex, the mRNA undergoes NMD^{142,143}. The distance between the PTC and the PABPC1 protein on the polyA tail

affects NMD activation^{144,145}. The probability of inducing NMD increases as this distance increases. Hence, physiological nonmutated transcripts with length of the 3'UTR greater than 1000 nt are susceptible to EJC-independent NMD¹⁴⁶. In addition, since UPF1 binding is promiscuous and is found on most cellular mRNAs¹⁴⁷, the likelihood of UPF1 occupancy is enhanced in case of a long 3'UTR, subsequently amplifying the possibility that the bound UPF1 will be phosphorylated and activate NMD. This hypothesis was supported by transcriptome-wide analysis in human cells with the finding that p-UPF1 was enriched on the 3' UTRs of EJC-independent NMD targets, as in the case of EJC-dependent NMD targets^{147,148}.

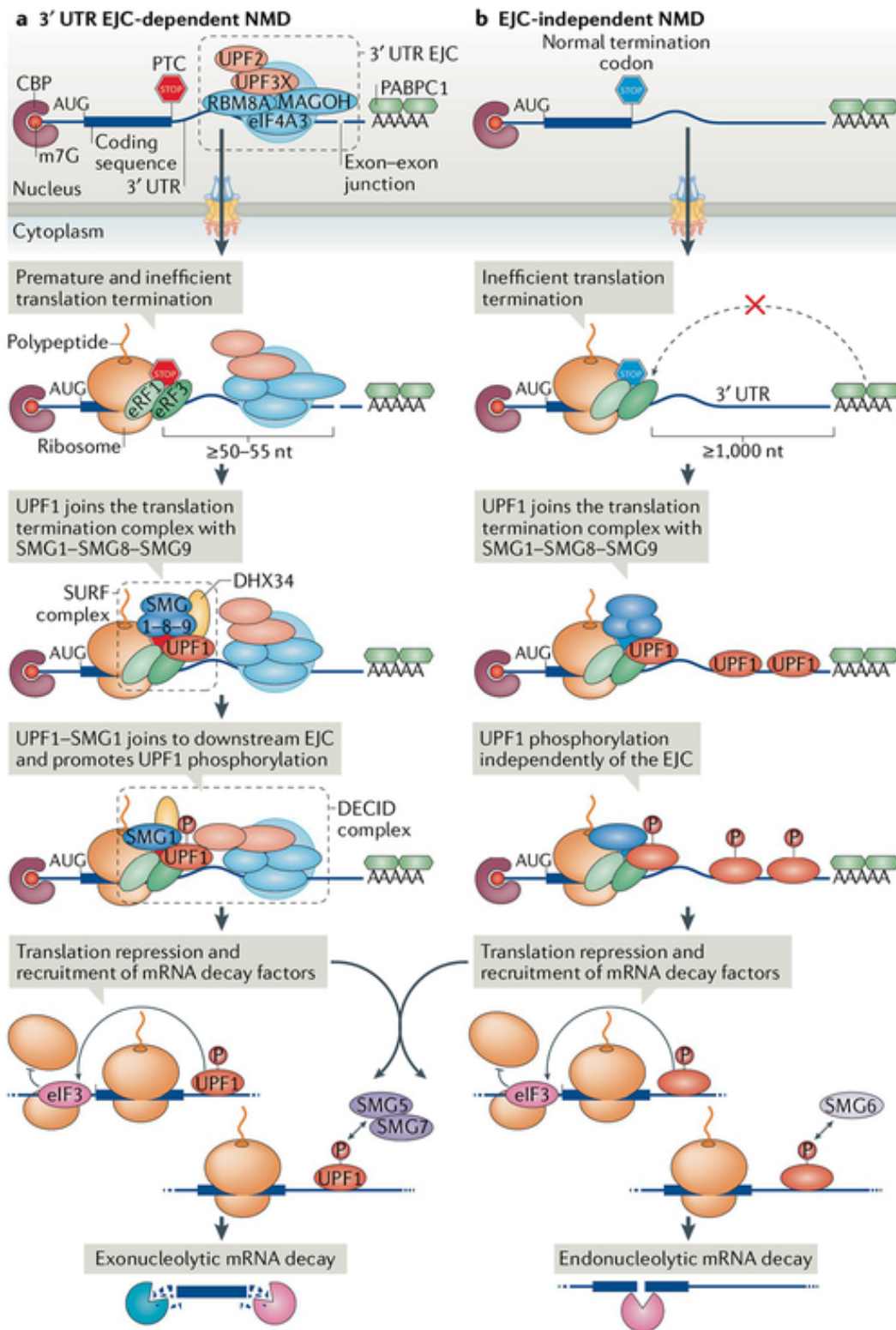


Figure 1.3.1. EJC-dependent and EJC-independent NMD pathway.

During normal termination, EJCs (that were deposited at every exon-exon junction post splicing) and any promiscuously bound UPF1 are typically cleared from the 5'UTR and CDS by translating ribosome. UPF1 cannot associate with the termination complex also because of PABPC1's interactions with eRF1-eRF3 or translation initiation factor eIF4G.

(a) **EJC-dependent NMD:** Unlike most termination codons that are located in the final exon and thus downstream of exon-exon junctions, if a PTC is located $\geq 50-55$ nt upstream of an exon-exon junction, it results in retention of EJC downstream and premature and inefficient translation termination. PABPC1 and eRF3 cannot interact properly because of the retained EJC. The NMD factors UPF1 and the SMG1 complex (SMG1, SMG8 and SMG9) associate with the eRF1-eRF3 translation termination complex to form the SURF complex. Interaction of SURF complex with EJC-UPF2-UPF3 results in DECID formation, which triggers SMG1-mediated phosphorylation of UPF1. This facilitates recruitment of mRNA decay factors SMG5/7 and/or SMG6 to degrade the PTC-containing mRNA by exonucleolytic and/or endonucleolytic cleavage.

(b) **EJC-independent NMD:** Physiological mRNAs that have unusually long 3'UTRs (>1000 nt) are also subject to NMD. With increased distance between PABPC1 and the PTC, translation termination is inefficient as PABPC1 cannot effectively recruit eRF1-eRF3 termination complex, resulting in retention of the many promiscuously bound UPF1 proteins on the 3'UTRs. This increases the likelihood of UPF1 phosphorylation, and thus NMD initiation. SURF complex is formed, and UPF1 phosphorylation occurs independent of EJC, subsequently followed by mRNA decay.

Coding sequence (CDS); Exon junction complex (EJC); Polyadenylate-binding protein 1 (PABPC1); eukaryotic release factor 3 (eRF3); Premature termination codon (PTC); release factors (eRF1-eRF3); SMG1-UPF1-eRF1-eRF3 (SURF); Decay inducing complex (DECID).

Figure from (Kurosaki T *et al*, 2019)¹²³

1.3.3. Key NMD effectors (UPF proteins, SMG proteins, EJC components)

Up-frameshift proteins (UPF)

The three UPF proteins, UPF1, UPF2 and UPF3B (also called SMG2, SMG3 and SMG4, respectively) that form the core machinery of the NMD pathway were discovered in genetic screens in *S. cerevisiae* and *C. elegans*^{138,149}, orthologs of which were described in humans, mice, and flies^{150,151}. The interaction of these proteins is critical for the recognition of the PTC-containing transcript, and the recruitment of NMD-related mRNA degradation factors. UPF1 is an ATP-dependent RNA helicase that contains 1) an N-terminal cysteine- and histidine-rich (CH) domain which is preceded by an unstructured proline-glycine rich region, 2) an RNA helicase domain (HD) in the middle, and 3) a C-terminal serine- and glutamine-rich (SQ) domain^{147,152} (**Figure 1.3.3a**). There are multiple experimentally validated phosphorylation sites targeted by SMG1 kinase in the amino-terminal unstructured region (T28 for SMG6) and the carboxy-terminal SQ domain of UPF1 (S1073, S1078, S1096 and S1116 for SMG5/7)¹⁵³. The distinct residue that undergoes phosphorylation determines which NMD factor (SMG6 or SMG5/7) will be recruited to induce decay downstream¹⁵⁴.

Inactive UPF1 has its CH domain tightly folded into its HD, forming a closed structure allowing it to clamp RNA but prevent the ATPase and RNA helicase activities¹⁵⁵⁻¹⁵⁷. Trans-binding of UPF2 to the regulatory CH domain of UPF1 during NMD results in a substantial conformational change giving it an open configuration which triggers UPF1 helicase activity^{155,158}, allowing protein clearance from the RNA to initiate the decay phase.

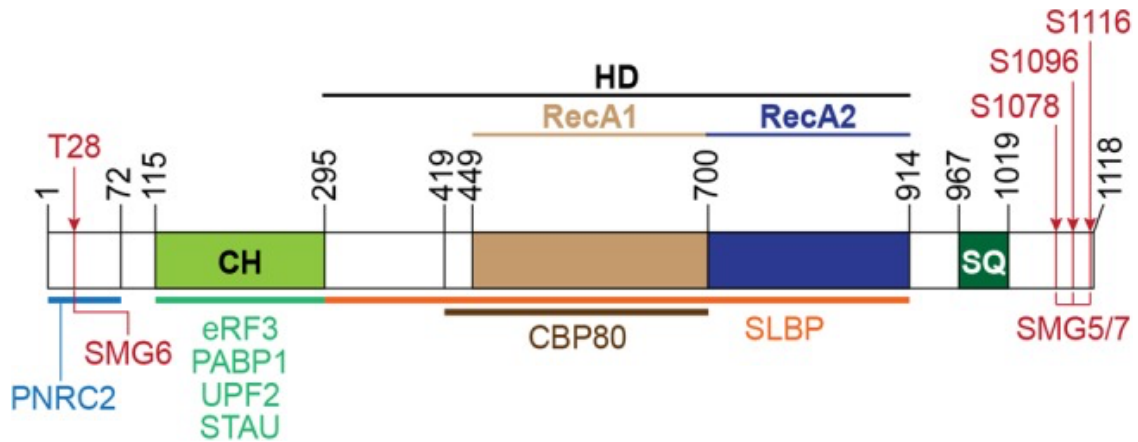


Figure 1.3.3a. Structure of UPF1 protein. UPF1 consists of: (1) N-terminal unstructured region, (2) a cysteine- and histidine-rich (CH) domain, (3) a central helicase domain which consists of two ATP-binding RecA-like domains (HD), (4) C-terminal serine- and glutamine-rich (SQ) domain. Phosphorylation sites exist in many [S/T] Q motifs in the amino-terminal unstructured region and the carboxy-terminal SQ domain of UPF1. Red depicts experimentally validated phosphorylation sites; Number depicts amino acid positions. Figure from (Kim YK *et al*, 2019)¹⁵⁹

The activity of UPF1 is stimulated during NMD by UPF2 and UPF3B, which are nonenzymatic components of the surveillance complex¹⁵⁵. Mendell *et al* observed perinuclear localization of UPF2, followed by recruitment to the mRNAs in the nucleus due to splicing¹⁶⁰. UPF2 acts as a molecular linker that can have interactions with several NMD factors. UPF2 can associate with UPF3B which is bound to the EJC, the release factor eRF3 recruited to the ribosome, and be involved in SMG1-UPF1 interaction¹⁶¹.

In vertebrates, the least conserved UPF protein is UPF3¹⁶², and two alternatively spliced isoforms of UPF3 exist; UPF3A and UPF3B^{150,163}. NMD is inhibited by UPF3A, while NMD is activated by its paralog, UPF3B¹⁶⁴. Functioning as an adaptor protein that allows interactions between UPF2 and EJC, UPF3B promotes UPF1 activation and premature translation termination. In mammals, compared to UPF3A, UPF3B has stronger binding affinity to the EJC hence acting as the dominant paralog carrying out UPF3-mediated functions in NMD. This was specifically due to the role of UPF3B in the recruitment of eRF3 to position it at the A site of the ribosome, followed by SMG1-mediated UPF1 phosphorylation¹⁶⁵. Since both proteins competitively bind to UPF2, these two proteins function differentially in NMD to modulate the level of gene expression during key processes such as neurogenesis, embryogenesis, apoptosis, and stress response^{123,164,166}. UPF3A could inhibit NMD by sequestering UPF2 from an NMD substrate RNA.

Suppressor with Morphological effects on Genitalia (SMG) proteins

SMG1 is a serine/threonine protein kinase and is one among the 6 members of the Phosphatidylinositol 3-kinase-related kinase (PIKK) family (ATM, ATR, DNA-PKcs, mTOR, TRRAP, and SMG1), all of which contain a HEAT domain followed by a C-terminal PI3K catalytic domain. The most studied function of SMG1 is its involvement as a critical component of the

NMD machinery, being the kinase that drives phosphorylation of the ATP-dependent RNA helicase UPF1, which is the rate-limiting step for NMD^{153,167}. Two other NMD factors, SMG8 and SMG9 form a stable heterodimer to complex tightly with SMG1, to regulate its kinase activity¹⁶⁸⁻¹⁷⁰ (**Figure 1.3.3b**). SMG9 binds to SMG1 directly and is necessary for the association of SMG1 with SMG8¹⁷⁰. In isolation, SMG8, which contains a C-terminal kinase inhibitory domain (KID), suppresses the kinase activity of SMG1 by steric hinderance of the catalytic kinase domain of SMG1¹⁷¹. Formation of the DECID complex during NMD triggers restoration of the kinase activity of SMG1 by providing accessibility to its catalytic domain. This is facilitated by a significant conformational change of SMG8-SMG9 heterodimer. Although the mechanism of activating SMG1 is yet to be explored, structural studies predict that GTP hydrolysis of SMG9 can drive the KID to shift out of the inhibitory position^{171,172}.

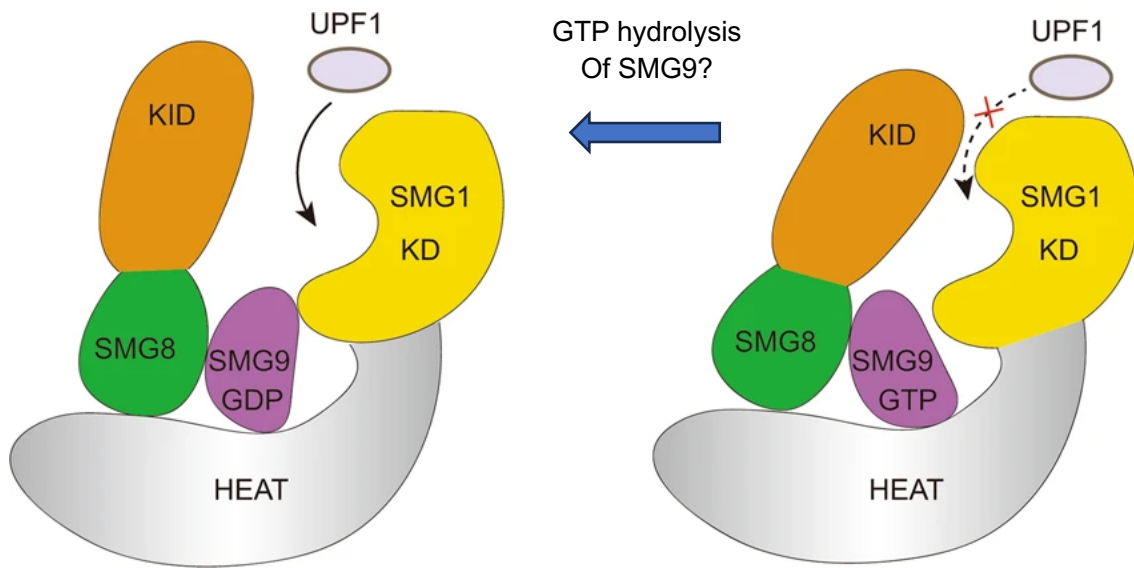


Figure 1.3.3b. Regulation of SMG1 kinase by SMG8-SMG9 heterodimer.

Right schematic: SMG1 has a kinase domain, and SMG8 has a kinase inhibitory domain. These two domains create a physical steric hindrance that prevents UPF1 to be accessed by SMG1. GTP-bound SMG9 facilitates this closed inactive conformation.

Left schematic: A conformation switch, possibly through GTP hydrolysis of SMG9 facilitates the catalytic pocket of SMG1 to be exposed for UPF1 binding, and subsequent phosphorylation.

Kinase domain (KD); Kinase inhibitory domain (KID). Figure adapted from (Zhu L *et al*, 2019)¹⁷¹

In vitro mutational analyses revealed that SMG1 can phosphorylate multiple serine/threonine residues such as LS1073QP, LS1078QD, LS1096QD and LS1116QY in the C-terminal SQ-rich region of UPF1^{154,173}. Among these, S1078 and S1096 are also verified as substrates for phosphorylation by SMG1 *in vivo*¹⁵³. SMG1-mediated phosphorylation of UPF1 on the faulty mRNA represents strong commitment to NMD since it precludes additional rounds of translation initiation. In addition, activated UPF1 creates an excellent platform for recruitment of crucial RNA degradation enzymes such as SMG6, SMG5/7 (described in section 1.6.4).

In addition to these, Yamashita *et al* showed that SMG1 can phosphorylate the oncogene p53 at the serine 15 position in its SQ motif, a known substrate of other PIKKs, as predicted from the sequence conservation of the PIKK domain¹⁵³. Trigger for p53-S15 specific phosphorylation was found to be exposure to UV/IR-induced genotoxic stress, but the mechanism of SMG1 activation in this context is unknown. In addition to its important role in NMD, SMG1 has been found to participate in other distinct processes which include cell cycle regulation through p53-dependent DNA damage response, maintaining telomere integrity and embryogenesis¹⁷⁴⁻¹⁷⁷.

Exon Junction complex (EJC) components

The EJC is a protein complex that assembles downstream of exon-exon junctions during the process of splicing. It consists of four RNA-binding proteins, including eIF4A3, Y14/MAGOH, and Barentsz (also known as MLN51 or CASC3) associating with the mRNA and ATP¹⁷⁸. The EJC marks the position of exon-exon junctions on the mRNA molecule. Being an ATP-dependent RNA helicase, eIF4A3 binds and unwinds mRNA to allow recruitment of the other EJC factors Y14/MAGOH and MLN51¹⁷⁹. A heterodimer is formed by the association of Y14 and MAGOH to inhibit the eIF4A3 ATPase activity, thus ensuring stable high affinity binding of

eIF4A3 with the RNA. In this conformation, eIF4A3 readily binds to MLN51 and stably loads other NMD-related proteins onto the mRNA. NMD factor UPF3B interacts with EJC-associated proteins, forming a complex that bridges the connection between the EJC and the ribosome stalled at the PTC. When a ribosome encounters a PTC within an mRNA, the presence of a stable tetrameric EJC downstream of an exon-exon junction is critical for recognition of the PTC. This renders the EJC to act as a signal that helps recruit the essential NMD machinery to the mRNA.

1.3.4. Degradation mechanisms of NMD target

Two crucial commitment steps occurring before the NMD-targeted mRNA is sent to the degradation phase is SMG1-mediated phosphorylation of UPF1 and translational repression^{147,180}. Continuous repression of translation initiation is achieved through the direct interaction of p-UPF1 with the translation initiation factor eIF3, thus inhibiting the conversion of 40S-bound mRNA to translationally active 80S-bound mRNA¹⁸⁰. The degradation phase begins with the binding of NMD effectors SMG5, SMG6 and SMG7 to p-UPF1, which triggers recruitment of endoribonucleolytic and exoribonucleolytic mechanisms^{154,181} (**Figure 1.3.4**).

Phosphorylation of UPF1 by SMG1 at position T28 in its amino-terminal unstructured region results in the direct recruitment of the endoribonuclease SMG6^{134,153}. In very close proximity to the termination codon, SMG6 cleaves the target mRNA to yield free 5'-cleavage fragments and 3'-cleavage fragments¹³⁴. The unprotected 5'-cleavage fragment is potentially degraded from the 3'-5' direction mediated by either the RNA exosome or the exosome-free nuclease DIS3L2¹⁸²⁻¹⁸⁴. The 3'-cleavage product that is still associated with UPF1 and NMD-related proteins are made accessible to 5'-to-3' exoribonuclease XRN1 for degradation after clearing of the RNA fragment from proteins by activated UPF1 helicase¹⁵².

On the other hand, if phosphorylation of UPF1 by SMG1 occurs at positions S1073, S1078, S1096 or S1116 in the carboxy-terminal SQ domain of UPF1, it results in the direct recruitment of the SMG5-SMG7 heterodimer, which facilitates deadenylation/decapping and degradation^{153,185}. SMG7 recruits the deadenylation machinery by direct interaction with the POP2 catalytic subunit of the CCR4–NOT deadenylase complex, which eliminates the polyA tail^{132,186,187}. Deadenylated mRNA undergoes exosome-mediated 3'-to-5' degradation¹⁸⁶. On the other hand, decapped mRNA is subjected to 5'-to-3' exoribonucleolytic cleavage^{186,188}. The decapping enhancer PNRC2 can elicit decapping by associating with SMG5 and other components of the decapping complex such as DCP1A and DCP2^{185,189}. Additionally, the deadenylase complex can also contribute to the recruitment of DCP2 to the mRNA⁸⁸.

Irrespective of the pathway utilized for the degradation of the target mRNA, it is followed by dephosphorylation of UPF1 facilitated by protein phosphatase 2A (PP2A), and SMG5-SMG7^{136,137,147,181}.

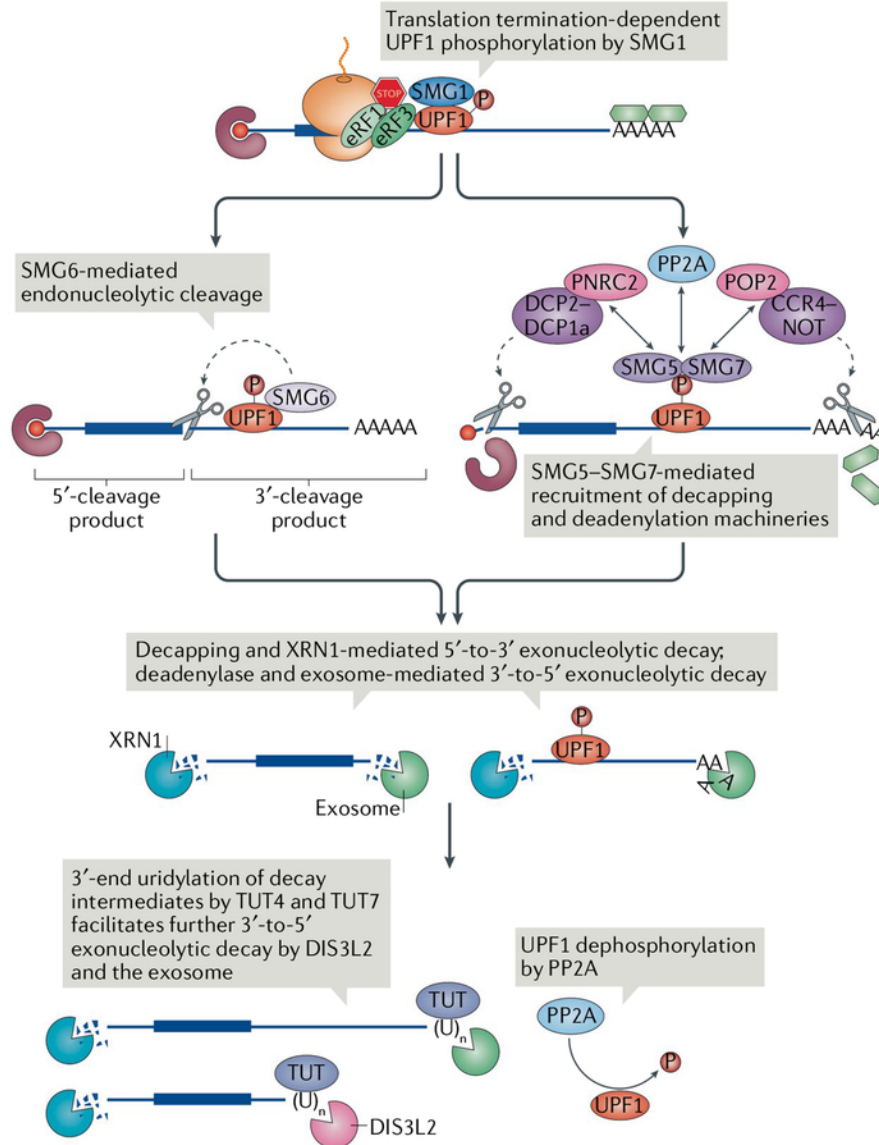


Figure 1.3.4. SMG6, SMG5/7 mediated mRNA degradation mechanisms. NMD initiation results in the formation of SURF complex, followed by DECID complex and UPF1 phosphorylation. SMG5, SMG6 and SMG7 are phospho-binding proteins that bind to p-UPF1 at specific sites. SMG6 being an endonuclease, it cleaves the mRNA in the vicinity of the PTC. Whereas decapping (DCPC-DCP1a and PNRC2) and deadenylation (CCR4-NOT) machineries are first recruited by SMG5/SMG7. Both pathways generate decay intermediates, including uridylated decay intermediates. These are preferably degraded 3'-to-5' by the exosome or the exosome-free 3'-to-5' exonuclease DIS3-like exonuclease 2 (DIS3L2). Non-uridylated decay intermediates undergo 5'-to-3' degradation by exonuclease XRN1. Figure from (Kurosaki T *et al*, 2019)¹²³

1.4. Regulators of NMD

In addition to serving as a quality control mechanism, NMD also functions as a master regulator of normal gene expression. This necessitates robust and controlled regulation of the process of NMD itself to ensure cellular protection from environmental and genetic insults. Potential mechanisms that cells employ for NMD regulation include altering the abundance of individual NMD factor availability, coordinated feedback loops with NMD autoregulating NMD factors, modulating NMD activity through phosphorylation of NMD factors, microRNAs and even alternative splicing.

1.4.1. Autoregulation of NMD

Depletion of NMD factors such as UPF1 and UPF3B resulted in upregulation of another NMD factor SMG5, suggesting an NMD feedback regulatory response^{160,190}. Other lines of evidence for NMD factors acting as NMD substrates themselves comes from Huang *et al* and Yepiskoposyan *et al*, in which transcriptomic analysis of HeLa cells depleted for UPF1, SMG6 or SMG7 revealed upregulation of mRNAs encoding seven NMD factors UPF1, UPF2, UPF3B, SMG1, SMG5, SMG6 and SMG7^{191,192}. Out of these, mRNAs encoding UPF1, UPF2, SMG1, SMG5, SMG6, and SMG7 had 3'UTR lengths >1200 nt^{191,192}. In addition, UPF2, SMG1, SMG5 and SMG7 also had an uORF in their 5'UTR^{191,192}. UPF1 RNA immunoprecipitation experiments¹⁹²⁻¹⁹⁴, RNA half-life studies^{191,192} and NMD reporter assays using the NMD-eliciting 5' and 3' UTR constructs^{146,192}, altogether proved that NMD factors are direct NMD targets, and are subject to autoregulation.

In cases where UPF3B is downregulated or eliminated, UPF3A is dramatically upregulated. Under normal conditions, UPF3A which is an NMD repressor, is typically unstable and has lower affinity than its paralog UPF3B to bind to EJC and UPF2. Consequently, depleting cells of UPF3B provides UPF3A the chance to steadily bind to UPF2 and EJC, and this binding makes UPF3A protein stable. This is a well-defined example of NMD regulation based on the abundance of individual NMD factors¹⁶⁶.

Here are some known examples of how post translational modifications including phosphorylation of NMD factors are used to control their activity and hence regulate NMD. The most well studied modification is the phosphorylation of the central NMD effector UPF1 by SMG1 kinase, which leads to a series of tightly regulated interactions with a downstream EJC, ultimately causing a rapid decay of the NMD targets¹⁹⁵. EJC factors such as Y14, RNPS1 and EIF4A3 are known to undergo post translational phosphorylation, and this was reported to interfere with their assembly onto EJC and interaction with NMD factors¹⁹⁶⁻¹⁹⁸.

1.4.2. microRNA-mediated regulation of NMD

Modulation of NMD efficiency through microRNA (miR) expression is a direct regulatory mechanism for buffering NMD in physiological contexts. Translational repression and/or rapid mRNA decay of certain mRNAs occur when they undergo targeted binding of certain small (22-nt) non-coding RNAs called microRNAs¹⁹⁹. MicroRNAs do not encode for proteins themselves but are involved in controlling post-transcriptional gene expression regulation.

During brain development, a brain specific microRNA, miR-128 is transcriptionally upregulated at the onset of neural differentiation²⁰⁰. In mouse and human cells, two key NMD effectors, UPF1 and MLN51 are targets of miR128-repression, resulting in the potent downregulation of NMD

activity²⁰⁰. Consequently, neural stem and progenitor cells are forced to exit their stemness phase and enter the differentiation phase by repressing TGF β signalling through stabilization of mRNAs promoting neural differentiation such as negative regulators of TGF β signalling (Smad7)²⁰¹. Lou *et al* also showed that another NMD activator UPF3B is repressed by miR128, and two other miRNAs (miR-124 and miR-9)²⁰¹. Other groups have shown that the miR-NMD circuit have roles beyond the brain, such as in T-cell development^{200,202}. These findings shed light on the influence of temporal and spatial miRNA expression on the regulation of NMD activity.

1.4.3. PABP as a human NMD antagonizing factor

The recruitment of UPF1 to the terminating ribosome can be stimulated or inhibited by specific 3' UTR-associated factors including poly(A)-binding protein (PABP). PABP is an RNA-binding protein that is deposited on the poly(A) tail of mRNA, which can stimulate normal translation termination and inhibit nonsense-mediated mRNA decay. The outcome exerted by PABP on translation termination depends on its location relative to the termination codon. In an mRNA undergoing normal eukaryotic translation termination, the canonical stop codon is positioned in its last exon followed by a relatively short 3' UTR. Normal termination is ensured by the interaction of PABPC1 with the ribosome-bound eRF3 as it promotes the release of the nascent polypeptide^{203,204}. Proper ribosome recycling is facilitated by a closed loop formation of the mRNA via the interaction of PABPC1 with another important translation initiation factor eIF4G^{205,206}. *In vitro* and *in vivo* studies provide evidence that PABPC1 competes with the NMD core factor UPF1 for eRF3 binding, to ensure normal termination and repression of NMD^{143,146,207}. In case of mRNAs containing long 3'UTRs, the distance between the terminating ribosome and the PABPC1 bound to the poly(A) tail is increased, and this has three consequences; (1) it leads to a failure in

the PABC1-eRF3 interaction, (2) it stimulates UPF1-eRF3 interaction to trigger NMD and (3) it impedes efficient ribosome recycling by eIF4G^{146,208} (**Figure 1.4.3**). Fatscher *et al* provided supporting evidence using NMD factor knockdown studies (SMG6, UPF1 and UPF2) by showing PABPC1 suppresses NMD and stabilizes target substrates²⁰⁸. In addition to humans, PABP antagonizing NMD is displayed in other organisms such as *S. cerevisiae* and *D. melanogaster*^{143,146,207,209,210}.

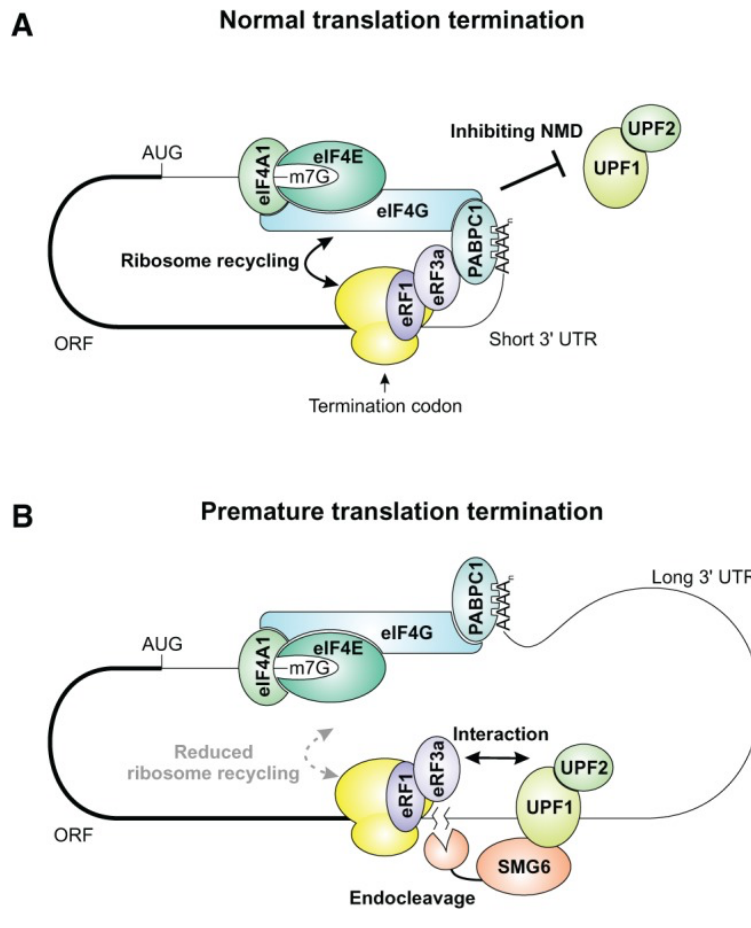


Figure 1.4.3. Interaction of cytoplasmic PABP with eIF4G suppresses NMD. (A) In case of a normal mRNA with a short 3'UTR, efficient translation termination and ribosome recycling is made possible through the interaction of PABPC1 with both eRF3a and eIF4G. This ensures UPF1 cannot access the eRF1-eRF3a translation termination complex thus preventing NMD from occurring. (B) With increased distance between PABPC1 and the PTC in case of a mRNA with long 3'UTR, translation termination is inefficient as PABPC1 cannot effectively recruit eRF1-eRF3a termination complex. The consequence of it is also prevention of ribosome recycling by eIF4G. Instead of PABPC1, UPF1 can potentially bind to the termination complex to elicit NMD. Figure from (Fatscher *et al*, 2014)²⁰⁸.

1.5. NMD as a critical regulator of the transcriptome

NMD was originally thought to function only as a mRNA quality control mechanism that rapidly degrades and eliminates transcripts harbouring PTCs arising due to errors in genomic mutations, errors in transcription, incorrect RNA processing or splicing^{122,123,211-213}. In addition to this canonical role, NMD has also been implicated in regulating ~15-20% physiological gene expression based on the nature of the mRNAs in context, thus shaping the transcriptome globally^{214,215}. Specific features in physiological mRNAs can act as a signal to promote PTC recognition and activate NMD, such as the presence of an upstream open reading frame (uORF) with a termination codon that resides ≥ 50 –55 nucleotides upstream of an exon–exon junction, one or more intron/s in the 3' untranslated region (3' UTR) and/or 3'UTRs of length >1000 nucleotides (nt), thereby unraveling novel substrates of the NMD pathway^{146,216,217} (**Figure 1.5**). Being a post-transcriptional mechanism, NMD functions as a master regulator of many cellular processes, particularly those involved in cell growth and differentiation, response to stress and development^{123,160,200,201,218-224}.

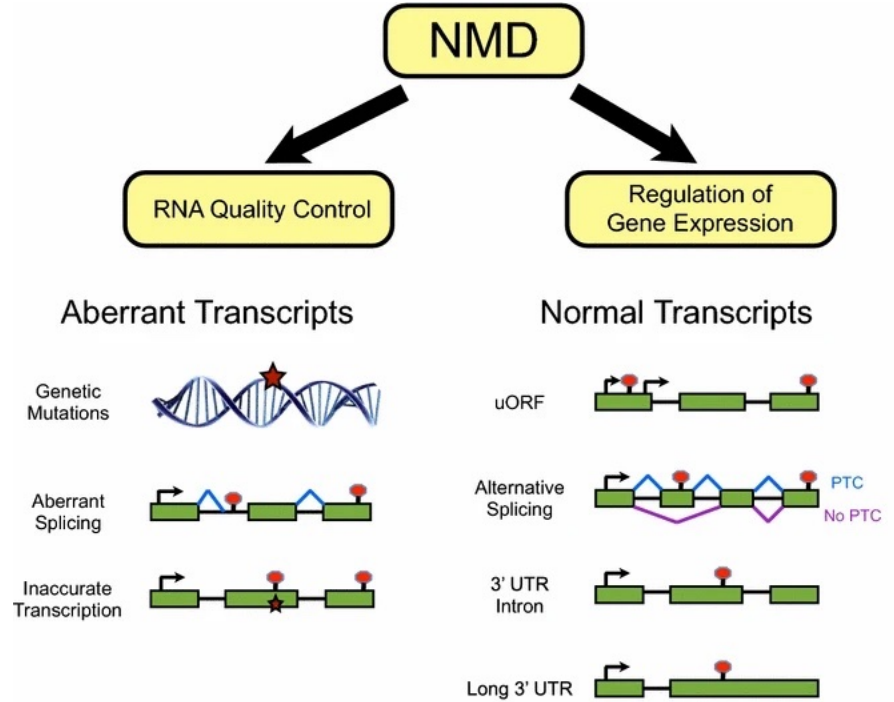


Figure 1.5. Dual roles of NMD. NMD functions as an RNA quality control pathway eliminating PTC containing transcripts that maybe produced due to genetic mutations, aberrant splicing or inaccurate transcription. NMD can also regulate naturally occurring mRNAs that contain specific NMD-eliciting features such as the presence of an uORF, long 3'/UTR (>1000nt), one or more introns in their 3'UTR and even alternatively spliced isoforms that may produce PTC transcripts. Red star: Genetic mutation; Red blob: Termination codon; Green boxes: Exons; Black lines: Introns; Black arrow: Transcription start site; Blue connecting lines: Regular splicing; Purple connecting lines: Alternative splicing. Figure from (Nickeless *et al*, 2017)²²⁵

1.5.1. Essentiality of NMD in mammalian viability and development

Wittkopp *et al* discovered that depletion of multiple NMD factors such as UPF1, UPF2, SMG5, or SMG6 in zebrafish displayed debilitating phenotypes in early patterning, viability, and embryonic development²²⁶. Following that, several groups have demonstrated that complete knockout of core NMD factors in mice resulted in embryonic lethality, strongly suggesting that NMD is an essential mechanism to maintain cell viability and development in mammals also^{174,219,227,228}. Being the central factor involved in all branches of NMD, UPF1 knockout mice displayed lethality at the earliest stage in embryonic development, i.e., shortly after implantation²²⁷. *In vitro* maintenance of these preimplantation blastocysts was unsuccessful because of severe apoptotic death²²⁷. Similarly, complete loss of the NMD endonuclease SMG6 lead to embryonic death, as early as the blastocyst stage²¹⁹. On the other hand, inducible deletion of SMG6 in embryonic stem cells (ESCs) in mice did not affect their proliferative capacity or morphology²¹⁹. However, they provided compelling evidence that NMD inactivation due to SMG6 depletion in mouse ESCs (1) prevented their ability to differentiate both *in vitro* and *in vivo* into all three germ layers and (2) upregulated mRNAs encoding pluripotency genes such as *c-Myc*²¹⁹. Whole body knockout of pan NMD factor SMG1 and UPF2 also lead to *in utero* death around E8.5 and E9.5 respectively, and both displayed severe developmental defects^{177,228}. Inducible deletion of UPF2 in four different tissue types/systems have been studied thus far. Liver-specific knockout of UPF2 at embryonic stage resulted in postnatal death due to the disruption of terminal differentiation of liver cells, and in adult mice caused severe liver damage and hindered regeneration²²⁹. Similarly, conditional knockout of UPF2 in the hematopoietic system led to postnatal (P10) death, due to the complete elimination of hematopoietic stem and progenitor

cells²²⁸. On the contrary, myeloid-specific knockout of UPF2 was viable and displayed normal phenotype²²⁸. Ablating UPF2 in testes lead to male infertility and severe testicular atrophy²³⁰. In conclusion, the requirement of NMD factors vary depending on the tissue type and developmental stage.

1.5.2. Alternative splicing coupled NMD in homeostatic regulation of splicing factors

Alternative splicing (AS) is greatly responsible for the proteomic diversity in cells, however unproductive or erroneous splicing is one of the major reasons for the production and accumulation of PTC-containing transcripts in mammalian cells²³¹⁻²³⁵. Crosstalk of AS with NMD allows homeostatic maintenance of productive and unproductive mRNA isoform levels^{236,237}. This post-transcriptional mechanism is also utilized by splicing activators and repressors to autoregulate their own levels²³⁸ (**Figure 1.5.2**). This is carried out by alternatively splicing their cognate pre-mRNAs for elimination by NMD^{239,240}. NMD-sensitive PTC-containing transcript is generated by promoting the insertion of stop codon exons in case of splicing activators and preventing the inclusion of a coding exon in case of splicing repressors²⁴¹. AS-NMD circuit is involved in regulating transcripts involved in other regulatory processes including mRNA metabolism, chromatin modification and biogenesis of lysosome-related organelles^{242,243}. Lower organisms such as zebrafish, plants, and even *S. cerevisiae* utilize AS-NMD as a gene expression mechanism²⁴⁴⁻²⁴⁶. This feedback loop in turn impacts the alternative splicing of all other pre-mRNAs in the cell.

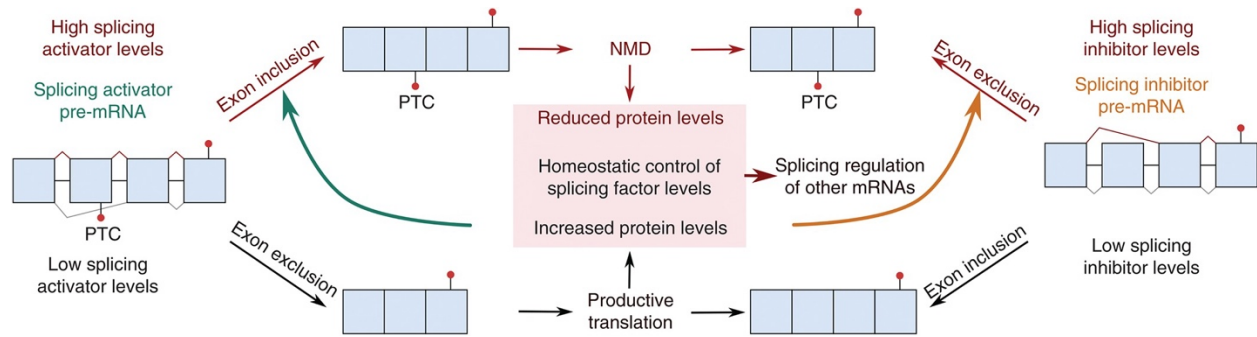


Figure 1.5.2. Alternative splicing coupled NMD in homeostatic autoregulation of splicing factor levels. To maintain physiological necessary levels of splicing factors in the cells, mRNAs undergo alternative splicing to generate unproductive PTC containing isoforms that are degraded by NMD. To generate PTC transcripts, splicing inhibitors avoid inclusion of a coding exon, while splicing activators favour the inclusion of stop codon exons. Alternative splicing of other mRNAs is dependent on this balance of splicing factor levels. Figure from (Karousis ED *et al*, 2016)²⁴⁷.

1.5.3. Physiological response of NMD to stress

A variety of cellular stresses, including amino-acid deprivation, viral infection, and oncogenic stressors such as oxygen deprivation (hypoxia) and reactive oxygen species (ROS) have been reported to inhibit NMD^{160,248}. A shared mechanism that these stressors possess is the capacity to activate kinases that phosphorylate the eukaryotic initiation factor 2 α (eIF2 α), commonly referred to as integrated stress response (ISR)^{223,249-251}. This is a critical step by which stress couples to NMD and represses it^{223,249}. Although the exact mechanism underlying eIF2 α phosphorylation-mediated NMD inhibition is unknown, a potential explanation is that stress-mediated eIF2 α phosphorylation inhibits the translation of newly synthesised and older mRNAs, and inhibiting translation represses NMD^{252,253}.

The stabilization and upregulation of important transcription factors of the stress-response pathways, the integrated stress response (ISR) and the unfolded protein response (UPR) to alleviate the stress is facilitated by NMD suppression (**Figure 1.5.3**). These mRNAs have characteristics that can trigger NMD, such as an uORF in the case of *ATF4* (activating transcription factor 4) and *CHOP/DDIT3* (CCAAT-Enhancer-Binding Protein Homologous Protein/ DNA Damage Inducible Transcript 3) and a premature termination codon introduced by alternative splicing (AS) in the case of *ATF3*, making them classic NMD targets^{223,254-256}. Once homeostasis has been re-established by ISR, NMD is reactivated to suppress these NMD targets. Of interest, *ATF4* has two uORFs that contribute to *ATF4* translation differentially: uORF1 is translated in response to stress, and uORF2 subjects it to NMD during non-stress conditions²⁵⁷.

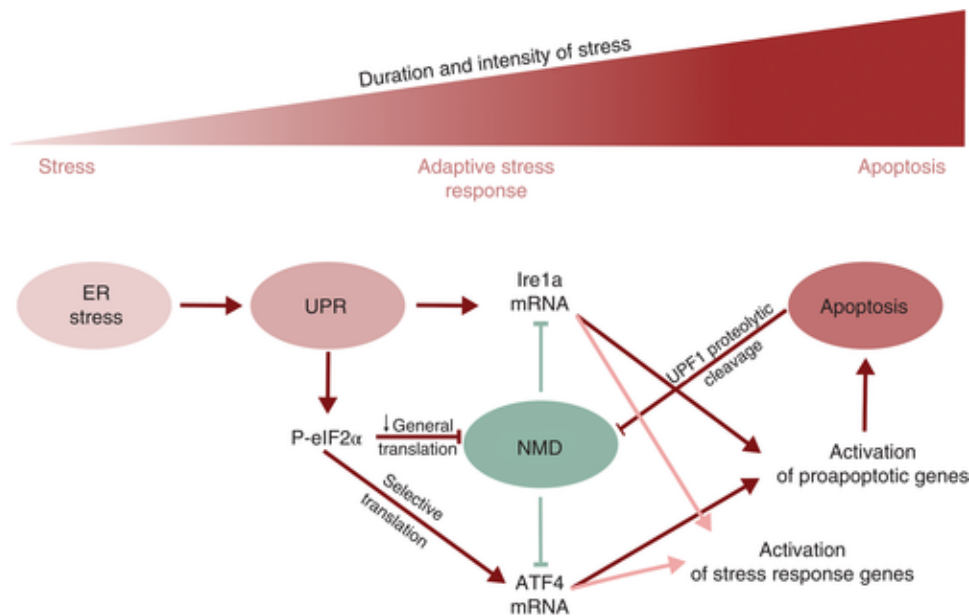


Figure 1.5.3. Role of NMD in Modulating the Stress Response. Various stressors including ER stress and hypoxia triggers eIF2 α phosphorylation in the initial phase of the stress response to activate the UPR pathway. NMD is repressed by eIF2 α phosphorylation resulting in the accumulation of NMD targets like the UPR component IRE1 α (due to the presence of a long 3'UTR), the transcriptional activator of the integrated stress response ATF4 (due to the presence of an uORF). With an increase in the duration and intensity of the stress, cells switch from an adaptive stress response to an apoptotic response, to ensure irreversible commitment of the highly stressed cell to apoptosis. UPF1 undergoes caspase-derived proteolytic cleavage to further inhibit NMD during this switch. Figure from (Karousis ED *et al*, 2016)²⁴⁷.

Another physiological response to stresses such as early hypoxia and serum starvation is translation repression through inhibition of the mammalian target of rapamycin complex 1 (mTORC1)²⁵⁸. The consequence of translation inhibition is not only impaired NMD but also cellular growth arrest²⁵⁹. In cells with arrested growth, Smith *et al* observed an increase in endogenous *GAS5* mRNA, a classic NMD target due to the presence of a PTC in an early exon in its very short ORF²⁵⁹. As supporting evidence, knockdown of NMD components such as UPF1, SMG1, SMG8 and SMG9 lead to accumulation of *GAS5* transcripts^{170,260}. Altogether, through NMD-mediated control of pro-apoptotic proteins such as *GAS5*, mammalian cell viability is maintained.

1.5.4. Role of NMD in neural development and function

In zebrafish, deficient NMD due to the knockdown of various NMD factors such as UPF1, UPF2, SMG5, or SMG6 rendered the embryos with CNS necrosis and defects in brain patterning, abnormal development of the eye and overall growth.

In higher order model organisms such as mice, NMD is subject to regulation over the course of neural development and dictates neural stem cell (NSC) fate decisions. Lou *et al* provided evidence that during early brain development around E14.5, NSC maintain their “stemness” through inherent upregulated levels of NMD factors/ NMD activity and neural stem cell differentiation is triggered when NMD is downregulated by a brain enriched microRNA (miR-128)²⁰¹. They also complement this data using knockdown (KD) studies of the NMD factor UPF1 and show that UPF1 promotes the decay of mRNAs encoding proliferation inhibitors such as p21 and p27 and differentiation factors such as SMAD7²⁰¹.

At later stages of neural development, Jolly *et al* showed that NMD exerts the exact opposite effect on mouse neural progenitor cells originating from E18.5 cortex, i.e., depleting the NMD activator UPF3B minimized their differentiating capacity²⁶¹. This indicates that the differentiation of already committed neural progenitor cells can be promoted by NMD. According to another study by Huang *et al*, NSCs from UPF3B-null mice differentiate poorly and instead exhibit increased self-renewal potential when cultured under normal differentiation inducing conditions, providing more proof that UPF3B promotes neuronal differentiation²⁶².

In the context of fully differentiated neurons, spatial and temporal regulation of NMD occurs in physiological processes. For instance, locally active NMD in axons regulates translation of NMD-sensitive mRNA isoform *Robo 3.2*, and thereby ROBO 3.2 protein synthesis during SLIT-ROBO3 mediated axon guidance²²¹. Another example is the decay of NMD-sensitive cytoskeletal-associated *Arc* mRNA specifically in the dendrites following synaptic stimulation²⁶³.

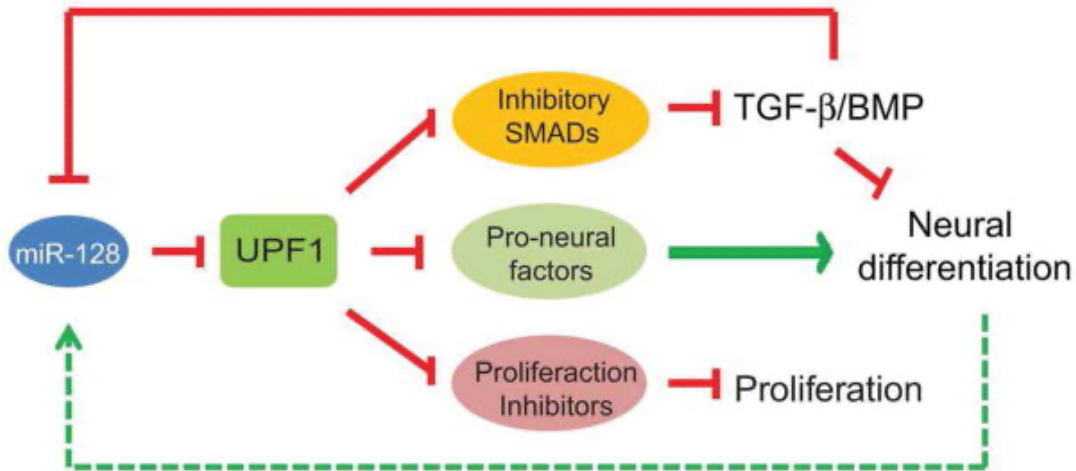


Figure 1.5.4. NMD controls neural stem cell fate. Neuronally expressed miR-128 is upregulated when a neural stem cell is ready to differentiate into a neuron. UPF1 is an miR-128 target, and drastically reduces UPF1 expression by binding to the long 3'UTR of UPF1, thereby inhibiting NMD. UPF1/ NMD is essential to maintain the stemness and proliferative nature of a neural stem cell, as it ensures degradation of mRNAs encoding differentiation factors such as *SMAD7* and proliferation inhibitors. Degradation of *SMAD* factors ensure upregulated TGF- β signaling, which further contributes to maintain the stemness. Figure from (Karousis ED *et al*, 2016)²⁴⁷.

1.6. NMD in disease

It is important for the NMD pathway to eliminate PTC containing transcripts because they can be problematic by resulting in production of truncated non-functional or/and dominant negative proteins. However, these aberrant transcripts can accumulate and associate with various diseases if 1) there are defects in the NMD pathway components, or 2) NMD factor levels and NMD activity magnitude are altered.

1.6.1. NMD-associated neural diseases

In humans, defects in some NMD components have been reported to impact neural development and cause neurological diseases. In mice, this is supported by increasing evidence that targeted disruption of mammalian core NMD factors leads to embryonic lethality, as observed for SMG1, UPF1, UPF2 and SMG6^{177,219,227,228,264}. Copy number variations in NMD genes such as UPF3B, UPF2 and SMG6 have been shown to be significantly associated with neurodevelopmental disorders, intellectual disabilities, and brain malformations, including macrocephaly^{264,265}. Another recent study showed that inhibition of UPF2 in the forebrain lead to an elevated expression of immune genes and brain inflammation which resulted in behavioral and neurophysiological abnormalities²⁶⁶. Hyperactivation of NMD due to a copy number loss in UPF3A, which encodes a NMD repressor, was shown to be associated with neural dysfunction, thus providing evidence that excessive NMD can also be detrimental for neural functioning¹⁶⁴. Additionally, loss of function mutations in SMG9, an essential interacting component of the SURF complex, that is required for SMG1 to phosphorylate UPF1, leads to cerebellar vermis hypoplasia and causes multiple congenital anomaly syndrome in humans²⁶⁷.

In conclusion, loss, or depletion of NMD factors in a variety of model organisms, including zebrafish, *Drosophila melanogaster*, and mice converges on the observation that it is associated with specific defects in the developing nervous system including behavioural and neurophysiological deficits. These findings suggest that NMD is important for brain development and function^{226,262,268}.

A branch of NMD is dependent on EJC, and it is not surprising that mouse mutants of multiple EJC components such as MAGOH, RMB8A and EIF4A3, exhibit severe neurodevelopmental defects such as microcephaly and several defects in the brain cortex²⁶⁹⁻²⁷¹. Despite being haploinsufficient for EJC factors, these mice exhibit more severe phenotypic defects compared to those observed in mice deficient for NMD factor. There could be two possible explanations for this observation. First, in addition to its role in the NMD pathway, EJC has important roles in pre-mRNA splicing, proper export and localization of mRNAs to the cytoplasm and distinguishing properly translated transcripts from newly produced transcripts, suggesting more impaired and debilitating impact on the developing nervous system^{272,273}. Second, due to multiple non-NMD roles of EJC, EJC factors are more limiting than core NMD factors such as UPF1 for executing NMD in neural cells.

Impairment of EJC function in the mutants can disrupt NMD and non-NMD functions, either of which could contribute to the severe phenotype. Mao *et al* provided causative evidence for inefficient NMD activity being a direct implication of impaired EJC function, by documenting very high levels of PTC-containing transcripts being generated in EJC factor-haploinsufficient neural progenitors²⁷¹. Similar to UPF3B-depleted cells and neural lineage committed UPF1-depleted cells, EJC factor (RBM8A) depletion also inhibited neural cell differentiation^{201,274}. Finally, microcephaly is observed as a common defining phenotype in patients with UPF3B

mutations and EJC factor insufficiency^{265,275}. The above indirect pieces of evidence converge on the observation that impaired EJC function is associated with perturbed NMD.

1.6.2. NMD and Cancer

SMG1 has been linked to various types of cancer. One group showed that in HPV-positive head and neck squamous cell carcinoma, SMG1 expression was diminished, and it was suggested to contribute to the enhanced response to therapy²⁷⁶. An important study showed that haploinsufficiency in SMG1 predisposes to a whole range of tumor formation, particularly lung and hematopoietic malignancies and inflammation. But this seemed to be independent of its NMD function, demonstrating that SMG1 can function as a tumor suppressor even without its involvement in the NMD route²⁷⁷.

On the other hand, SMG1 knockout mice are embryonically lethal at E8.5. Deep sequencing of RNA from SMG1-deficient embryos revealed a pronounced accumulation of premature termination codon (PTC)-containing splice variant transcripts with NMD eliciting events. This list included genes involved in the splicing process itself, as well as genes not previously known to be subject to alternative splicing coupled NMD, including several involved in transcription, membrane dynamics, metabolism, and cell death¹⁷⁷. Yahui *et al* showed that SMG1 acts as a novel potential tumor suppressor in acute myeloid leukemia owing to the effect of epigenetic regulation of *SMG1* expression²⁷⁸. All these studies indicate that SMG1 is crucial both in an NMD-dependent and independent manner to maintain homeostasis at mRNA level and play a role in tumorigenesis. However, more work is required to fully understand the role of SMG1 in cancer.

In the case of cancers, the role of NMD is complex and not always unidirectional, depending on tumor type and location, cell/tissue of origin of tumors, evolutionary history of the tumors, developmental stage at which the tumors develop, etc. Thus, each tumor type needs to be viewed as a unique disease with varying levels of NMD attenuation. Some tumors select for mutations to inactivate tumor suppressors and downregulate gene expression by exploiting NMD²⁷⁹⁻²⁸³. In other cases, tumors adjust NMD activity to adapt to their microenvironment rendering it advantageous for tumor progression^{249,284,285}. Mutations in the NMD apparatus have also been described in a few cancers in literature. Somatic UPF1 mutations that either disrupt UPF1 pre-mRNA splicing or cause exon skipping leads to a loss of function of UPF1 and were found to be frequently detected in adenosquamous carcinoma (ASC) pancreatic tumors and lung inflammatory myofibroblastic tumors, respectively^{286,287}. Stresses such as hypoxia (which is prevalent in some cancers) is another parameter in tumor that inhibits NMD, which results in stabilization of NMD-sensitive targets such as ATF4, ATF3 and DDIT3 (CHOP) which are all components of the integrated stress response pathways. Understanding how particular tumors exploit NMD for their benefit may help the development of new therapeutic interventions.

Chapter 2

Rationale and contribution to original knowledge

In our lab, we used the *Ptch1*^{+/-} mouse model of MB to establish the “three” step model of MB formation and progression, with the first step being *Ptch1* heterozygosity in GCPs, followed by *Ptch1* LOH resulting in the formation of preneoplastic MB lesions, and finally requiring additional genetic mutations collaborating with *Ptch1* LOH. With the aim to identify and characterize other co-driver mutations of Shh-MB, we performed deep RNA sequencing (RNA Seq) on the spontaneous tumors that developed from the *Ptch1*^{+/-} mouse MB model. It was a serendipitous discovery that one of the spontaneous tumors harboured a somatic missense substitution S3220F mutation in *SMG1* and another spontaneous tumor harboured a somatic missense substitution L178P mutation in *SMG5*. The *SMG1* somatic tumor variant had a high allelic frequency of 0.543 and was indicative of a potential cancer functionality. Although, the *SMG5* somatic tumor variant had a very low allelic frequency of 0.055, it is still interesting that two distinct, critical NMD effectors were found to be mutated in spontaneous Shh-MB mouse tumors. This finding also raised the possibility of NMD as a pathway collaborating with *Ptch1* LOH to drive MB tumorigenesis.

Mutations in other components of the NMD apparatus have also been described in a few cancers, such as somatic inactivating mutations in *UPF1* in ASC, pancreatic tumors, and lung inflammatory myofibroblast tumors. However, we did not detect any spontaneous mutations in other NMD factors (*UPF1*, *SMG6* or *SMG7*) from our RNA Seq data.

Since *SMG1* is a very large gene (16062 bp), it would be technically very challenging to successfully generate point mutant *SMG1* cDNA constructs to perform in vivo functional assays using these large *SMG1* constructs. Of note, several groups have demonstrated that *SMG1* haploinsufficiency/complete inactivation, or epigenetic regulation of *SMG1* facilitates *SMG1* to function as tumor suppressor in different types of cancers. Furthermore, COSMIC mutational

distribution in *SMG1* gene is suggestive that a missense substitution mutation in *SMG1* is probably an Inactivating mutation. Keeping all these considerations in mind, rather than studying the specific effect of the spontaneous mutations that we identified, in my thesis I have focused on the effect of *NMD* inactivation on GCPs and MB *in vitro* (using siRNA against *SMG1* or *UPF1*, or *NMD* pharmacological inhibitor) and *in vivo* (using CRISPR-Cas9).

Impairment of *NMD* machinery can have a wide range of effects on key regulatory mechanisms in cells including proliferation, differentiation, apoptosis, and stress response. This can be through generation of transcripts that encode for truncated oncogenic proteins, destruction of key tumor suppressor mRNAs and/or dynamic regulation of physiological genes critical for driving tumorigenesis. Thus, many cancers can adopt *NMD* inhibition as a pro-oncogenic mechanism. Therefore, we hypothesized that *NMD* acts as a novel tumor suppressor mechanism in MB formation, and we aim to elucidate the underlying molecular mechanisms. To this date, *NMD* has not been studied in MB, and this additionally propelled us to explore our hypothesis.

In Chapter 3 of this thesis, my initial focus was to understand the role of *NMD* in GCPs (which are the cell of origin of Shh-MB) both *in vitro* and *in vivo*. We used primary cultures of P5 GCPs from developing cerebellum as a model system to demonstrate that *NMD* inactivation upregulates Shh signaling effectors, its transcriptional targets which are essential for driving GCP proliferation, and consequently GCP proliferation.

Having established a functional role of *NMD* in GCPs, we investigated the mechanism by which Shh signalling is being regulated by *NMD*. To address this, we utilised a combination of the following techniques: (1) a β -globin *NMD* reporter assay to test the contribution of these identified putative *NMD*-inducing features in their *NMD*-mediated degradation, and (3) p-*UPF1* RNA immunoprecipitation to identify if mRNAs of the Shh effectors are bound to the central *NMD*

marker p-UPF1, followed by quantitative RT-PCR to estimate their fold enrichment in p-UPF1 bound lysates. We identified and confirmed that the 3'UTRs of *Smo* and *Gli2* mRNA were NMD-sensitive and were marked for degradation by p-UPF1.

Our *in vivo* studies were achieved as follows: (1) NMD inactivation achieved through CRISPR-Cas9 mediated inactivation of NMD components: SMG1, UPF1, SMG6, SMG7 individually in the *Ptch1*^{+/-} mouse model of MB and (2) NMD activation via lentivirus-mediated overexpression of UPF1 in an aggressive Math1-Cre driven overactivated SmoM2 mouse MB model.

We demonstrate that inactivation of *NMD* components cooperate with *Ptch1* inactivation to accelerate MB progression and aggressiveness *in vivo*. Conversely, *NMD* activation causes a delay in MB tumor latency and improves survival in mice.

Chapter 3
Methodology

3.1. Mouse lines

All animal work in this study was performed according to the Canadian Council on Animal Care guidelines. The animal protocol 2020-02-FC was approved by the Montreal Clinical Research Institute Animal Care Committee and all mice were maintained in the IRCM specific pathogen-free animal facility. All mice were maintained on a C57BL/6 (The Jackson Laboratory RRID :IMSR_JAX:000664) background. *Ptch1^{+/-lacZ}* (referred to as *Ptch1^{+/-}*) mice⁴² were backcrossed with C57BL/6 mice. The *R26SmoM2^{110,288}* and the *Math1-Cre²⁸⁹* mouse strains obtained from Jackson Laboratory were crossed to generate the *Math1-Cre; SmoM2* mouse line.

3.2. GCP isolation and culture

P5 GCPs were isolated as previously described²⁰. Briefly, cerebella were isolated from P5 mice and chopped into small pieces. The tissue was washed with HBSS and treated with 0.25% trypsin for 20 minutes at 37°C. Single cell suspensions obtained by trituration were centrifuged through a 30% to 65% Percoll step gradient, and cells were collected at the 30% interphase.

For most of the experiments, GCPs were grown in serum-free Neurobasal media supplemented with 2% B27, 1X GlutaMAX (Gibco 35050-61), 1X sodium pyruvate (Gibco 11360-070) and 0.25% Pen/Strep and were cultured in plates precoated with 100 µg/ml poly-D-lysine (Sigma P0899), for the duration as indicated in different assays. Cells were cultured in the presence of 5 nM Shh (R&D Systems; 1845-SH). When indicated, siSMG1, siUPF1, or siControl were transfected, and pmCMV-GFP or pLenti-UPF1-cMyc-DDK-P2A-Puro were transduced by lentivirus into freshly isolated GCPs. Lentiviral transduction of GCPs were performed as previously described¹²⁰.

3.3. Cell culture

NIH 3T3, Gli luciferase reporter-NIH 3T3, MEF, and HEK 293T cells were maintained in DMEM supplemented with 10% fetal bovine serum and 1% penicillin/streptomycin in a 5% CO₂ humidified incubator. Cells were seeded one day before transfection with plasmid DNA or siRNA using Lipofectamine 3000 (Invitrogen). After incubation for 24-48 hours, the cells were lysed with hypotonic lysis buffer for western blotting/ IP or RLT Plus buffer from the RNeasy kit (Qiagen) for RT-qPCR. When indicated, pmCMV-GI-Norm, pmCMV-GI-39Ter, phCMV-MUP, pmCMV-GI-mSmo3'UTR, pmCMV-GI-mGli2-3'UTR, pmCMV-GFP or pLenti-UPF1-cMyc-DDK-P2A-Puro were transfected into NIH 3T3 cells. For silencing the expression of specific endogenous genes, the siRNAs were transfected for 48-72 hours, as indicated. All the sequences of siRNAs are listed in **Table 3.16.5** (Integrated DNA Technologies, USA). As a control, cells were transfected with non-targeting siControl for siRNA-mediated knockdown.

3.4. siRNA transfection

For transfection of GCP culture, 2×10^6 cells were freshly isolated, plated on PDL coated plates and incubated for 1 hour to allow adherence to the plate. The siRNA oligonucleotides were prepared by mixing with Lipofectamine 3000 (Invitrogen) in Opti-MEM reduced serum medium and incubated for 20 minutes before addition to the cells. The cells were incubated at 37°C for 4-6 hours. The transfection mixture was replaced with fresh serum-free Neurobasal media supplemented with 2% B27, 1X GlutaMAX (Gibco 35050-61), 1X sodium pyruvate (Gibco 11360-070) and 0.25% Pen/Strep. The cells were incubated for an additional 48-72 hours to allow for efficient gene knockdown. The cells were then harvested for further downstream analysis, such

as western blotting to assess the efficiency of siRNA-mediated knockdown, immunofluorescence, or quantitative RT-PCR for assessing gene expression.

3.5. Lentivirus preparation

Lentiviruses were prepared as previously described¹²⁰. Briefly, highly proliferating 293T cells (2×10^7 /150 mm plate) cultured in DMEM supplemented with 10% FBS and 1% P/S were used for lentivirus generation when they reached 80% confluency. Prior to transfection, cells were switched to a virus production medium (DMEM supplemented with 0.5% FBS, 1% P/S and 2mM caffeine). Lentiviruses were generated by co-transfecting 15 μ g of lentiviral vector, 15 μ g of pLp1, 7 μ g of pLp2 and 10 μ g of pVSVG packaging vector into the cells using Lipofectamine 2000 (Sigma). Supernatants were collected 48 hours and 72 hours after transfection, centrifuged for 5 min to remove cell debris and then filtered through a 0.45 μ m membrane. 10 ml of PEG6000-NaCl solution was added to the supernatant in a 1:4 ratio (PEG6000-NaCl: virus supernatant) and the mix was incubated overnight at 4 °C with rotation. The PEG6000/virus mixture was further centrifuged at 3750 rpm to precipitate the virus. After removal of the PEG solution, precipitates were resuspended in Neurobasal medium. This was followed by another 5 minutes of centrifugation at 12000 rpm before the virus was ready to use.

3.6. Western blotting

Cells lysis was performed using 140 mM KCl, 1.5 mM MgCl₂, 20 mM Tris-HCL at PH 7.4, 0.5% NP-40, 0.5 mM dithiothreitol, protease inhibitors (Roche 11873580001), and PhosSTOP phosphatase inhibitors (Roche 4906837001) and boiled in SDS sample buffer at 95°C for 10 minutes. Protein samples were separated by SDS-PAGE and transferred to PVDF membrane. The

membranes were blocked with 5% BSA (Wisent, 800-095-EG) in TBST (0.01 M Tris-HCl pH 7.5, 150 mM NaCl, 0.1% Tween20), followed by overnight incubation of primary antibody in 5% BSA at 4°C in TBST and 1 hour incubation of secondary antibody at room temperature. The western blots were then visualized with chemiluminescence.

3.7. Immunostainings

3.7.1. Dissociated GCP IF

To fix the cells, an equal volume of 8% PFA in PBS was added to the cell culture media, and the plates were then incubated at 4°C for 15 minutes. This was followed by washing the coverslips in PBS. Permeabilization of cells was performed in 0.3% triton for 15 minutes, followed by washes in PBS. Cells were then incubated in blocking solution made of 10% serum (goat/donkey), 0.1% triton in PBS for 1 hour at RT. This was followed by an overnight incubation at 4°C with primary antibody(s) diluted in 1% serum, 0.1% triton. This was followed by washes in 1% serum, 0.1% triton solution. The cells were incubated in diluted fluorophore-conjugated secondary antibody(s) for 1 hour at RT and then washed again in 1% serum, 0.1% triton solution. Finally, cells were counterstained with DAPI, and coverslips were mounted onto slides with mowiol. For all cell-based visualizations, the Leica DM6 microscope was used to acquire fluorescence.

3.7.2. Mouse MB tissue section IF

Animals were anesthetized using ketamine/xylazine (IP) and perfused with saline (0.9% NaCl). Whole cerebella (including intact tumor tissue) were dissected, postfixed with 4% paraformaldehyde (PFA) for 24 hours, and cryoprotected with 30% sucrose for at least 48 hours at 4°C. Cerebellar hemispheres were frozen in OCT and sliced into 12 μ M sagittal sections using a

cryostat. Only for tissue sections stained with the UPF1 antibody, antigen retrieval was performed on cryosections at 98°C for 1 hour using sodium citrate buffer (10mM sodium citrate, 0.05% tween 20 in water, pH 6.0). Following a PBS wash, tissue was permeabilized in 0.3% triton for 15 minutes at RT. To reduce autofluorescence, slides were washed in PBS first and then with 0.3M glycine. The tissue was again washed in PBS before being blocked in 10% goat/donkey serum and 0.1% triton in PBS for an hour at RT. This was followed by an overnight incubation with diluted primary antibody (1% goat/donkey serum and 0.1% triton in PBS). After PBS washes to remove any unbound primary antibody, tissues were incubated for 1 hour at RT with a diluted Alexa fluor-conjugated secondary antibody, then washed once more and counterstained with DAPI. Slides had coverslips affixed to them with mowiol. The tissues were visualized cells using the Zeiss LSM 710 confocal microscope.

3.8. Luciferase assays

For NMD activation, expression vectors for UPF1 and GFP were transfected into Gli luciferase reporter NIH 3T3 cells using Lipofectamine 3000 (Invitrogen) at 90% confluency. Transfected cells were cultured for 24 hours, followed by 24 hours of serum starvation. Cells were stimulated with different concentrations of Shh (R&D Systems; 1845-SH) for 24 hours. Cells were lysed and assayed using a luciferase reporter assay system consisting of the substrate BD Monolight D-Luciferin (BD Biosciences 556888) in GloMax® Navigator Microplate Luminometer (Promega).

For NMD inactivation experiments, cells were plated to attain 90% confluency, followed by 24 hours of serum starvation. Cells were concomitantly treated with different concentrations of NMDi14 drug (5 nM, 25 nM, 50 nM and 500 nM) and Shh (5 nM, 10 nM and 25 nM) for 24 hours, followed by luciferase assay.

As a control, cells were transfected with an RSV-luciferase plasmid (luciferase under a Rous sarcoma virus promoter) along with GFP or UPF1 expression plasmids in NIH 3T3 cells for NMD activation, and with NMDi14 drug for NMD inactivation. Transfected/drug treated cells were cultured for 24 hours, followed by the luciferase assay as described above.

3.9. NMD efficiency measurement

NMD activity was measured using the beta-globin reporter system²⁹⁰. For assessing the impact of NMD activation on various constructs, NIH 3T3 cells were plated to attain 90% confluency and the cells were co-transfected 24 hr later with 0.5 µg of pCMV-MUP plasmid (transfection control) and 1 µg of either β-globin full length plasmid (normal termination codon), β-globin-39Ter plasmid (premature termination codon), β-globin-Smo 3'UTR plasmid (3'UTR length=1080 nt) or β-globin-Gli2 3'UTR plasmid (3'UTR length=1724 nt) and 1 µg of UPF1 or GFP expression vectors using Lipofectamine 3000 (Invitrogen) according to the manufacturer's protocol. After 24 hr, media was changed and 48 hr later, the cells were harvested for qRT-PCR analysis. The levels of pCMV-β-globin-39Ter, β-globin-Smo 3'UTR and β-globin-Gli2 3'UTR plasmids were plotted relative to levels of β-globin full length plasmid.

3.10. p-UPF1 RNA Immunoprecipitation -qPCR

p-UPF1 RNA Immunoprecipitation protocol was adapted from the protocol described previously^{147,291}. Briefly, HEK293T cells (8×10^6 in each 10 cm dish) were incubated for 3 hours with 200 nM okadaic acid. Cell pellets were harvested, washed with ice cold PBS, and lysed using hypotonic gentle lysis buffer (containing RNaseOUT) for 10 min in ice. 3 µl of DNase was added to the collected supernatant, and the mix was incubated for 10 minutes in a 37°C water bath. To

minimize background and non-specific binding, lysates were pre-cleared before the immunoprecipitation step. Cellular RNAs bound by p-UPF1 were immunoprecipitated using 5 µg of anti-p-UPF1(S1116) [Millipore, anti-phospho-Upf1(Ser1127)] or rabbit IgG as control, and Dynabeads protein A magnetic beads (Life Technologies). The RNA in bead-bound RNA-p-UPF1(S1116) complexes was eluted using 2X SDS-PAGE sample elution buffer by incubating at 95°C for 5 minutes after thorough washing with ice-cold NET-2 buffer (0.1% NP40), ice-cold NET-2 buffer (0.5% NP40), and high salt wash buffer. TRIZOL was used for RNA extraction and purification in accordance with the manufacturer's instructions. Following this, RNA was converted to cDNA, and qRT-PCR was performed as described below, with primers specific to the common backbone of all the constructs used.

3.11. qRT-PCR

qRT-PCR on genes of interest was performed as described⁵¹. Briefly, RNA was purified using the RNeasy Mini Plus kit (QIAGEN). cDNA was synthesized using the Transcriptor first strand cDNA synthesis kit (Roche) using total RNA. Real-time PCR mixes were prepared using SYBR Green qPCR mastermix (Applied Biosystems). Results were analyzed using the Comparative Ct method. Primer sequences used are listed in **Table 3.16.6**.

3.12. In utero electroporation

The anaesthetic, Isoflurane (2%) was used to sedate the pregnant mice. To gain access to the uterus and find the embryos, a minor incision was made. The uterine horn was gently pulled out to access the embryos from one side of the midline and visualize using a light source. The surgical region was periodically moistened with PBS, as needed. The embryos were positioned such that the dorsal

side of the head was facing upwards and near the uterine wall. The target plasmid DNAs were injected laterally into the rhombic lip of the 4th ventricle using a microinjection equipment (sterile 7mm capillary needles). To aid the entry of the plasmid DNA into the site of interest, electrical pulses were applied via electrodes connected to an electroporation device (35mV, 5 pulses, 950ms in Pico spritzer injector (Science Products, GmbH). After carefully reintroducing the embryos into the body, the incision was sutured. To prevent any infection, polysporine was topically administered.

3.13. Orthotopic transplantation

Cerebella of post-natal day 5 wildtype C57BL6 pups were used for orthotopic transplantation of virally transduced GCPs¹²⁰. The recipient pups were anaesthetized by hypothermia for 3-4 minutes. This was immediately followed by an injection of 1×10^6 previously transduced *Math1-Cre⁺; Smo^{+M2}* GCPs (with GFP or UPF1 lentivirus) into the cerebellum of each recipient pup using a Pico spritzer injector (Science Products, GmbH). A volume of 2 μ l was injected. The pups were allowed to recover from the procedure for 20 minutes after injections, and their health condition was monitored weekly until symptoms of MB were evident.

3.14. Statistical Methods

Unless otherwise indicated, all data are expressed as mean \pm SEM. The statistical tests used to measure differences are indicated in the appropriate legends. Statistical significances are indicated as follows: *p < 0.05; **p < 0.01; ***p < 0.001; n.s., not significant, and the p values are indicated in the appropriate legends.

3.15. Bioinformatics

3.15.1. NMD feature prediction

The Ensembl gene annotation for *Mus musculus*. GRCm38.85 was used to identify transcripts with the below NMD-inducing features:

- (1) A 3'UTR at least 1000kb in length
- (2) One or more introns in the 3'UTR
- (3) A uORF in the 5'UTR defined by an ATG start site that encodes at least 10 amino acids

3.15.2. NMD target signature generation and human MB data analysis

All the analysis pertaining to this section was performed on R2 Genomics Analysis and Visualization Platform. Using published lists of NMD targets generated by the Burge laboratory (CLIP-seq used to identify direct UPF1 binding targets) and the Maquat laboratory (p-UPF1 RIP-seq), we generated two NMD target gene signatures (288 genes for the Burge signature and 104 genes for the Maquat signature). These signatures were used to perform expression analysis on a published cohort of human MB samples (Cavalli dataset) and stratify the samples into high and low NMD target expression. Kaplan-Meier overall survival probability analysis was performed on these high and low groups.

3.16. Supplemental information

3.16.1. Reagents

Shh was purchased from R&D Systems (1845-SH) and was used at following concentrations: 5 nM, 10 nM, 25 nM, 50 nM, 100 nM or 200 nM, as indicated. NMDi14 (NMD inhibitor) was purchased from MedChemExpress (HY-111374), and was used at following concentrations: 5 nM, 25 nM, 50 nM, 500 nM or 5 μ M, as indicated.

3.16.2. Plasmids

pmCMV-GI-Norm, pmCMV-GI-39Ter and phCMV-MUP were gifts from Dr. Lynne Maquat²⁹⁰. pmCMV-GI-mSmo3'UTR and pmCMV-GI-mGli2-3'UTR were derived from pmCMV-GI-Norm using the In-Fusion kit (Clontech 639648) by replacing the 3'UTR of β -globin with the 3'UTR of mSmo (3'UTR length=1080 nt) and mGli2 (3'UTR length=1724 nt) respectively. pLenti-UPF1-cMyc-DDK-P2A-Puro was purchased from Origene (MR216969L3V). pmCMV-GFP was obtained from Addgene (Plasmid #11657). For CRSIPR-Cas9 mediated genetic engineering, a cloning backbone for sgRNA targeting specific genes was obtained from Genscript (pSpCas9 BB-2A-GFP (PX458)). The specific sgRNAs sequences are listed in **Table 3.16.4**.

3.16.3. Antibodies

Antibodies against the following targets were used: SMG1 (Anti-Smg1 antibody (ab30916), 1:1000 for WB), UPF1 (Recombinant Anti-RENT1/hUPF1 ab109363, 1:1000 for WB, 1:500 for IF), phospho-UPF1 (Anti-phospho-UPF1 Ser1116 antibody- antiphospho-UPF1 (Ser1127), EMD Millipore, 5 μ g for IP); Pan-actin (Cell Signaling (NEB) 4968S, 1:1000 for WB), GAPDH (Millipore/Sigma MAB374 clone 6C5, 1:1000 for WB), β -Tubulin (Recombinant Anti-beta Tubulin antibody (ab179513), 1:1000 for WB), GFP (Invitrogen A11122, 1:1000 for IF), Ki67 (Recombinant Anti-Ki67 antibody [SP6] ab16667, 1:1000 for IF on cells, 1:1000 for IF on tissues). Secondary antibodies that were used: Goat anti-mouse IgG-HRP (Jackson ImmunoResearch, 115-035-003, 1:10000 for WB), Goat anti-rabbit IgG-HRP (Jackson ImmunoResearch, 111-035-003, 1:10000 for WB), Donkey anti-Rabbit IgG-Cy3 (Jackson ImmunoResearch, 111-165-144, 1:1000 for IF), Isotype Control rabbit IgG polyclonal (Abcam, ab37415, 5 μ g as control for IP)

Table 3.16.4: sgRNA sequences:

Gene	sgRNA sequence
Smg1-1	ATTCCAGCTCCGCGGGTACTTGG
Smg1-2	ATTCAGCTGTGGTGTCTCGGCAAAGGCAC
Smg6	CCTATTATCTTTGCGCTGTCTGG
Smg7	TACCTGTCATTTACAGCCTTCAGG
Upfl	CGCCGGGGGGCGTCTGCGTCTGG

Table 3.16.5: siRNA duplex sequences:

siRNA against:	Duplex sequence
Scrambled siRNA	5'-rCrUrUrCrCrUrCrUrCrUrUrCrUrCrUrCrCrCrUrUrGrUGA-3' 5'-rUrCrArCrArArGrGrGrArGrArGrArArArGrArGrArGrArArGrGrA-3'
siSmg1 B	5'-rGrGrCrUrUrArUrUrArGrUrUrGrArGrArArGrCrUrArArACA-3' 5'-rUrGrUrUrUrArGrCrUrUrCrUrCrArArCrUrArArUrArArGrCrCrArA-3'
siSmg1 C	5'-rArCrArGrCrArArArArUrUrGrUrArGrArUrArArArCrUrUTC-3' 5'-rGrArArArGrUrUrUrArUrCrUrArCrArArUrUrUrUrGrCrUrGrUrArG-3'
siUpfl Y	5'-rGrUrCrArUrCrArArGrGrUrUrCrCrUrGrArUrArArUrUrATG-3' 5'-rCrArUrArArUrUrArUrCrArGrGrArArCrCrUrUrGrArUrGrArCrGrU-3'
siUpfl Z	5'-rGrGrUrGrArUrGrArGrUrUrUrArArArUrCrArCrArGrArUTG-3' 5'-rCrArArUrCrUrGrUrGrArUrUrUrArArArCrUrCrArUrCrArCrCrGrA-3'

Table 3.16.6: Primer sequences used for quantitative RT-PCR

Gene	Primer sequence
mGusb: Forward primer	5' CTGCCACGGCGATGGA 3'
mGusb: Reverse primer	5' ACTGCATAATAATGGGCACTGTTG 3'

mAtf4: Forward primer	5' CACAACATGACCGAGATGAG 3'
mAtf4: Reverse primer	5' CGAAGTCAAACCTCTTTCAGATCC 3'
mDdit3: Forward primer	5' CTGGAAGCCTGGTATGAGGAT 3'
mDdit3: Reverse primer	5' CAGGGTCAAGAGTAGTGAAGGT 3'
mGas5: Forward primer	5' TTTCCGGTCCTTCATTCTGA 3'
mGas5: Reverse primer	5' TCTTCTATTTGAGCCTCCATCCA 3'
mSnord22: Forward primer	5' GCCAGGCCTGTTCAATTTTA 3'
mSnord22: Reverse primer	5' TGCCTGAGATTTGTCACCAG 3'
mGli2: Forward primer.	5' AGCACTACCTCCGGTCTGTG 3'
mGli2: Reverse primer	5' CATGAGGGTTCATCTGGTGGT 3'
mSmo: Forward primer	5' GCTGTGGGATTCAGTGTGAG 3'
mSmo: Reverse primer	5' CAGGGTAGCGATTGGAGTTC 3'
mGli1: Forward primer	5' GCAGTGGGTAACATGAGTGTCT 3'
mGli1: Reverse primer	5' AGGCACTAGAGTTGAGGAATTGT 3'
mHk2: Forward primer	5' GGACTAAGGGGTTCAAGTCCA 3'
mHk2: Reverse primer	5' GACCAATCTCGCAGTTCTGA 3'
mCnd1: Forward primer	5' TTGACTGCCGAGAAGTTGTG 3'
mCnd1: Reverse primer	5' CTGGCATTTTGGAGAGGAAG 3'
mUpf1: Forward primer	5' CTGCCTGCGTGGTTTACTGT 3'
mUpf1: Reverse primer	5' GTAGCACTCCAGCACGGTCT 3'
h β -globin: Forward primer	5' GCTCGGTGCCTTTAGTGATG 3'
m β -globin: Reverse primer	5' CCCAGCACAAATCACGATCATA 3'
hGli2: Forward primer	5' CGAGGGTTCATCTGGTGGTAA 3'
hGli2: Reverse primer	5' GAGCACTACCTCCTGTCTGT 3'
hHprt: Forward primer	5' TTCGTGGGGTCCTTTTCACC 3'
hHprt: Reverse primer	5' TGACCAGTCAACAGGGGACA 3'
hSmo: Forward primer	5' GGACATGCACAGCTACATCG 3'
hSmo: Reverse primer	5' CCAATGCTGCCACAAAGAA 3'
hAtf4: Forward primer	5' TCGTCCTGGTGGGATCTAGG 3'
hAtf4: Reverse primer	5' TCTGGCATGGTTTCCAGGTC 3'
hGli1: Forward primer	5' CTTCTGCCACCAAGCTAACC 3'
hGli1: Reverse primer	5' CGACAGAGGTGAGATGGACA 3'

Chapter 4

Results

4.1. The NMD pathway is functional in cerebellar granule cell precursors (GCPs).

NMD is a translation-dependent mechanism involving degradation of faulty transcripts through a highly orchestrated sequence of protein-protein interactions involving core NMD factors such as UPF1, UPF2, UPF3B, SMG1, SMG5, SMG6 and SMG7¹²⁵ (**Figure 4.1A**). To test whether NMD is functional in cerebellar GCPs, we performed siRNA-mediated knockdown of two key NMD components: SMG1 (siSMG1; **Figure 4.1B-C**) and UPF1 (siUPF1; **Figure 4.1D-E**). 72 hr after SMG1 or UPF1 siRNA transfection, we assessed the levels of well-established, direct NMD targets harboring various NMD-inducing features (*Atf4*, *Ddit3*, *Gas5*, and *Snord22*)^{160,214,223,228,292-296} (**Figure 4.1F** for the list of NMD features present in these NMD target genes). We found that knockdown of either SMG1 or UPF1 gave similar results and led to an increase in the mRNA levels of *Atf4*, *Ddit3*, *Gas5*, and *Snord22*, while not affecting the housekeeping gene *Gusb*, used as an internal control (**Figure 4.1G-H**). The fact that knockdown of two NMD signaling components give similar results supports that the observed effect is due to inhibition of NMD, rather than inhibition of another signaling mechanism. Thus, inhibition of the NMD pathway leads to the upregulation of NMD target mRNAs in GCPs, indicating that the NMD pathway is functional in GCPs.

We next tested the opposite and assessed whether NMD activity can be upregulated in GCPs. Increased expression of UPF1 has been shown to activate NMD in many cell types and cause a decrease in NMD target levels^{150,223,284,297}. We first confirmed that we could achieve elevated levels of UPF1 protein and mRNA expression by lentivirus transduction of GCPs (**Figure 4.1I-J**). As anticipated, this led to the downregulation of the NMD target *Atf4* (**Figure 4.1K**), consistent with NMD being activated in GCPs upon increased expression of UPF1. Together, these experiments

demonstrate for the first time that the NMD pathway is functional in GCPs and that it can regulate its targets positively or negatively, depending on whether NMD is down- or up-regulated.

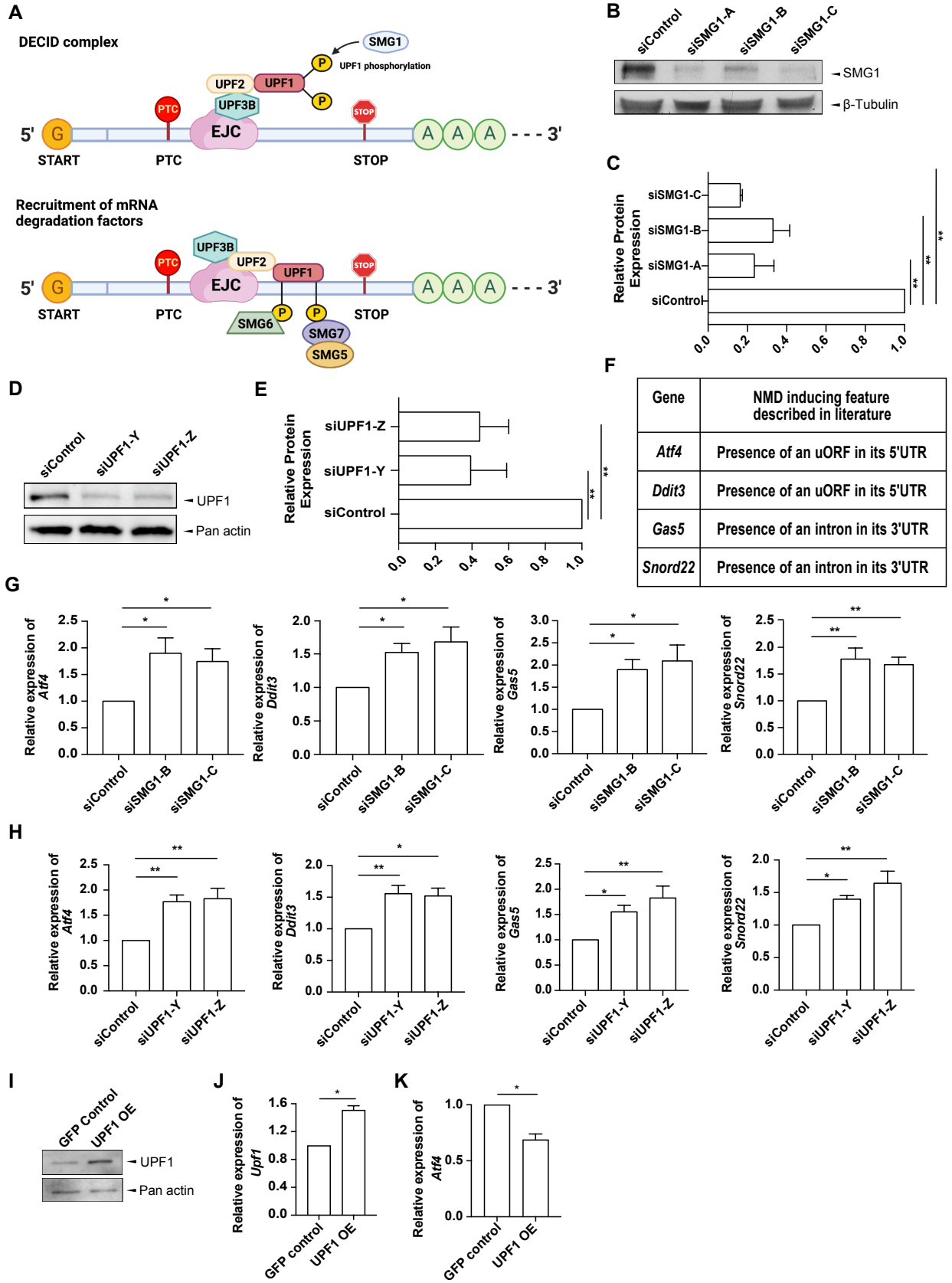


Figure 4.1. The NMD pathway is functional in cerebellar granule cell precursors (GCPs).

- (A) Schematic of the NMD pathway. Detection of a transcript containing a premature termination codon leads to interaction of UPF1 with the UPF2-UPF3 bound to EJC, triggering the phosphorylation of UPF1 by SMG1 kinase, to form the DECID complex. NMD-mediated exonucleolytic degradation of the transcript occurs through interaction of UPF1 with the final effectors of NMD- SMG5 and SMG7, and/or through endonucleolytic cleavage by SMG6.
- (B) Freshly isolated P5 C56BL6 GCPs were transfected with three different siRNAs against SMG1 targeting three different exons, or a control non-targeting siRNA, as indicated. The total cell lysates were analyzed by western blotting with the indicated antibodies; β -tubulin was used as the loading control.
- (C) Densitometric quantification of SMG1 in siSMG1 GCPs; n=3. Data are normalized such that the siControl treatment is 1.
- (D) Freshly isolated cerebellar GCPs were transfected with two different siRNAs against UPF1 or a control non-targeting siRNA, as indicated. The total cell lysates were analyzed by western blotting with the indicated antibodies; Pan-actin was used as the loading control.
- (E) Densitometric quantification of UPF1 in siUPF1 GCPs; n=3. Data are normalized such that the siControl treatment is 1.
- (F) NMD-inducing features described in literature for four classic NMD targets: *Atf4*, *Ddit3*, *Gas5* and *Snord22*.
- (G) Relative endogenous mRNA levels of well-established NMD targets; *Atf4*, *Ddit3*, *Gas5* and *Snord22* in siSMG1 GCPs, as measured by qRT-PCR; n>3.
- (H) Relative endogenous mRNA levels of well-established NMD targets; *Atf4*, *Ddit3*, *Gas5* and *Snord22* in siUPF1 GCPs, as measured by qRT-PCR; n>3.
- (I) P5 C56BL6 GCPs were infected with UPF1 lentivirus to activate NMD, or GFP lentivirus as control. The total cell lysates were analyzed by western blotting with the indicated antibodies; Pan-actin was used as the loading control.
- (J) Relative mRNA levels of *Upf1* in UPF1 OE GCPs, as measured by qRT-PCR; n=3.
- (K) Relative endogenous mRNA levels of well-established NMD target - *Atf4* in UPF1 OE GCPs, as measured by qRT-PCR; n=3.

Transcript levels were normalized to *Gusb* in (G, H, J, K). One- way ANOVA with Dunnett's multiple comparison post-test was performed in (G, H, J, K). Error bars represent SEM.

4.2. NMD regulates Shh pathway activity, expression of proliferation-regulating genes, and GCP proliferation.

While in some cell types NMD was shown to regulate proliferation^{201,220,228,261}, whether NMD regulates the proliferation of GCPs remains unknown. Thus, we next investigated the consequences of inactivating NMD on GCP proliferation. In GCPs with knockdown of SMG1 or UPF1, we observed a ~2-fold increase in the percentage of cells positive for the proliferation marker Ki67⁺ (**Figure 4.2A-D**). While in some contexts NMD regulates proliferation, in other cellular contexts, NMD has been shown to regulate differentiation^{201,220,228,261}. To evaluate whether NMD also plays a role in GCP differentiation, we assessed if inhibition of NMD affects GCP differentiation into granule neurons. Knockdown of SMG1 did not affect the expression of early or late granule neuron differentiation markers such as *Cntn2* (Tag1), *Rbfox3* (NeuN), or *Tubb3* (neuronal β -tubulin) (**Figure 4.2E**). Thus, our data indicate that NMD regulates proliferation of GCPs but does not regulate their differentiation.

As the Shh signaling pathway is an important regulator of GCP proliferation^{17,18}, we explored whether Shh pathway activity is regulated by NMD. We first looked at *Gli1* mRNA, a transcriptional target of the Shh pathway which reflects the activity of the pathway (**Figure 4.2F**). When SMG1 or UPF1 was knocked-down in GCPs, we found that *Gli1* levels were upregulated (**Figure 4.2G-H**), suggesting an upregulation of Shh pathway activity. To confirm this, we looked at two additional Shh pathway targets, *CyclinD1* (*Ccnd1*) and *Hexokinase2* (*Hk2*)^{35,54,298-300}. We found that, similarly to *Gli1*, *Ccnd1* and *Hk2* mRNA levels were also upregulated in SMG1- and UPF1-knocked-down GCPs (**Figure 4.2G-H**). Together, these results indicate that Shh pathway activity is upregulated when NMD is inactivated.

We next explored the mechanism underlying this effect. We hypothesized that modulation of Shh pathway activity by NMD might be due to an effect of NMD on the mRNA(s) of Shh pathway components. In support to this, we found that *Smo* and *Gli2*, two key mediators of Shh signaling (**Figure 4.2F**), each contain three NMD features in their mRNA (**Figure 4.3E**), thus making them prime candidates for regulation by NMD. Consistent with our hypothesis, we found that the mRNA levels of *Smo* and *Gli2* were upregulated in SMG1- and UPF1-knockdown GCPs (**Figure 4.2I-J**). For these mRNA changes to result in an increase in Shh pathway activity, they need to also result in changes in proteins levels. Immunoblot analysis showed that the amounts of Smo and Gli2 proteins were increased in SMG1- and UPF1-knockdown GCPs (**Figure 4.2K-L**), consistent with the *Smo* and *Gli2* mRNA increases that we observed. Thus, NMD inhibition increases Shh pathway activity, expression of proliferation-regulating genes, and GCP proliferation.

We next assessed whether upregulation of NMD activity would lead to the downregulation Shh pathway transcriptional targets and Shh signaling pathway components. We achieved upregulation of NMD activity by increasing expression of UPF1 in GCPs (**as in Figure 4.1I-J**) and found that the Shh pathway targets *Gli1*, *Ccnd1*, and *Hk2* were downregulated (**Figure 4.2M**). In addition, we found that increased expression of UPF1 in GCPs led to a decrease in protein levels of Smo and Gli2 (**Figure 4.2N**). In summary, our data show that NMD can modulate key Shh signaling pathway components (Smo and Gli2) and their Shh pathway targets (*Gli1*, *Ccnd1*, and *Hk2*) in either activating or inactivating direction, depending on the status of NMD activity.

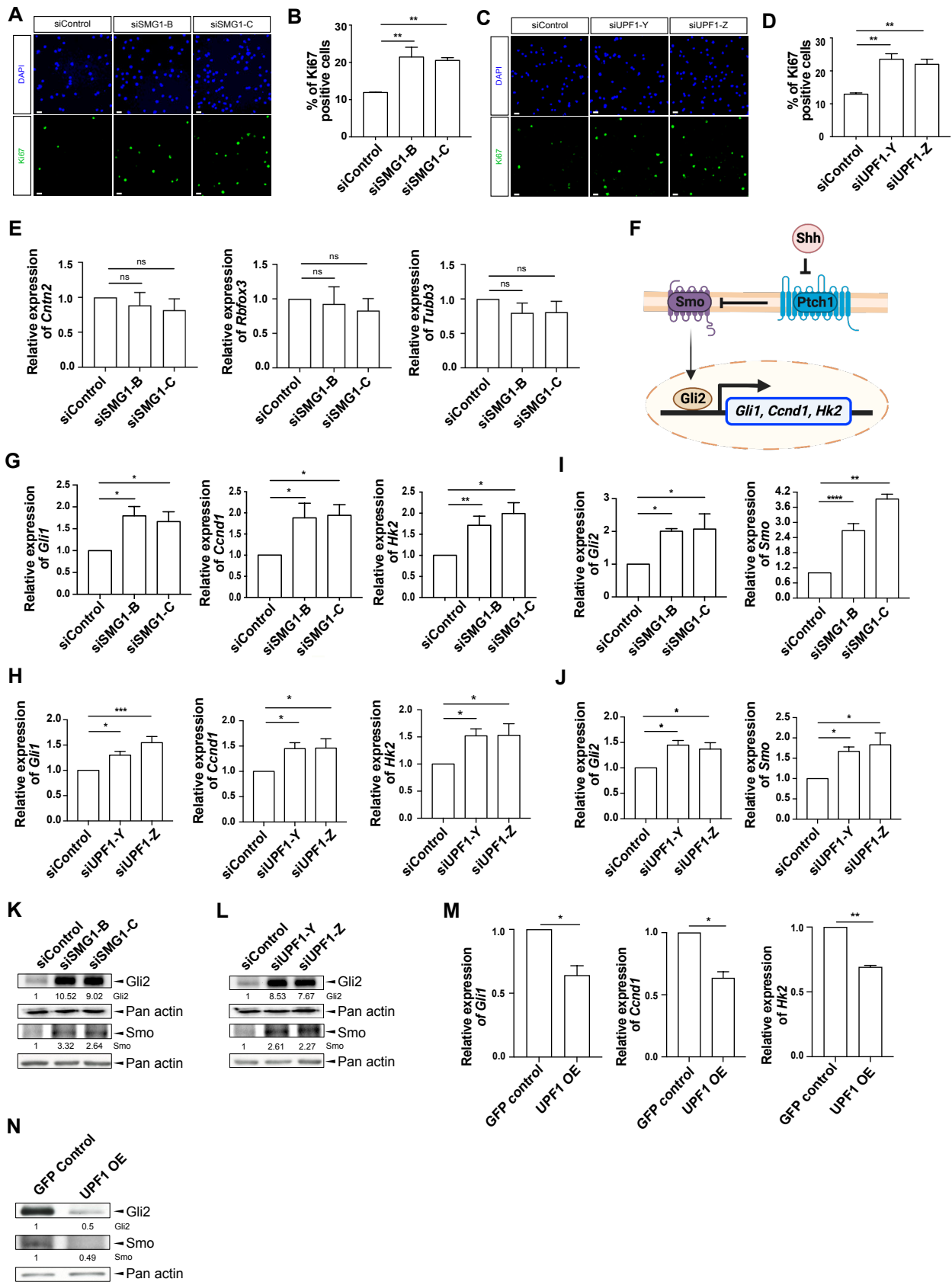


Figure 4.2. NMD regulates Shh pathway activity, expression of proliferation-regulating genes, and GCP proliferation.

- (A) Immunofluorescence of siSMG1 GCPs with an antibody against Ki67 to assess proliferation.
- (B) IF quantification of Ki67 positive staining of siSMG1 GCPs; n=3.
- (C) Immunofluorescence of siUPF1 GCPs with an antibody against Ki67 to assess proliferation.
- (D) IF quantification of Ki67 positive staining of siUPF1 GCPs; n=3.
- (E) Relative endogenous mRNA levels of GCP differentiation genes; *Cntn2*, *Rbfox3* and *Tubb3* upon SMG1 KD, as measured by qRT-PCR; n=3.
- (F) Schematic of canonical Shh signaling pathway. In the absence of Shh ligand, Ptch1 inhibits the constitutive activation of the pathway. In presence of Shh, it binds to Ptch1, thus relieving Ptch1 inhibition on Smoothed (Smo), leading to activation of *Gli* transcription factors and its downstream targets.
- (G) Relative endogenous mRNA levels of *Gli2* transcriptional targets that are known to regulate GCP proliferation (*Gli1*, *Ccnd1*, *Hk2*) upon SMG1 KD, as measured by qRT-PCR; n>3.
- (H) Relative endogenous mRNA levels of *Gli2* transcriptional targets that are known to regulate GCP proliferation (*Gli1*, *Ccnd1*, *Hk2*) upon UPF1 KD, as measured by qRT-PCR; n=3.
- (I) Relative endogenous mRNA levels of Shh pathway activators; *Gli2* and *Smo* upon SMG1 KD, as measured by qRT-PCR; n>3.
- (J) Relative endogenous mRNA levels of Shh pathway activators; *Gli2* and *Smo* upon UPF1 KD, as measured by qRT-PCR; n>3.
- (K) Endogenous protein levels of Shh pathway effectors; Gli2 full length and Smo in siSMG1 GCPs, as measured by immunoblotting with the indicated antibodies. Gli2 and Smo levels measured in KD conditions are relative to siControl.
- (L) Endogenous protein levels of Shh pathway effectors; Gli2 full length and Smo in siUPF1 GCPs, as measured by immunoblotting with the indicated antibodies. Gli2 and Smo levels measured in KD conditions are relative to siControl.
- (M) Relative endogenous mRNA levels of Shh pathway activators; *Gli2*, *Gli1* and *Smo* upon UPF1 OE, as measured by qRT-PCR; n=3.
- (N) Endogenous protein levels of Shh pathway effectors; Gli2 full length and Smo upon UPF1 OE, as measured by immunoblotting with the indicated antibodies. Gli2 and Smo levels was measured in OE conditions and normalised to GFP control.

In (A-D), GCP proliferation was measured as a percentage of number of cells positively stained for Ki67 relative to total number of DAPI stained cells per condition.

Scale bar represents 10 μm in (A, C). In (E, G, H, I, J, M), transcript levels were normalized to *Gusb* and One-way ANOVA with Dunnett's multiple comparisons post-test was performed; Error bars represent SEM. Pan-actin was used as the loading control in (K, L, M).

4.3. NMD regulates Shh signaling by modulating *Gli* transcriptional activity.

To show that the transcriptional output of the Shh pathway is modulated by NMD in a direct manner, we used a Gli-dependent reporter assay. In this assay, a heterologous cell line (NIH 3T3) harbors a stably integrated construct composed of Gli DNA binding sites upstream of a luciferase reporter gene. Shh pathway activation is achieved by Shh stimulation. To investigate the impact of NMD modulation on the transcriptional activity of the Shh pathway, we inhibited NMD using varying concentrations (5, 25, 50, and 500 nM) of NMDi14, an NMD inhibitor that disrupts the interaction between SMG7 and UPF1 by targeting a pocket in the SMG7 protein³⁰¹. As expected, we observed a dose-dependent increase in Shh activity with Shh treatments of 5, 10, and 25 nM. Concomitant NMD inhibition with Shh stimulation showed enhancement of Gli-mediated transcription by ~1.5-2 fold (**Figure 4.3A**). To ensure that the changes observed in the Gli-reporter response were not caused by a non-specific effect on the reporter, we also used a luciferase reporter driven by a Rous sarcoma virus (RSV) promoter. We did not detect any effect of NMDi14 on the RSV-luciferase reporter, even when we used a much higher dose of 5 μ M NMDi14 (**Figure 4.3B**). Conversely, to look at the effect of increasing NMD on Gli activity, we used lentivirus mediated UPF1 overexpression. Increased NMD activity led to a decrease in Gli-driven luciferase transcription (**Figure 4.3C**). This was supported by a change in the EC₅₀ of Shh from 16.32 nM in control condition to 28.55 nM in the UPF1 overexpression condition. Again, the changes observed in the Gli-reporter response were not caused by a non-specific effect on the reporter as we did not detect any effect on the RSV-luciferase reporter upon NMD activation (**Figure 4.3D**). Together, these data show that NMD modulates Gli-dependent transcriptional activity, but it does not affect a non-Gli-driven transcriptional reporter.

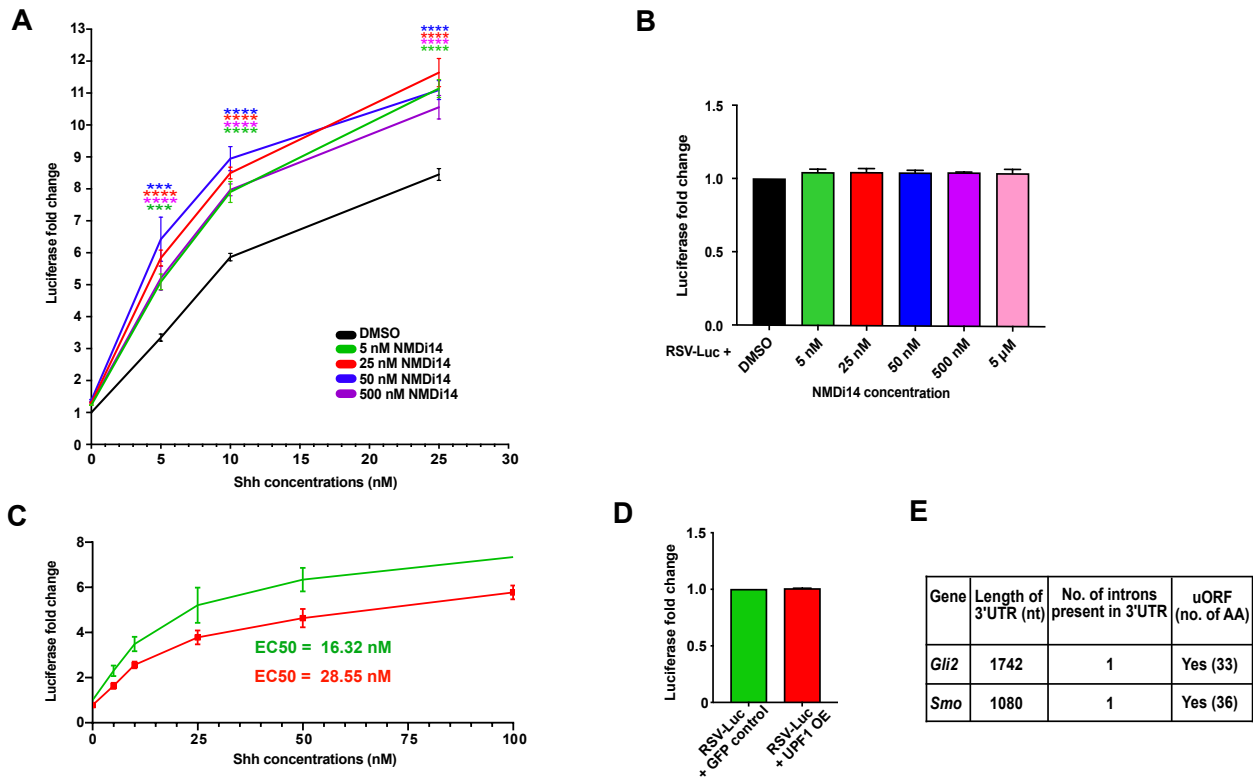


Figure 4.3 NMD regulates Shh signaling by direct modulation of *Gli* transcriptional activity.

- (A) Stimulation of *Gli2*-promoter driven luciferase reporter activity in NIH3T3 cells subjected to simultaneous NMD inactivation using NMDi14 and Shh stimulations for 24 hours; n=3. The different concentrations of NMDi14 used: 5nM, 25nM, 50nM, 500nM and the different concentrations of Shh used: 5nM, 10nM, 25nM.
- (B) Stimulation of luciferase activity in NIH3T3 cells that were transfected with RSV-luciferase, were subjected to NMD inactivation using different concentrations of NMDi14; n=3.
- (C) Stimulation of *Gli2*-promoter driven luciferase reporter activity in NIH3T3 cells subjected to NMD activation by transfecting an UPF1 overexpression plasmid or a control GFP plasmid for 48 hours, followed by Shh stimulation at doses: 5nM, 10nM, 25nM, 50nM and 100nM for 24 hours; n=3.
- (D) Stimulation of luciferase activity in NIH3T3 cells that were transfected with RSV-luciferase, were subjected to NMD activation by transfecting an UPF1 overexpression plasmid or a control GFP plasmid for 48 hours; n=3.
- (E) NMD-inducing features predicted from the Ensemble database for *Gli2* and *Smo*.

4.4. The 3'UTRs of *Smo* and *Gli2* are targets of NMD-mediated degradation.

Since *Smo* and *Gli2* mRNA levels are modulated by NMD (**Figure 4.2I-J**) and their mRNA each contain three predicted NMD features (long 3'UTR, presence of an intron in 3'UTR, and uORF; **Figure 4.3E**), we hypothesized that they might be direct targets of NMD. To test this, we used the β -globin mini-gene reporter system where the impact of an exogenous RNA sequence can be tested on β -globin mRNA stability²⁹⁰. This reporter system has been used to identify and characterize novel NMD targets^{290,294}. As a negative control, we used a construct containing full length β -globin (with its normal termination codon) and its 3'UTR (referred to as β -globin full length). This construct does not have NMD features and is not targeted by NMD^{290,294}. As a positive control, we used the same construct but harboring a premature termination codon (PTC) at the 39th position of the β -globin ORF (39 Ter β -globin). Since this construct has an NMD feature (PTC), it is targeted by NMD^{290,294,302-305}. In addition, we generated two chimeric constructs, both containing the full length β -globin ORF followed by replacing the 3'UTR of β -globin with either the intron-containing 1080 nt-long 3'UTR of *Smo* mRNA (β -globin-*Smo* 3'UTR) or intron-containing 1724 nt-long 3'UTR of *Gli2* mRNA (β -globin-*Gli2* 3'UTR) (**Figure 4.4A**).

We transfected these reporters into NIH 3T3 cells and assessed their *β -globin* mRNA levels by qRT-PCR. First, we observed that in DMSO control conditions, transcripts from our β -globin-*Smo* and β -globin-*Gli2* 3'UTR chimeric constructs were downregulated two-fold compared to β -globin full length (**Figure 4.4B**). This downregulation was similar to the decrease observed for the NMD-targeted 39 Ter β -globin mRNA. To show that the downregulation of *Smo* and *Gli2* 3'UTR chimeric constructs are due to targeting by NMD, we assessed the effect of NMD inhibition on the stability of these mRNAs. We observed that transcript levels of *Smo* and *Gli2* 3'UTR chimeric constructs progressively increased with treatment of NMDi14, ultimately reaching levels similar

to the NMD-insensitive *β -globin* full length transcript (**Figure 4.4B**). These results show that the *Smo* and *Gli2* 3'UTR are NMD targets.

We next sought to determine whether elevating NMD activity would lead to an enhanced degradation of *Smo* and *Gli2* 3'UTR chimeric constructs. Indeed, upon increased expression of UPF1, we observed more than two-fold decrease in chimeric transcript levels compared to the control GFP condition (**Figure 4.4C**). Thus, NMD activation leads to increased degradation of *Smo* and *Gli2* 3'UTR chimeric constructs, further supporting that *Smo* and *Gli2* are novel NMD targets.

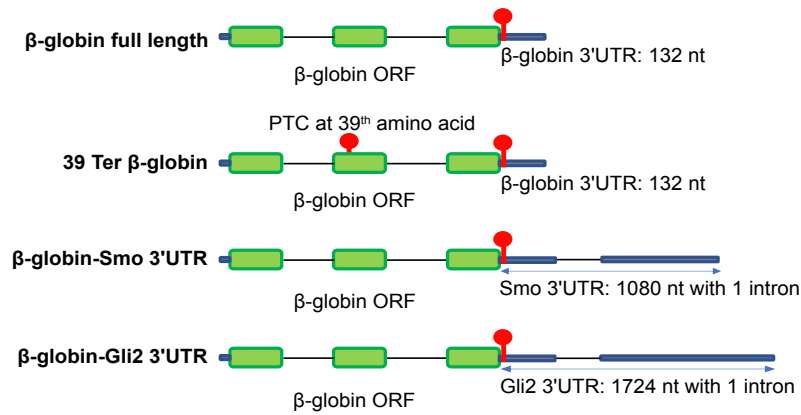
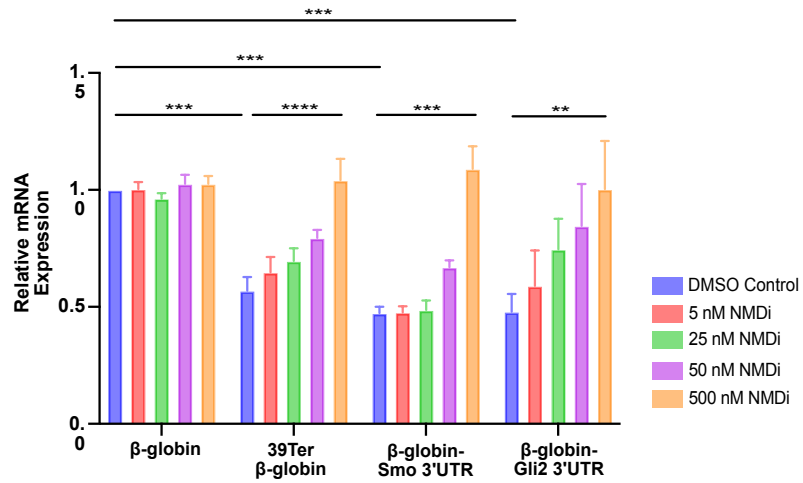
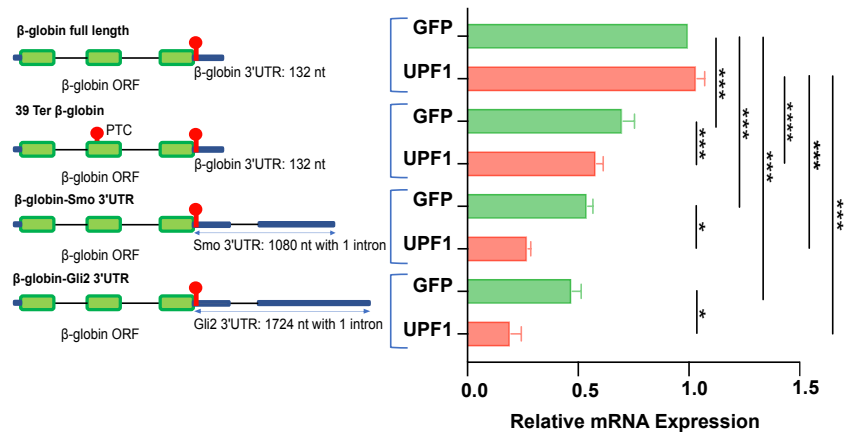
A**B****C**

Figure 4.4. The 3'UTRs of *Smo* and *Gli2* are targets of NMD-mediated degradation.

(A) Schematic of different NMD reporter constructs used: (1) β -globin full length reporter construct (used as a negative control for NMD degradation): encoding the β -globin opening reading frame followed by β -globin 3' UTR or (2) 39 Ter β -globin NMD reporter construct (used as a positive control for NMD degradation): encoding premature termination codon-containing at 39th amino acid position in the β -globin opening reading frame followed by β -globin 3' UTR or (3) β -globin *Smo* 3'UTR chimeric construct: encoding the β -globin opening reading frame followed by the *Smo* 3' UTR of length 1080 nt or (4) β -globin *Gli2* 3'UTR chimeric construct: encoding the β -globin opening reading frame followed by the *Gli2* 3' UTR of length 1742 nt. Green boxes are exons (open reading frames), black lines are introns, red is a termination codon and blue is a 3'UTR.

(B) Relative levels of transcripts from the β -globin full length, 39 Ter β -globin and β -globin *Smo* 3'UTR and β -globin *Gli2* 3'UTR constructs following NMD inactivation using different doses of NMDi14 as indicated in figure; n=3. Data are normalized such that the β -globin full length treated with DMSO is set to 1.

(C) Relative levels of transcripts from the β -globin full length, 39 Ter β -globin and β -globin *Smo* 3'UTR and β -globin *Gli2* 3'UTR constructs following NMD activation by UPF1 OE or GFP as control in NIH3T3 cells; n=3. Data are normalized such that the β -globin full length transfected with GFP control is set to 1.

All error bars are SEM.

4.5. p-UPF1 binds to the 3'UTRs of *Smo* and *Gli2* to mark and target their mRNAs for NMD.

Phosphorylation of UPF1 (p-UPF1) by SMG1 kinase is crucial for triggering NMD-mediated degradation of its targets^{127,180}. Phosphorylated steady state UPF1 binds, gets stabilized and enriched on the 3'UTR of NMD targets¹⁴⁷. Kurosaki et al. developed a p-UPF1 RNA immunoprecipitation (RIP) method for the identification of direct NMD targets^{147,291}. This approach involves treating cells with okadaic acid (OA), an inhibitor of protein phosphatase 2A (PP2A), which not only increases the steady-state fraction of p-UPF1 in the bulk of cellular UPF1 to allow easier detection of p-UPF1 marking NMD targets, but also inhibits immediate degradation of the targets, thus enabling an increase in their transcript levels for more sensitive detection by qRT-PCR^{147,153,180,306}. While our findings thus far show that *Smo* and *Gli2* mRNAs are subject to NMD degradation (**Figure 4.2**) and that their 3'UTR are targeted by NMD (**Figure 4.4**), we further confirmed that they are direct NMD targets by assessing whether p-UPF1 marks *Smo* and *Gli2* transcripts for NMD-mediated degradation. For this, we used OA to enhance p-UPF1 levels in HEK293T cells and performed p-UPF1 RIP using an antibody against p-UPF1 (p-S1116) or rabbit IgG (rIgG) as a control, followed by a qRT-PCR (**Figure 4.5A**). 10% of the cell lysate that was used as input before IP confirmed a large increase in cellular p-UPF1 levels upon OA treatment (**Figure 4.5B**). We also verified by western that our IP using an antibody against p-UPF1 efficiently enriched p-UPF1 protein, as seen by a considerable increase in p-UPF1 levels with OA treatment compared to the rIgG controls (**Figure 4.5B**). Assessing p-UPF1 mRNA transcript levels relative to the rIgG background upon OA treatment by qRT-PCR revealed a very high fold enrichment in *Smo* of ~40-fold and in *Gli2* of ~200-fold, similar to what we observed with the well-established NMD target *Atf4* (~70-fold; **Figure 4.5C**). Notably, we detected enrichment of *Smo* and *Gli2* even

in absence of OA treatment, on the order of ~25 and ~70-fold, respectively. This key finding that p-UPF1 marks *Smo* and *Gli2* transcripts for NMD-mediated degradation demonstrate that these positive effectors of the Shh pathway are directly targeted by NMD. Together, our results demonstrate that *Smo* and *Gli2* mRNAs are novel NMD targets.

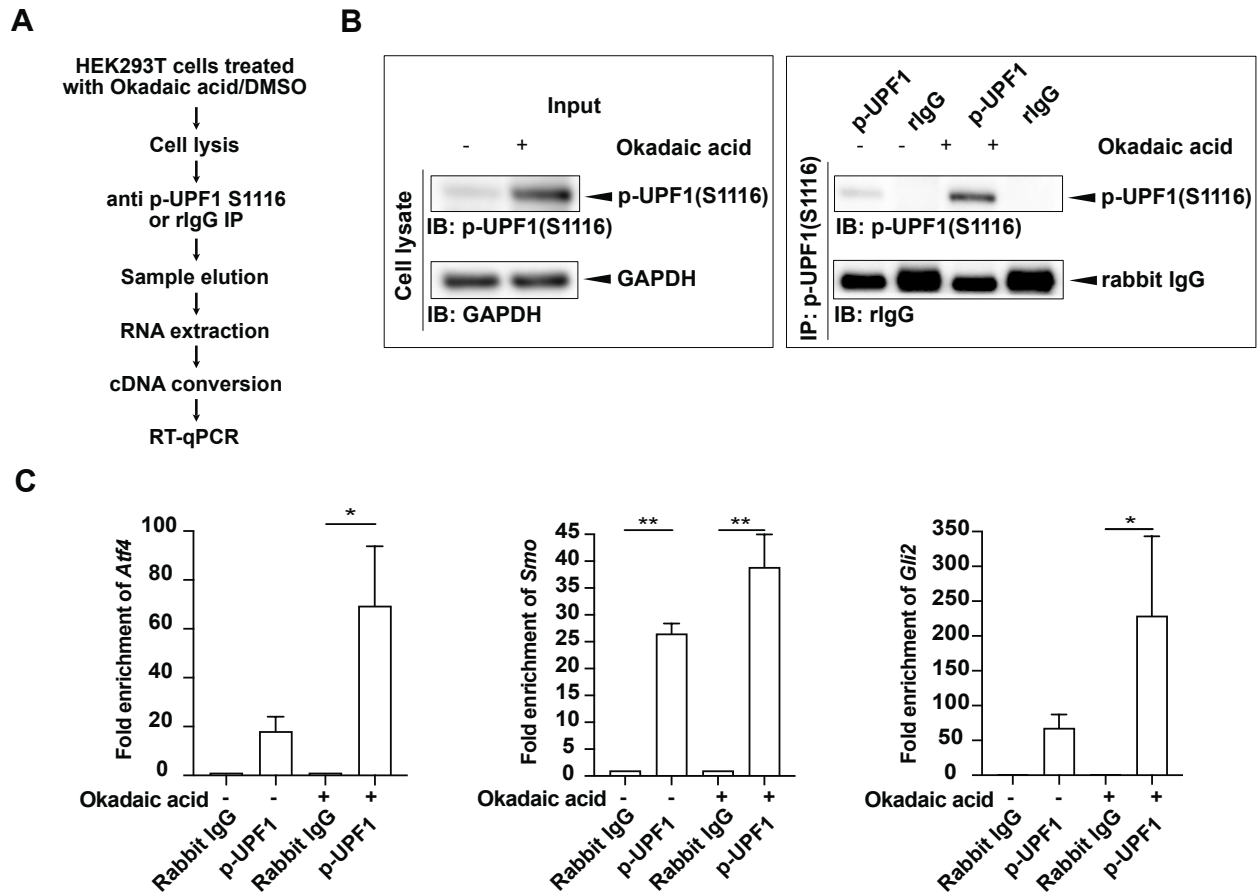


Figure 4.5. p-UPF1 binds to the 3'UTRs of *Smo* and *Gli2* to mark and target their mRNAs for NMD.

(A) Schematic for p-UPF1 RIP-Seq (details in Methodology Chapter 3.10).

(B) Immunoprecipitation of HEK293T cell lysates was performed using anti-p-UPF1(S1116) or, as a control, rabbit IgG. Immunoblot (left) represents the input sample, which contain the total cellular proteins before IP, using indicated antibodies; GAPDH was used as a loading control. Right blot represents immunoblot after p-UPF1 immunoprecipitation using indicated antibodies.

(C) RT-qPCR on samples analyzed in (B), for the assessment of fold enrichment of endogenous *Atf4*, *Gli2* and *Smo* bound to p-UPF1.

All error bars are SEM.

4.6. NMD inactivation cooperates with *Ptch1* inactivation to enhance medulloblastoma tumorigenesis.

Having established that NMD regulates the Shh signaling pathway and GCP proliferation, we next aimed to determine if this could play a role in Shh pathway-induced pathologies. GCPs are the cell of origin of Shh-medulloblastoma⁴⁴⁻⁴⁶; we thus sought whether NMD regulation of Shh signaling might play a role in medulloblastoma tumorigenesis. *PTCH1* is one of the most commonly mutated gene in Shh-medulloblastoma⁸⁵. As a Shh-medulloblastoma mouse model, we used *in utero* electroporation of the rhombic lip (the zone where GCPs are generated) to perform CRISPR-Cas9-mediated inactivation of *Ptch1*, alone or jointly with *SMG1* inactivation (**Figure 4.6.1A**; gRNA details in **Table 3.16.4**). We first investigated whether NMD impacts formation of early medulloblastoma tumors (preneoplasia) at postnatal day 21 (P21), a time when preneoplastic lesions can be distinctly observed¹²⁰. Histological assessment revealed that inactivation of *Ptch1* alone led to an incidence of preneoplasia of 9.5% at P21 (**Figure 4.6.1B**). Remarkably, double inactivation of *Smg1* and *Ptch1* led to a drastic increase in preneoplasia incidence from 9.5% to 60%, while single *Smg1* inactivation alone did not have tumorigenic effect on its own (0% incidence). In addition to increased incidence, we also observed that *Smg1* inactivation considerably increased (~5-fold) the area of preneoplastic lesions, from ~20 mm² in *Ptch1*-inactivated preneoplasia to ~100 mm² in *Ptch1*+*Smg1*-inactivated preneoplasia (**Figure 4.6.1C-D**). These results indicate that SMG1 modulates *Ptch1*-tumorigenesis, and this impacts the incidence and the size of early medulloblastoma.

We next examined if this effect on early tumors would result in differences in medulloblastoma aggressiveness at later stages. We performed *in utero* electroporation as described above and, after their birth, monitored the animals over time for the appearance of behavioral phenotypes related

to medulloblastoma, such as severe ataxia and coordination defects. Upon detection of these phenotypes, the animals were euthanized and autopsied to confirm the presence of a medulloblastoma. In all cases, a medulloblastoma tumor was confirmed. We observed that *Ptch1+Smg1* inactivation increases the incidence of advanced medulloblastoma by ~9-fold, from 3.6% in *Ptch1*-inactivated tumors to 30.6% *Ptch1+Smg1*-inactivated tumors (**Figure 4.6.1E**). This data was used to perform a Kaplan-Meier survival analysis. We found that *Ptch1+Smg1* inactivation significantly decreases survival, compared to *Ptch1* inactivation alone (**Figure 4.6.1F**). Thus, *Smg1* inactivation cooperates with *Ptch1* inactivation to enhance tumorigenesis by increasing the incidence and growth of early medulloblastoma, resulting in an increased incidence of late stage medulloblastoma and a decreased survival.

We next confirmed that inactivating *Smg1* was resulting in a decrease in NMD activity in these tumors. First, we validated that the protein level of SMG1 was highly decreased in *Ptch1+Smg1*-inactivated tumors compared to *Ptch1*-inactivated tumors (**Figure 4.6.2A-B**). Consistent with NMD being inactivated, we observed an increase in the classic NMD targets (*Atf4*, *Ddit3*, *Gas5*, and *Snord22*) in *Ptch1+Smg1*-inactivated tumors compared to *Ptch1*-inactivated tumors (**Figure 4.6.2C**). Similar to what we described in GCPs, we observed that *Smg1* inactivation in *Ptch1* tumors increases the NMD-sensitive Shh pathway effectors *Gli2* and *Smo* (**Figure 4.6.2D**). Consistent with an increase in Shh pathway activity, we also observed an increase in the Shh pathway transcriptional targets *Gli1*, *Hk2*, and *Ccnd1* (**Figure 4.6.2E**). Together, these results indicate that Shh pathway activity is upregulated in medulloblastoma tumors when *Smg1* is inactivated.

To further confirm that the effect of inactivating *Smg1* on medulloblastoma aggressiveness reflects a role of SMG1 in NMD, we also used the CRISPR-Cas9 approach to inactivate *Upf1*, another key

NMD component. Combined inactivation of *Ptch1+Upf1* increased medulloblastoma incidence ~6-fold, from 3.6% (*Ptch1* alone) to 22% (*Ptch1+Upf1*; **Figure 4.6.1E**). In addition, *Ptch1+Upf1* inactivation decreased survival compared to *Ptch1* inactivation alone (**Figure 4.6.1G**). Thus, NMD inactivation cooperates with *Ptch1* inactivation to increase medulloblastoma tumorigenesis.

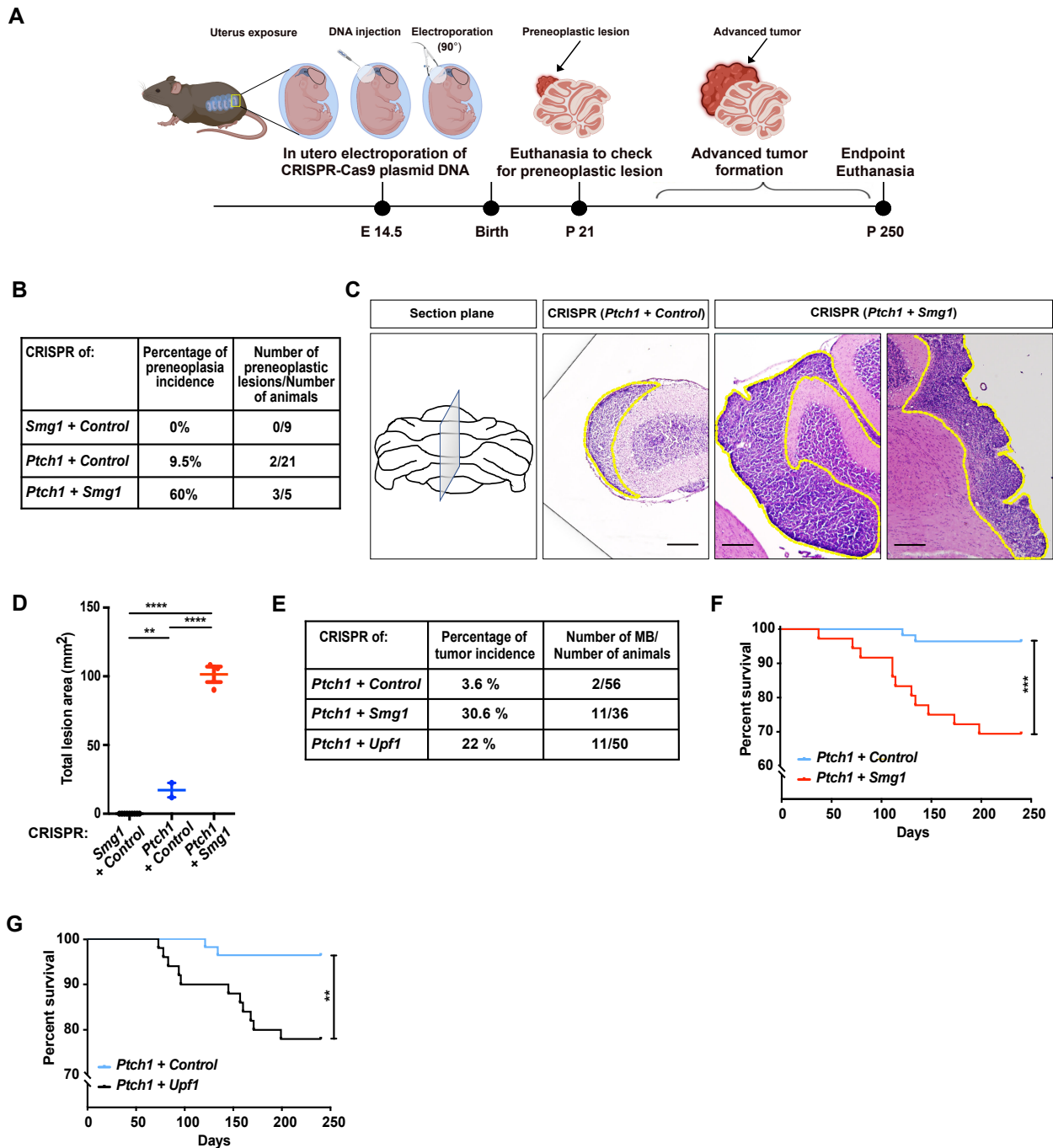


Figure 4.6.1. NMD inactivation cooperates with *Ptch1* inactivation to enhance medulloblastoma tumorigenesis.

(A) Schematic of in-utero electroporation of CRISPR-Cas9 gRNA-mediated inactivation of NMD components in combination with *Ptch1* inactivation to study the impact on *Ptch1* MB formation and progression.

- (B) Summary table indicating percentage of preneoplasia incidence and the ratio of no. of mice positive for preneoplastic lesions to total no. of animals in each group, CRISPR (*Smg1* + *Control*), CRISPR (*Ptch1* + *Control*), and CRISPR (*Ptch1* + *Smg1*).
- (C) MB lesions at postnatal 21 (P21) days in mice with inactivation of *Ptch1* + *Control* (n=2/21) compared to mice with combined inactivation of *Ptch1* + *Smg1* (n=3/5) and mice inactivated for *Smg1* only (n=0/9). Yellow dotted lines represent the area of tumor growth.
- (D) Quantification of the total lesion area in mm² per group in (C).
- (E) Summary table indicating percentage of tumor incidence and the ratio of no. of mice positive for MB to total no. of animals in each group; CRISPR (*Ptch1* + *Control*), CRISPR (*Ptch1* + *Smg1*) and CRISPR (*Ptch1* + *Upf1*).
- (F) Kaplan-Meier survival curves comparing mice with combined inactivation of *Ptch1*+*Control* (n=2/56) (vs) *Ptch1*+*Smg1* (n=11/36).
- (G) Kaplan-Meier survival curves comparing mice with combined inactivation of *Ptch1*+*Control* (n=2/56) (vs) *Ptch1*+*Upf1* (n=11/50).

Scale bar represents 200µm in (C). One- way ANOVA with Tukey's multiple comparison post-test was performed for (D). Error bars represent SEM. Log-rank (Mantel-Cox) test was performed in (F-G).

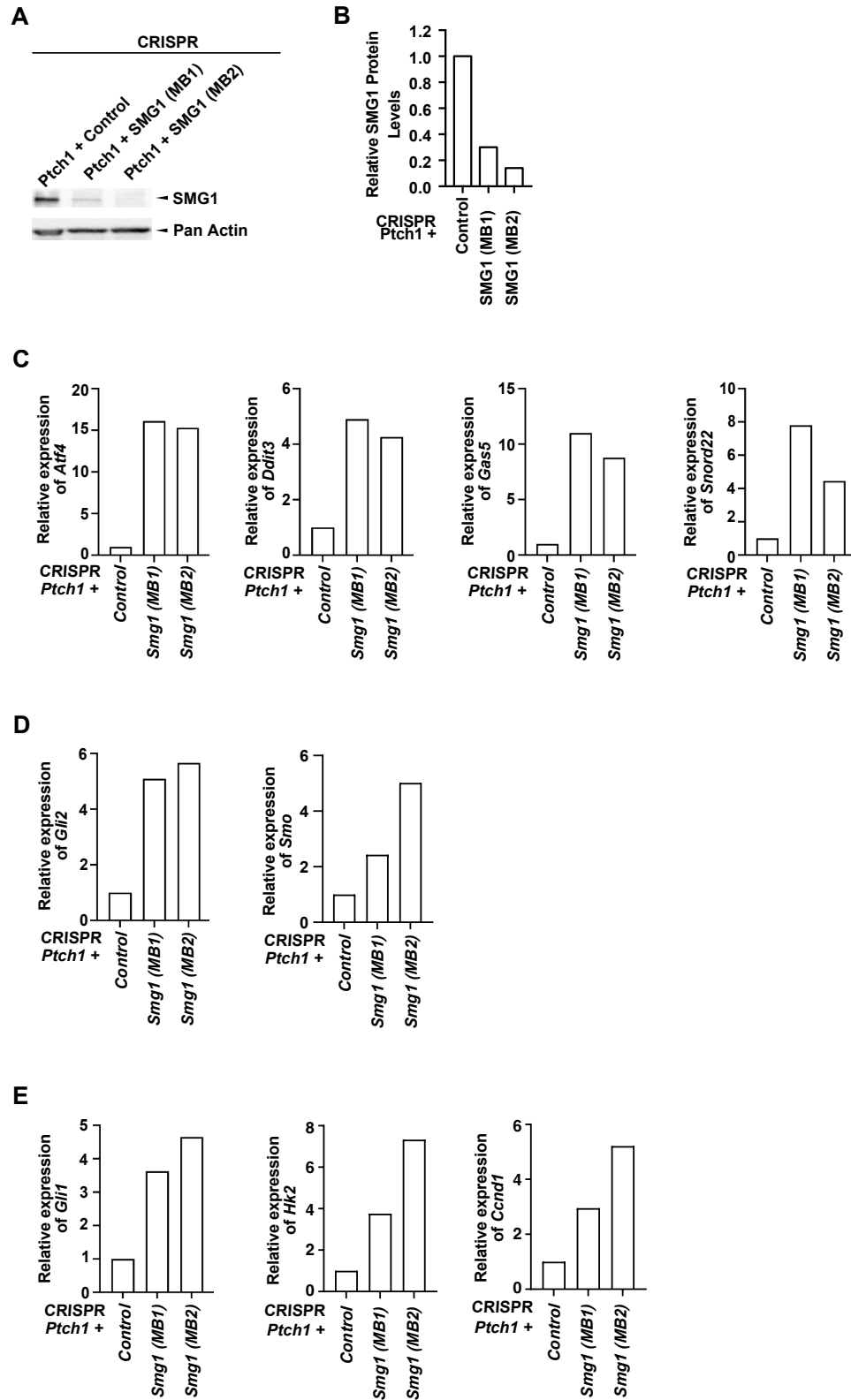


Figure 4.6.2. Shh pathway activity is upregulated in medulloblastoma tumors when *Smg1* is inactivated *in vivo*

- (A) Representative Immunoblot of total cell lysates from tumor tissue obtained by CRISPR-Cas9 mediated combined inactivation of (*Ptch1* + *Control*) and (*Ptch1* + *Smg1*). MB1 and MB2 represent two individual tumors. The total cell lysates were analyzed by western blotting with the indicated antibodies; Pan-actin was used as the loading control.
- (B) Densitometric quantification of (A). Data are normalized such that the CRISPR (*Ptch1* + *Control*) tumor group is set to 1.
- (C) Relative endogenous mRNA levels of well-established NMD targets; *Atf4*, *Ddit3*, *Gas5* and *Snord22* in CRISPR (*Ptch1* + *Control*) vs CRISPR (*Ptch1* + *Smg1*) tumors, as measured by qRT-PCR.
- (D) Relative endogenous mRNA levels of Shh pathway activators; *Gli2* and *Smo* CRISPR (*Ptch1* + *Control*) vs CRISPR (*Ptch1* + *Smg1*) tumors, as measured by qRT-PCR.
- (E) Relative endogenous mRNA levels of *Gli* transcriptional targets that are known to regulate GCP proliferation (*Gli1*, *Ccnd1*, *Hk2*) in CRISPR (*Ptch1* + *Control*) vs CRISPR (*Ptch1* + *Smg1*) tumors, as measured by qRT-PCR.
- In (C,E), each bar represents the value of one tumor and transcript levels were normalized to *Gusb*.

4.7. NMD upregulation decreases tumor cell proliferation and aggressiveness of medulloblastoma tumors.

Since we showed that increased expression of UPF1 activates NMD in GCPs, thereby causing a reduction in Shh signaling and a decrease in GCP proliferation, we wondered whether increased expression of UPF1 could also have a similar effect in tumorigenic GCPs, where the Shh pathway is driven by SmoM2, a constitutively active form of Smo. For this, we generated *Math1-Cre⁺; Smo^{+M2}* mice, where SmoM2 is driven in GCPs by the Math1-Cre promoter. This is a very aggressive medulloblastoma mouse model with 100% incidence and 0% survival. We isolated tumorigenic GCPs from P5 *Math1-Cre⁺; Smo^{+M2}* cerebella and infected them with a lentivirus expressing UPF1. This resulted in an increase in UPF1 protein levels (**Figure 4.7.1A**). Consistent with an increase in NMD activity, we observed a decrease in the expression level of NMD targets (*Atf4*, *Ddit3*, *Gas5*, and *Snord22*) and a decrease in the NMD-sensitive Shh pathway effectors *Gli2* and *Smo* (**Figure 4.7.1B-C**). Consistent with a decrease in Shh pathway activity, we also observed a decrease in the Shh pathway transcriptional targets *Gli1*, *Hk2*, and *Ccnd1* (**Figure 4.7.1D**). In line with these targets being important drivers of tumorigenic GCP proliferation, increased NMD activity also led to a reduction in tumorigenic GCP proliferation (**Figure 4.7.1E-F**). Together, these results indicate that, even in highly tumorigenic GCPs, NMD activation downregulates Shh pathway activity and proliferation.

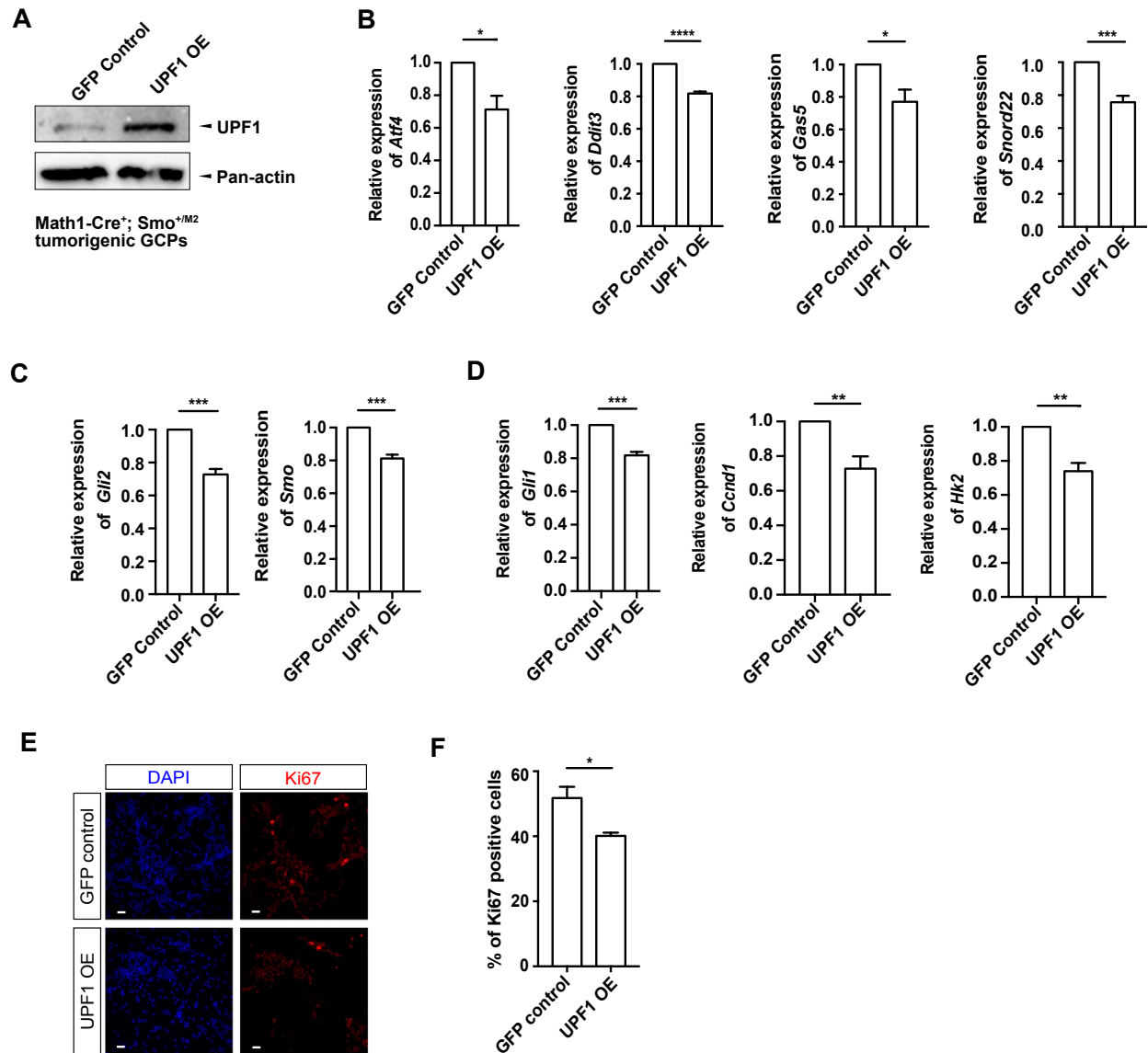


Figure 4.7.1 NMD upregulation decreases tumor cell proliferation *in vitro*.

(A) P5 *Math1-Cre⁺; Smo^{+M2}* tumorigenic GCPs were infected with UPF1 to upregulate NMD or GFP as a control. The total cell lysates were analyzed by western blotting with the indicated antibodies; Pan-actin was used as the loading control.

(B) Relative endogenous mRNA levels of known NMD targets; *Atf4*, *Ddit3*, *Gas5* and *Snord22* upon NMD upregulation in *Math1-Cre⁺; Smo^{+M2}* tumorigenic GCPs, as measured by qRT-PCR; n=3.

(C) Relative endogenous mRNA levels of Shh pathway activators; *Gli2* and *Smo* upon NMD upregulation in *Math1-Cre⁺; Smo^{+M2}* tumorigenic GCPs, as measured by qRT-PCR; n=3.

(D) Relative endogenous mRNA levels of Gli2 transcriptional targets that are known to regulate GCP proliferation (*Gli1*, *Ccnd1* and *Hk2*) upon NMD upregulation in *Math1-Cre⁺*; *Smo^{+M2}* tumorigenic GCPs, as measured by qRT-PCR; n=3.

(E) P5 *Math1-Cre⁺*; *Smo^{+M2}* tumorigenic GCPs infected with UPF1 or GFP control followed by immunofluorescence with an antibody against Ki67. Proliferation of infected GCPs was measured as a percentage of number of cells positively stained for Ki67 relative to total number of DAPI stained cells per condition.

(F) IF quantification of Ki67 positive staining in (E); n=3.

Transcript levels were normalized to *Gusb* in (B-D). In (E-F), Unpaired t-test was performed, and error bars represent SEM.

We next wanted to determine whether NMD upregulation could decrease tumor cell proliferation and the aggressiveness of medulloblastoma tumors *in vivo*. To test this, we performed orthotopic transplantation of tumorigenic *Math1-Cre⁺; Smo^{+M2}* GCPs that were isolated from P5 cerebella and then transduced for one hour with either a UPF1 or GFP control lentivirus, and then immediately transplanted into the cerebella of P5 wildtype recipient mice (**Figure 4.7.2A**). Animals were monitored frequently and when symptoms of medulloblastoma were apparent the animals were euthanized and the presence of a medulloblastoma was confirmed by autopsy. Tumor tissue was collected for further analyses. Increased expression of UPF1 was confirmed in the tumor tissue by immunoblotting and immunostaining (**Figure 4.7.2B-D**). Consistent with NMD upregulation, i) classic NMD targets, ii) the NMD-sensitive Shh pathway effectors *Gli2* and *Smo*, and iii) the Shh pathway transcriptional targets *Gli1*, *Hk2*, and *Ccnd1* were all downregulated in UPF1 overexpressing tumors compared to GFP control tumors (**Figure 4.7.2E-G**). In line with the Shh pathway and its targets being important drivers of tumorigenic GCP proliferation, increased NMD activity led to a reduction in GCP proliferation (**Figure 4.7.2H-I**). Together, these results indicate that, even in highly aggressive Smo-M2 tumors, NMD activation downregulates Shh pathway activity and proliferation.

Lastly, we assessed if this would impact survival. Kaplan-Meier analysis showed that NMD activation causes a delay in medulloblastoma tumor latency and extends survival time by 31% ($p=0.0018$; **Figure 4.7.2J**). Thus, NMD upregulation decreases tumor cell proliferation and decreases the aggressiveness of mouse medulloblastoma tumors.

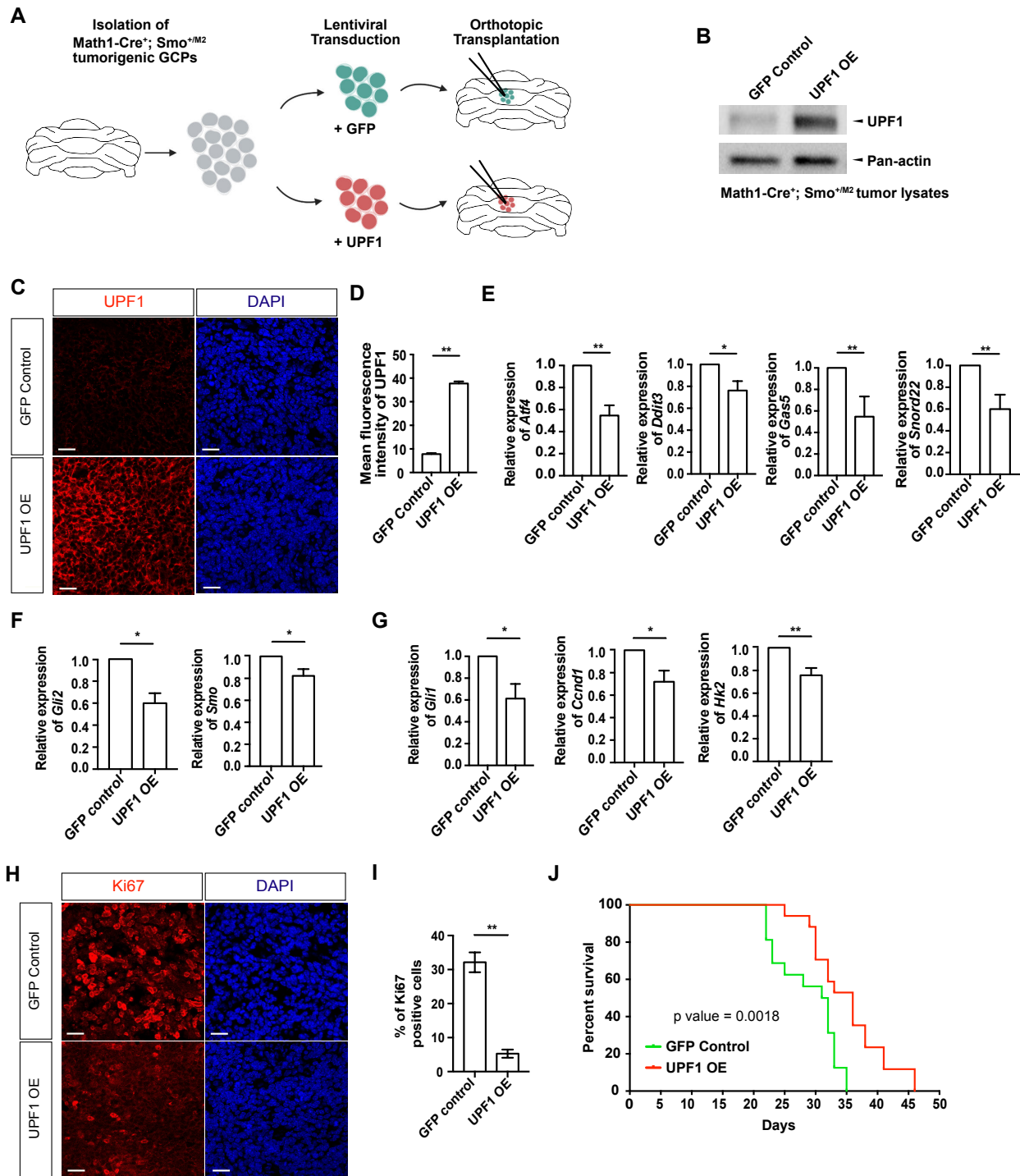


Figure 4.7.2. NMD upregulation leads to a delay in MB tumor latency and significantly improved survival *in vivo*.

(A) Schematic depicting the orthotopic transplantation approach where tumorigenic *Math1-Cre⁺; Smo^{+M2}* GCPs were transduced by spin-inoculation with either a GFP or a UPF1 lentivirus before transplantation into P5 C56BL6 wildtype recipient mice.

- (B) Representative immunoblot of total cell lysates from tumor tissue obtained from mice with UPF1 OE or GFP as control as depicted in (A); Pan-actin was used as the loading control.
- (C) Sections of MB tumors from C56BL6 mice that received cerebellar transplants of *Math1-Cre⁺*; *Smo^{+M2}* tumorigenic GCPs infected with UPF1 or GFP were stained with UPF1 antibody to confirm UPF1 OE.
- (D) Quantification of mean UPF1 fluorescence intensity in (C).
- (E) Relative endogenous mRNA levels of known NMD targets; *Atf4*, *Ddit3*, *Gas5* and *Snord22* upon NMD upregulation in tumors, as measured by qRT-PCR; n=3.
- (F) Relative endogenous mRNA levels of Shh pathway activators; *Gli2* and *Smo* upon NMD upregulation in *Math1-Cre⁺*; *Smo^{+M2}* tumorigenic GCPs, as measured by qRT-PCR; n=3.
- (G) Relative endogenous mRNA levels of Gli2 transcriptional targets that are known to regulate GCP proliferation (*Gli1*, *Ccnd1* and *Hk2*) upon NMD upregulation in *Math1-Cre⁺*; *Smo^{+M2}* tumorigenic GCPs, as measured by qRT-PCR; n=3.
- (H) P5 *Math1-Cre⁺*; *Smo^{+M2}* tumorigenic GCPs infected with UPF1 or GFP control followed by immunofluorescence with an antibody against Ki67. Proliferation of infected GCPs was measured as a percentage of number of cells positively stained for Ki67 relative to total number of DAPI stained cells per condition.
- (I) IF quantification of Ki67 positive staining in (H); n=3.
- (J) Kaplan-Meier survival analysis of C56BL6 mice that received cerebellar transplants of *Math1-Cre⁺*; *Smo^{+M2}* tumorigenic GCPs infected with UPF1 (red) or GFP (green).

Scale bar represents 35 μ m in (C, H). Transcript levels were normalized to *Gusb* in (E-G). Unpaired t-test was performed, and error bars represent SEM in (E-G, I).

4.8. NMD activity level is a determinant of prognosis in specific subgroups of human medulloblastoma.

All data presented thus far were obtained in MB mouse model; thus, we next used bioinformatics analyses to assess whether NMD might also play a role in human MB. For this, we analyzed human MB cohorts from published datasets (Pecan, cBioportal, Medullo500) for the presence of mutations in genes involved in the NMD machinery. We found that less than 1% of MB have mutations and/or copy number loss in NMD components (data not shown). This indicates that mutations/deletions of NMD components is not a main event in MB tumorigenesis. However, other molecular mechanisms could lead to inactivation of NMD in MB: For example, mutations could occur in the regulatory sequences of genes involved in the NMD process (such as promoters and enhancers), in transcription factors controlling the expression of NMD genes, at the epigenetic level (and affect the expression of NMD components), or could occur in signalling pathways controlling NMD component activity^{201,307 192,308-310}.

Regardless of the cause, events leading to a downregulation/inactivation of NMD activity would lead to an upregulation of mRNAs that are NMD targets. Thus, in addition to looking for mutations in NMD components, we also looked to see whether the NMD activity status of human MB tumors are affected in some MB tumors. For this, we used a published list of NMD targets (UPF1 binding targets identified using crosslinking/immunoprecipitation-sequencing (CLIP-seq; which we refer to as the *Burge signature*)³¹¹. As expected, this list contains many of the classic NMD targets, such as ATF4, DDIT3, etc. We used this list to generate an NMD target gene signature of ~200 genes. We then analyzed gene expression in a published cohort of 763 MB samples (Cavalli) for this signature. Of interest, some MB exhibit low levels of NMD targets, while others exhibit high levels of NMD targets. This suggests that some MB samples have an inactivation or a severe decrease in

their NMD process, while other samples do not. Next, we looked at the overall survival of individuals with tumors exhibiting high NMD targets, for each of the four MB subgroups (**Figure 4.8A**). Interestingly, we found that NMD-deficient tumors (thus exhibiting high NMD targets) have a worse survival prognosis compared to tumors having low NMD targets. This effect was significant for SHH-MB, Group3-MB and Group4-MB, but not for WNT-medulloblastoma (**Figure 4.8B-E**) We also performed this analysis using an independent NMD target signature, this time identified by the immunoprecipitation of phospho-UPF1, followed by the sequencing of the bound mRNAs (*Maquat signature*)¹⁴⁷ and we observed similar results (**Figure 4.8F**). Overall, these human data are consistent with our results indicating that when NMD is inactivated in the *Ptch1* Shh-MB mouse model (through *Smg1* or *Upf1* inactivation), the survival of these mice is significantly decreased. Together, these results suggest that NMD inactivation makes MB tumors more aggressive.

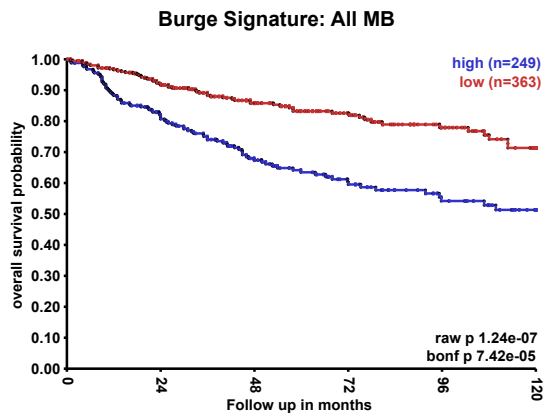
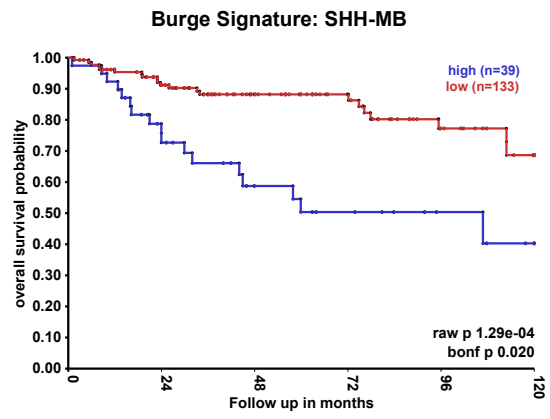
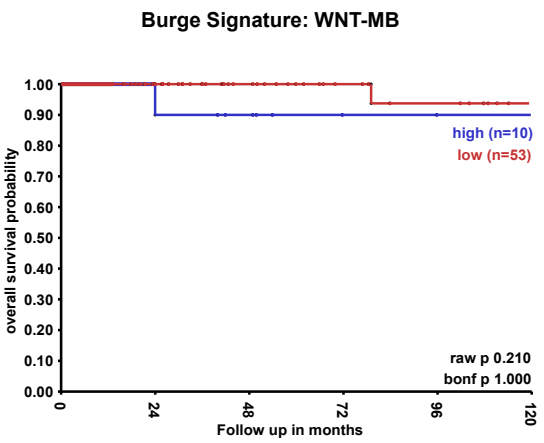
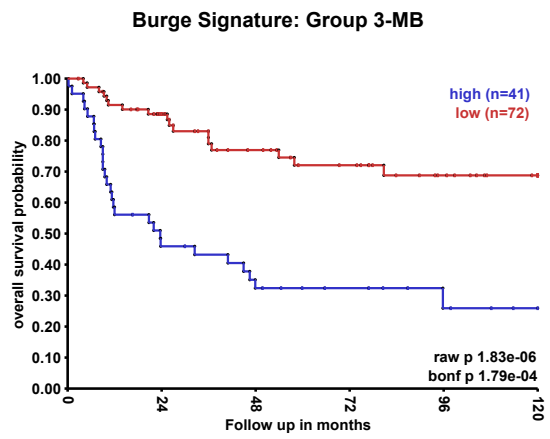
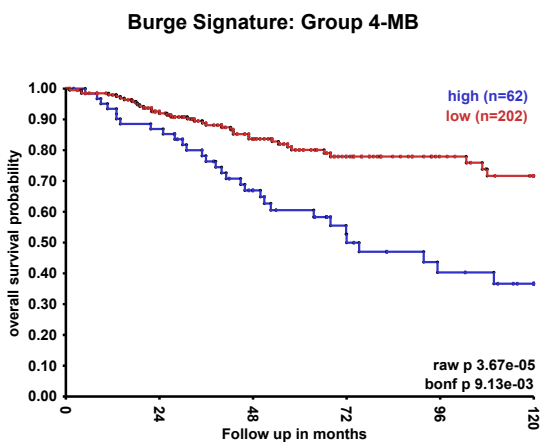
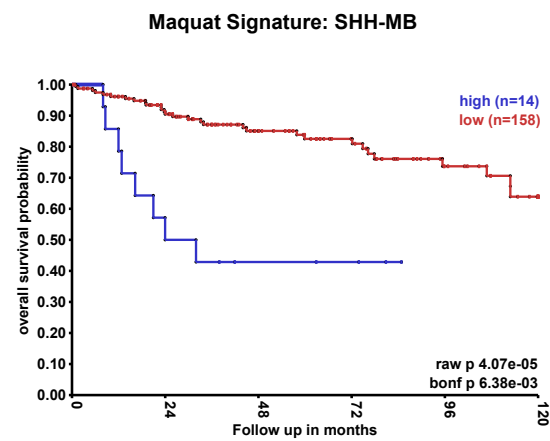
A**B****C****D****E****F**

Figure 4.8. NMD activity level is a determinant of prognosis in specific subgroups of human medulloblastoma.

Using published lists of NMD targets generated by the Burge laboratory (CLIP-seq used to identify direct UPF1 binding targets) and the Maquat laboratory (p-UPF1 RIP-seq), we generated two NMD target gene signatures (288 genes for the Burge signature and 104 genes for the Maquat signature). Using the R2 Genomics platform, these signatures were used to perform expression analysis on a published cohort of human MB samples (Cavalli dataset) and stratify the samples in high (blue) and low (red) NMD target expression. Kaplan-Meier overall survival probability analysis was performed on these high and low groups. The overall survival probability for MB patients having high vs low NMD target expression of the Burge signature is plotted in (A-E) and for Maquat signature in (F):

(A) All four MB subgroups combined; (B) SHH-MB subgroup; (C) WNT-MB;
(D) Group 3-MB; (E) Group 4-MB; (F) SHH-MB.

The raw p-values, Bonferroni corrected p-values, and the samples sizes for high vs low groups are indicated in the respective graphs.

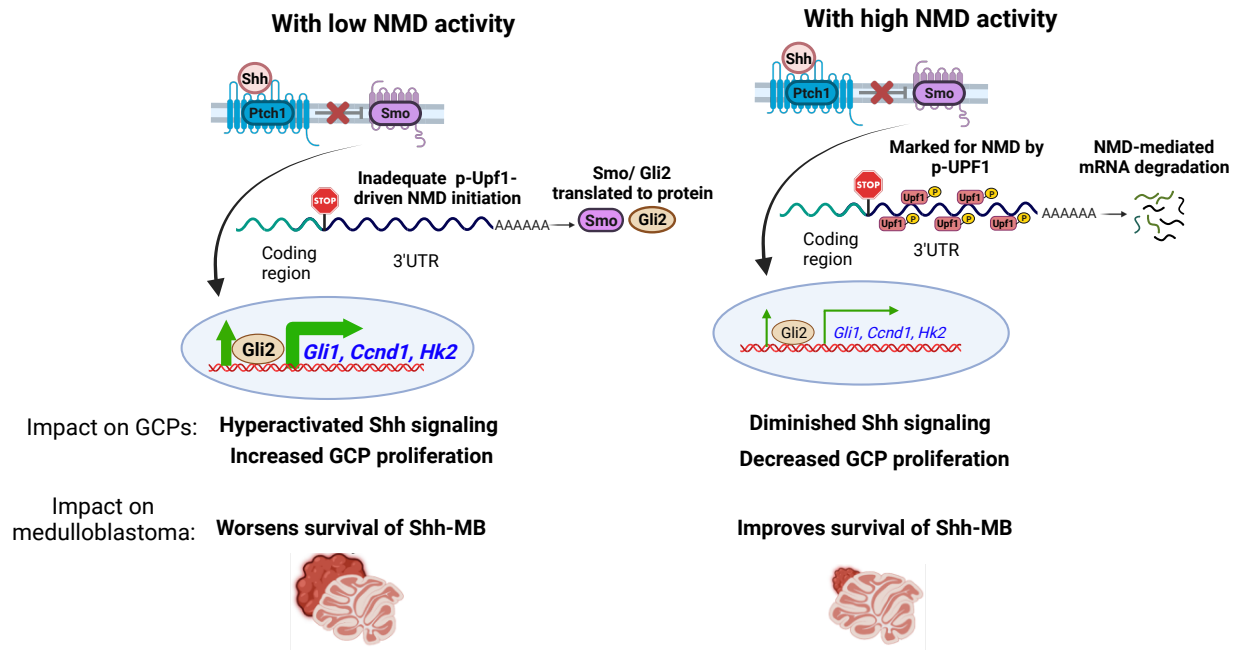
Chapter 5
General Discussion

In the present study, we have identified that suppression of a post-transcriptional gene expression modulator such as NMD increased Shh pathway activity in cerebellar GCPs and delineated the mechanism of NMD-mediated regulation of the Shh pathway. We identified the presence of one or more “NMD-inducing” features in the transcripts of positive regulators of the Shh pathway (*Smo* and *Gli2*) using a genome-wide bioinformatic approach for NMD feature prediction. Several reports have shown that presence of long 3' UTRs or 3'UTR introns in endogenous mRNAs can be a potential trigger of NMD^{142,194,311-313}. *Smo* and *Gli2* mRNAs possessed (1) 3'UTRs of length greater than 1000 nt, and (2) one intron within this long 3'UTR. Their expression levels were observed to be regulated by NMD, as proven using an NMD translational reporter assay. Furthermore, using p-UPF1 RIP-qRT-PCR assay, we demonstrate that the NMD pathway activator p-UPF1, which acts as a marker of NMD targets directly interacts with NMD sensitive Shh signaling components (*Smo* and *Gli2*) on their 3'UTRs to propel them for subsequent degradation. To date, this is the first study to identify *Smo* and *Gli2* as novel and direct NMD targets due to the NMD-sensitive nature of their 3'UTRs. Future studies will have to be performed to assess if and how the other NMD-triggering feature in *Smo* and *Gli2*, such as uORF also contribute to their NMD-mediated degradation.

We observed hyperactivated Shh signaling in GCPs upon NMD inhibition led to their excessive proliferation through the upregulation of genes important for cell proliferation. Overactivation of Shh pathway leads to MB, and thus NMD can have serious implications in MB. Combined inactivation of NMD and *Ptch1* increased tumor incidence, size, and decreased survival. Increased transcriptional activity of the Shh pathway was reflected in these NMD inactivated tumors. Conversely, NMD activation delayed tumor latency, improved survival and displayed reduced Shh signaling activity. This is supported by our bioinformatic analyses on publicly available human

MB datasets, wherein we discovered human MB with low NMD activity having worse survival than tumors with normal/high NMD activity. In summary, NMD senses the nature of 3'UTR, such as the length of 3' and presence of intron in 3'UTR, to function as a direct regulator of Shh signaling components, and subsequently also functions as a novel tumor suppressor in Shh-MB.

Graphical abstract



NMD modulates Shh signaling in cerebellar progenitors, and functions as a novel tumor suppressor in MB progression.

- (A) Low NMD activity results in hyperactivation of Shh signaling in GCPs, as positive effectors of the pathway *Smo* and *Gli2*, which we identified as de novo NMD targets were upregulated, facilitating increased GCP proliferation. This reflected in worse survival in mice with Shh-MB.
- (B) High NMD activity diminishes Shh signaling in GCPs resulting in decreased GCP proliferation due to the p-UPF1 mediated NMD degradation of *Smo* and *Gli2*. This reflected in delaying the tumor latency and improving time of survival *in vivo*.

5.1. Interdependency of NMD regulation and Shh signaling in MB

Here, we report that a subset of human MB with hyperactivated Shh signaling have reduced activity of the post transcriptional surveillance process of NMD owing to their enriched NMD target signature and display poor survival when compared to SHH-MBs with proper functional NMD activity. Complementary to our findings, analysis of genome wide CHIP-Seq analysis of *Gli1* binding sites performed in embryonic stem cell (ESC)-derived neural progenitors revealed *Upf3a*, a potent NMD inhibitor as a putative gene bound to Gli1^{164,314}. Furthermore, another study identified *Upf3a* was co-activated to higher levels by STAT3 and GLI via mining of Gli1 and STAT3 ChIP-seq datasets³¹⁵. They also show that high expression of *Upf3a* gene is associated in breast cancers with worse survival, an effect similarly observed by us in NMD deficient SHH-MB. Of note, a study by Yuan *et al* revealed Smo-mediated Shh signaling in Shh MB cells is dependent on STAT3 and STAT3 is required for Shh-MB cell proliferation and survival³¹⁶. Based on these observations, it is indicative that either GLI1 on its own and/or GLI1 and STAT3 together work to control NMD activity via UPF3A. Together with our experiments showing that NMD inhibition in GCPs stimulates Shh signaling and stimulates GCP proliferation in a Smo-Shh signaling-dependent manner, these results suggest a possible mechanism that NMD participates in a feedback loop with Shh pathway, wherein elevated Shh signaling stimulates UPF3A expression which leads to an intrinsic inhibition of NMD, that further aids to maintain hyperactivated Shh signaling in MB tumorigenesis.

5.2. Role of NMD in maintaining the equilibrium between proliferation and differentiation

We demonstrate that inhibition of NMD in GCPs led to their increased proliferation. NMD plays a role in regulating proliferation and maintaining cellular homeostasis by controlling the expression of key genes involved in cell cycle regulation, differentiation, and tissue development. Although high magnitude of NMD promotes the neural stem cell (NSC) state, i.e. proliferation of NSCs at early stages of neural development (E14.5) to ensure availability of high pool of NSCs, NMD has the opposite role at later stages of neural development close to birth (E18.5) where it promotes neural differentiation^{201,261}. In this study, NMD inhibition via UPF3B depletion in E18.5 neural progenitor cells (NPCs) increases their proliferation and impairs neurite formation, suggesting that NMD promotes the differentiation of already committed neural progenitor cells. In contrast, other groups have reported that hematopoietic stem cells and embryonic stem cells depend on NMD for their proliferation, and on NMD suppression for their differentiation^{201,220,228}.

In the developing cerebellum, the role of NMD specifically in post-mitotic GN remains to be explored. *Ccnd1* is an important gene that is downregulated in GCPs to initiate their cell cycle exit and differentiation²⁹⁸. We show that NMD activation downregulates *Ccnd1*. This raises a possibility that NMD is required for normal GCPs to differentiate to GN by downregulating *Ccnd1*. Cheng *et al* demonstrated that tumor cell differentiation suppresses MB growth³¹⁷. Of note, we observe that NMD activation in tumorigenic GCPs, lead to a delayed MB onset, and improved time of survival.

Our model shows that NMD inhibition increases the proliferation of postnatal GCPs, which are defined as committed precursor cells destined to differentiate into granule neurons, however we do not observe any impact on P5 GCP differentiation *in vitro*.

Such diverse roles of NMD in maintaining proliferation vs differentiation can be attributed to several reasons. First and foremost, it is crucial to keep in mind that different cell types can control and uphold the equilibrium between proliferation and differentiation depending on the spatial (location of NMD action) and temporal (embryonic/postnatal date) NMD regulation during every developmental stage, as the examples discussed above. Second, the culture conditions employed in the different studies may necessitate distinct proliferation and differentiation programs, thereby yielding diverse responses and biological outcomes when NMD is modulated *in vitro*. Third, gene manipulation strategies employed in these studies vary, reflecting in their diverse efficiencies to generate NMD magnitude-based responses. Fourth, different NMD factors have been investigated by these groups, and the NMD-independent functions of these factors might contribute to these biological variations/discrepancies.

The role of NMD in cancer can be seen as a "double-edged sword". In the context of various cancers such as colorectal cancer, gastric cancer, fibrosarcoma, colorectal adenocarcinoma, lymphoma, papillary adenocarcinoma, acute myeloid leukemia, NMD acts a suppressor of tumor proliferation, similar to Shh-MB^{277,278,297,308,318,319}. Whereas in others such as colorectal cancers with microsatellite instability and MDM2-overexpressed TP53 wild-type cancers, NMD promotes tumor proliferation^{320 321}. Altogether, the differential effect of NMD can be due to a complex interplay of intrinsic and extrinsic factors that can vary depending on the cell type, developmental stage, environmental cues, mRNA features, genetic and epigenetic factors, alternative splicing, core NMD factor/regulator levels and even crosstalk with stress pathways or other RNA degradation pathways such as miRNA-mediated degradation.

5.3. NMD, genomic instability and MB: the sisterhood

Genomic stressors including DNA lesions, secondary DNA structures, R-loops and oncogenes can induce replication stress and DNA damage. Of note, SHH-MB is associated with the loss of genes involved in homologous recombination or non-homologous end joining (NHEJ) processes, suggesting strongly that the cell of origin of these tumors, GCPs are highly responsive to DNA repair mechanisms. In addition, GCPs proliferating in the EGL *in vivo* exhibit higher γ -H2AX levels (a readout for DNA damage levels), and DNA breaks *in vitro*^{51,52}. Shh signalling in GCPs is a mitogenic pathway, but hyperactivation of the pathway causes MB. The underlying mechanism for this neoplastic transformation is the induction of replication stress by Shh, specifically increased replication origin firing and fork speed⁵². In the *Ptch1*^{+/-} mice, this causes DNA damage, and an increase in somatic recombination events such as LOH of *Ptch1*, which leads to ligand-independent constitutive signalling, associated with the development of preneoplasia^{52,120}. Additional oncogenic drivers like *p53* mutations promote advanced tumor development¹²⁰. This study from our lab established the link between genomic instability in GCPs and SHH-MB initiation⁵².

My experiments demonstrated that NMD inhibition in *Ptch1*^{+/-} mice hyperactivated Shh signaling and resulted in advanced MB formation. Hence, it will be interesting to determine whether NMD directly plays a role in DNA damage and replication stress, specifically in response to Shh in GCPs.

An interesting study showed that UPF1 is essential to maintain genomic stability. In addition to NMD inhibition, depletion of UPF1 also resulted in (1) early S-phase arrest in HeLa cells, (2) more γ -H2AX-positive cells and (3) increase in chromosomal aberrations due to the arrest of replication forks³²². This DNA-damage response induced by UPF1 depletion occurs in an ATR

dependent manner, which is a PIKK primarily involved in regulating the cellular response to replication block³²². In support, a very recent study by Nie *et al* demonstrated that DNA replication was impaired with AS-NMD inhibition³²³. They revealed that UPF1 knockdown had a significant impact on replication fork speed and symmetry³²³. Furthermore, in human tumor cell lines, depletion of SMG1 results in constitutive phosphorylation/activation of CHK2 and p53, increase in H2AX foci and number of chromosomal abnormalities¹⁷⁴. Thus, these studies reveal important roles for NMD factors in DNA replication and DNA repair to maintain genomic integrity.

Another putative link between NMD-genomic instability-MB is described below. A subset of patients with SHH-MB were found to harbor *BRCA2* mutations⁹⁶. In mice with complete loss of *BRCA2* driven by a *Nestin-Cre* promoter, rapid development of MB was reported. Although, *BRCA2* is a well-known tumor-suppressor gene, it is also an essential protein for repairing DNA strand breaks, specifically those high frequency, naturally occurring breaks in neurons during neurogenesis³²⁴⁻³²⁶. Intriguingly, *BRCA2* is a UPF3B-dependent NMD target²⁶². This raises the possibility that NMD can target *BRCA2* mRNA for degradation and thus influence the repair of these DNA breaks in neurons, and potentially lead to suppression of MB tumorigenesis. Nickless *et al* demonstrated that persistent DNA damage diminishes NMD activity in a p38 α MAPK dependent manner, causing an increase in the NMD-sensitive stress inducible transcription factor, ATF3 and transcriptional regulation of its downstream targets involved in stress³²⁷.

In conclusion, our study together with other published data described above points to a potential feedback loop in Shh-MB which involves (1) Shh-induced oncogenic transformation of GCPs, (2) replication stress and DNA damage, (3) genomic instability in turn inhibits NMD and (4) NMD inhibition results in subsequent hyperactivation of Shh signaling. Further research is

required in the context of Shh-MB to understand if and how SHH-replication stress and DNA damage can regulate NMD, and if NMD is involved in mediating genomic instability in GCPs.

5.4. NMD activation as potential therapy for SHH-MB

Existing treatments for MB comprise of surgery followed by chemotherapy and/or radiotherapy, which are non-specific to the tumor subtype, aggressive and renders patients with severe neurological deficits. Therefore, it is necessary to improve our knowledge of the molecular mechanisms underlying MB in order to increase treatment specificity. Our data not only shows that NMD activation in a very aggressive Shh-MB mouse model decreases tumor cell proliferation through negative regulation of Shh signalling, but also an improvement in survival of mice *in vivo*. This is the first report to identify NMD as a novel tumor suppression mechanism in MB formation, in addition to identifying *Smo* and *Gli2* as *de novo* NMD targets and elucidating that 3'UTR length recognition is the mechanistic trigger of their NMD. Our study provides a proof of concept for the design of NMD activation as a novel MB therapeutic approach. To my knowledge, proper NMD activators have not yet been definitively identified. Below, I describe some of the ways NMD activation could be achieved.

1) We can identify potential NMD-activating small molecules by performing a high throughput screen of compounds and testing their NMD efficiency using the well-established beta-globin NMD reporter system, as described in Chapter 4.4. Nickless *et al* utilised this approach to successfully identify NMD inhibitors, but also identify four putative compounds that were suggested to activate NMD, including Tranilast³²⁸. Tranilast, potentially through NMD activation has been shown to protect against the neurotoxicity caused by arginine-rich dipeptide repeats-mediated NMD inhibition in human neuroblastoma cell line and *Drosophila*. Although the exact

mechanism of action of Tranilast is unknown, this oral drug is traditionally used to treat bronchial asthma, so it is well-tolerated, has low toxicity and is known to cross the blood-brain barrier, thus making it a potential treatment choice³²⁹.

Given UPF1 phosphorylation is a central and essential function in NMD, it is logical that agents that promote this process will activate NMD. The kinase SMG1 is responsible for UPF1 phosphorylation, thus screening for small molecules that would trigger SMG1 kinase activity, for instance, could be a prime approach to activate NMD. In line with this suggestion, Huang et al and other groups have shown that SMG1 overexpression triggers NMD^{153,191}. Alternatively, inhibitors of phosphatases that target UPF1 would be expected to activate NMD by allowing phosphorylation of UPF1. For example, Durand et al showed NMD is activated when UPF1 is hyperphosphorylated¹⁷³. Screening for compounds that stimulate UPF1 to associate with UPF1-binding partners necessary for NMD, is an alternative method to finding compounds that enhance UPF1 phosphorylation. This idea arises from work by Sanchez *et al*, who observed degradation of subsets of NMD targets due to NMD activation aided by the high expression of Coactivator-Associated Methyltransferase-1 (*CARM1*) in the motor neuron disease Spinal muscular dystrophy³³⁰. This is through direct UPF1 association with *CARM1* in an RNA-dependent manner³³⁰. As a result, NMD could potentially be activated by agents that increase *CARM1* expression or activity.

Studies from Shum *et al* demonstrate UPF3A competes with its paralog UPF3B for EJC binding to inhibit NMD¹⁶⁴. Thus, NMD can be activated by inhibiting UPF3A, or its binding. Small molecule screening for NMD activators should include (1) inhibitors specific to UPF3A, but not UPF3B or any other UPF factors and/or (2) drugs that can result in transcriptional repression of UPF3A and/or (3) agents that prevent binding of UPF3A to EJC or UPF2.

2) Another approach is to use a recent antisense approach to modulation of gene expression. Antisense oligonucleotides (ASO) have the capacity to promote NMD-mediated degradation of specific oncogenic transcripts. The NMD-inducing oligonucleotides don't exert a global effect on activating the NMD pathway but rather specifically bind and block the translation initiation of NMD substrates. For instance, Tano *et al* used an NMD-inducing morpholino against STAT3 in human breast cancer cells to decrease oncogenic STAT3 expression³³¹. Another successful example is from Liang *et al*, where they observe ASO triggering NMD pathway even in NMD impaired conditions to reduce mRNA levels of alternatively spliced NMD-sensitive *NCL*³³².

3) To date, NMD induction as gene therapy for cancer has not been tested, but there is growing literature for promising results in neurodegenerative diseases. Increasing expression of human UPF1 in a rat paralysis model for amyotrophic lateral sclerosis abrogated the devastating motor paralysis phenotype³³³. Additional evidence provided by another group shows overexpression of UPF1 in human gastric cancer cells decreased tumor cell proliferation, cell cycle progression, cell migration and invasion and increased apoptosis²⁹⁷. Future studies are pertinent to test the success of the UPF1 induction approach in more cancer models.

A serious implication of chemotherapy is excessive NMD inhibition through UPF1 and UPF2 cleavage, the consequence of which is upregulation of apoptosis related NMD targets^{334,335}. Therefore, NMD activation therapy could potentially be used in combination with chemotherapy to protect normal cells from apoptosis, by reversing the NMD inhibition caused by chemotherapeutics³³⁶. Proving NMD activation therapy can protect or improve normal cell survival during chemotherapy is crucial, which may allow for higher doses of chemotherapy to be administered, thereby facilitating better recovery post chemotherapy³³⁶. UPF1 OE has also been

shown to improve the sensitivity of cancer cells to the chemotherapeutic drug doxorubicin, opening the possibility of this approach to enhance efficiency of chemotherapy²⁹⁷.

In conclusion, our work identifies NMD as a critical regulator of the Shh pathway, through 3'UTR length recognition of activators of this crucial neurodevelopmental pathway, both in the developing cerebellum and in MB. Furthermore, it provides strong evidence that NMD activation has a great potential to be used as a targeted therapy for MB.

Chapter 6

Conclusion

With the broad goal to discover novel druggable targets to aid in precision medicine treatment approaches for MB, my PhD dissertation research primarily sought to advance our understanding of medulloblastoma progression by identifying potential collaborators of *Ptch1* LOH. With the discovery of more than one NMD factor being mutated in the spontaneous *Ptch1*^{+/-} mouse MB model, my research expanded to addressing more questions:

- (1) Can NMD regulate Shh signaling in cerebellar GCPs?
- (2) Can NMD accelerate neoplastic transformation of cerebellar GCPs? and
- (3) What is the mechanism mediating regulation of Shh signaling by NMD?

I have utilized three key tools to answer these questions: mouse cerebellar GCPs, *Ptch1*^{+/-} mouse MB model, and Math1-Cre driven overactivated SmoM2 mouse MB model.

The developing cerebellum is a highly dynamic environment; hence it is logical that the cerebellar progenitors rely heavily on a tightly regulated post-transcriptional control of gene expression for the temporal localisation of only the essential mRNAs and elimination of the redundant or unproductive transcripts postnatally. RNA-binding proteins including NMD factors (UPF, SMG and EJC protein families) and their corresponding protein and RNA interactomes play a major role in this mRNA regulation. This can modulate key cellular processes such a proliferation and differentiation.

In this thesis, I identify a hitherto unknown role for NMD as a molecular pathway that is involved in regulating the proliferation of cerebellar progenitors. My experiments not only shows that NMD inhibits GCP proliferation, but it does so by acting directly on GCP proliferation regulators, which we identify as novel NMD targets. Our results support the idea that inactivation of NMD may promote the progenitor cell state by stimulating GCP proliferation, which is the

perfect driver for tumor progression. This is further strengthened by our observation that NMD inhibition in the *Ptch1*^{+/-} mouse MB model results in more aggressive MB tumors.

This thesis identifies physiological *Smo* and *Gli2* mRNAs which are positive effectors of the Shh pathway as *de novo* NMD targets, due to the presence of NMD triggering features. We also show that phosphorylation occurs on UPF1 bound to these targets to eventually induce mRNA decay. *In silico* genome-wide prediction of NMD features revealed *Ccnd1* and *Hk2* were also found to have NMD triggering features, how these features may contribute to MB tumorigenesis is yet to be explored. Finally, with our UPF1 over expression experiments *in vivo*, we also provide strong evidence for the design of NMD activation as a potential MB therapeutic approach.

Our research aims to produce clinically impactful discoveries in neuroscience that will improve the survival and quality of life of patients with brain diseases. While this approach of precision medicine ultimately strives for a cure, insights from our work is a small step taken towards the aim of lengthening patient survival by reducing the neurological and cytotoxic side effects of radio-chemotherapy on patients. On a broader level, it also contributes to better patient stratification, identification of prognostic markers and ultimately improved clinical trial designs.

Chapter 7
Bibliography

1. Leto, K., Arancillo, M., Becker, E.B., Buffo, A., Chiang, C., Ding, B., Dobyns, W.B., Dusart, I., Haldipur, P., Hatten, M.E., et al. (2016). Consensus Paper: Cerebellar Development. *Cerebellum* 15, 789-828. 10.1007/s12311-015-0724-2.
2. Hoshino, M., Nakamura, S., Mori, K., Kawauchi, T., Terao, M., Nishimura, Y.V., Fukuda, A., Fuse, T., Matsuo, N., Sone, M., et al. (2005). Ptf1a, a bHLH transcriptional gene, defines GABAergic neuronal fates in cerebellum. *Neuron* 47, 201-213. 10.1016/j.neuron.2005.06.007.
3. Leto, K., and Rossi, F. (2012). Specification and differentiation of cerebellar GABAergic neurons. *Cerebellum* 11, 434-435. 10.1007/s12311-011-0324-8.
4. Hatten, M.E., and Heintz, N. (1995). Mechanisms of neural patterning and specification in the developing cerebellum. *Annu Rev Neurosci* 18, 385-408. 10.1146/annurev.ne.18.030195.002125.
5. Laine, J., and Axelrad, H. (2002). Extending the cerebellar Lugaro cell class. *Neuroscience* 115, 363-374. 10.1016/s0306-4522(02)00421-9.
6. Morales, D., and Hatten, M.E. (2006). Molecular markers of neuronal progenitors in the embryonic cerebellar anlage. *J Neurosci* 26, 12226-12236. 10.1523/JNEUROSCI.3493-06.2006.
7. Dino, M.R., Schuerger, R.J., Liu, Y., Slater, N.T., and Mugnaini, E. (2000). Unipolar brush cell: a potential feedforward excitatory interneuron of the cerebellum. *Neuroscience* 98, 625-636. 10.1016/s0306-4522(00)00123-8.
8. Fink, A.J., Englund, C., Daza, R.A., Pham, D., Lau, C., Nivison, M., Kowalczyk, T., and Hevner, R.F. (2006). Development of the deep cerebellar nuclei: transcription factors and cell migration from the rhombic lip. *J Neurosci* 26, 3066-3076. 10.1523/JNEUROSCI.5203-05.2006.
9. Wang, V.Y., Rose, M.F., and Zoghbi, H.Y. (2005). Math1 expression redefines the rhombic lip derivatives and reveals novel lineages within the brainstem and cerebellum. *Neuron* 48, 31-43. 10.1016/j.neuron.2005.08.024.
10. Alder, J., Cho, N.K., and Hatten, M.E. (1996). Embryonic precursor cells from the rhombic lip are specified to a cerebellar granule neuron identity. *Neuron* 17, 389-399. 10.1016/s0896-6273(00)80172-5.
11. Leto, K., Carletti, B., Williams, I.M., Magrassi, L., and Rossi, F. (2006). Different types of cerebellar GABAergic interneurons originate from a common pool of multipotent progenitor cells. *J Neurosci* 26, 11682-11694. 10.1523/JNEUROSCI.3656-06.2006.
12. Machold, R., and Fishell, G. (2005). Math1 is expressed in temporally discrete pools of cerebellar rhombic-lip neural progenitors. *Neuron* 48, 17-24. 10.1016/j.neuron.2005.08.028.
13. Haldipur, P., and Millen, K.J. (2019). What cerebellar malformations tell us about cerebellar development. *Neurosci Lett* 688, 14-25. 10.1016/j.neulet.2018.05.032.
14. Englund, C., Kowalczyk, T., Daza, R.A., Dagan, A., Lau, C., Rose, M.F., and Hevner, R.F. (2006). Unipolar brush cells of the cerebellum are produced in the rhombic lip and migrate through developing white matter. *J Neurosci* 26, 9184-9195. 10.1523/JNEUROSCI.1610-06.2006.
15. Roussel, M.F., and Hatten, M.E. (2011). Cerebellum development and medulloblastoma. *Curr Top Dev Biol* 94, 235-282. 10.1016/B978-0-12-380916-2.00008-5.

16. Parmigiani, E., Leto, K., Rolando, C., Figueres-Onate, M., Lopez-Mascaraque, L., Buffo, A., and Rossi, F. (2015). Heterogeneity and Bipotency of Astroglial-Like Cerebellar Progenitors along the Interneuron and Glial Lineages. *J Neurosci* 35, 7388-7402. 10.1523/JNEUROSCI.5255-14.2015.
17. Wallace, V.A. (1999). Purkinje-cell-derived Sonic hedgehog regulates granule neuron precursor cell proliferation in the developing mouse cerebellum. *Curr Biol* 9, 445-448. 10.1016/s0960-9822(99)80195-x.
18. Wechsler-Reya, R.J., and Scott, M.P. (1999). Control of neuronal precursor proliferation in the cerebellum by Sonic Hedgehog. *Neuron* 22, 103-114. 10.1016/s0896-6273(00)80682-0.
19. Dahmane, N., and Ruiz i Altaba, A. (1999). Sonic hedgehog regulates the growth and patterning of the cerebellum. *Development* 126, 3089-3100. 10.1242/dev.126.14.3089.
20. Izzli, L., Levesque, M., Morin, S., Laniel, D., Wilkes, B.C., Mille, F., Krauss, R.S., McMahon, A.P., Allen, B.L., and Charron, F. (2011). Boc and Gas1 each form distinct Shh receptor complexes with Ptch1 and are required for Shh-mediated cell proliferation. *Dev Cell* 20, 788-801. 10.1016/j.devcel.2011.04.017.
21. Miyata, T., Maeda, T., and Lee, J.E. (1999). NeuroD is required for differentiation of the granule cells in the cerebellum and hippocampus. *Genes Dev* 13, 1647-1652. 10.1101/gad.13.13.1647.
22. Miyazawa, K., Himi, T., Garcia, V., Yamagishi, H., Sato, S., and Ishizaki, Y. (2000). A role for p27/Kip1 in the control of cerebellar granule cell precursor proliferation. *J Neurosci* 20, 5756-5763. 10.1523/JNEUROSCI.20-15-05756.2000.
23. Pan, N., Jahan, I., Lee, J.E., and Fritzsche, B. (2009). Defects in the cerebella of conditional Neurod1 null mice correlate with effective Tg(Atoh1-cre) recombination and granule cell requirements for Neurod1 for differentiation. *Cell Tissue Res* 337, 407-428. 10.1007/s00441-009-0826-6.
24. Sillitoe, R.V., and Joyner, A.L. (2007). Morphology, molecular codes, and circuitry produce the three-dimensional complexity of the cerebellum. *Annu Rev Cell Dev Biol* 23, 549-577. 10.1146/annurev.cellbio.23.090506.123237.
25. Tamayo-Orrego, L., and Charron, F. (2019). Recent advances in SHH medulloblastoma progression: tumor suppressor mechanisms and the tumor microenvironment. *F1000Res* 8. 10.12688/f1000research.20013.1.
26. Briscoe, J., and Therond, P.P. (2013). The mechanisms of Hedgehog signalling and its roles in development and disease. *Nat Rev Mol Cell Biol* 14, 416-429. 10.1038/nrm3598.
27. Yang, L., Xie, G., Fan, Q., and Xie, J. (2010). Activation of the hedgehog-signaling pathway in human cancer and the clinical implications. *Oncogene* 29, 469-481. 10.1038/onc.2009.392.
28. Teglund, S., and Toftgard, R. (2010). Hedgehog beyond medulloblastoma and basal cell carcinoma. *Biochim Biophys Acta* 1805, 181-208. 10.1016/j.bbcan.2010.01.003.
29. Murone, M., Rosenthal, A., and de Sauvage, F.J. (1999). Sonic hedgehog signaling by the patched-smoothed receptor complex. *Curr Biol* 9, 76-84. 10.1016/s0960-9822(99)80018-9.

30. Haycraft, C.J., Banizs, B., Aydin-Son, Y., Zhang, Q., Michaud, E.J., and Yoder, B.K. (2005). Gli2 and Gli3 localize to cilia and require the intraflagellar transport protein polaris for processing and function. *PLoS Genet* *1*, e53. 10.1371/journal.pgen.0010053.
31. Allen, B.L., Song, J.Y., Izzi, L., Althaus, I.W., Kang, J.S., Charron, F., Krauss, R.S., and McMahon, A.P. (2011). Overlapping roles and collective requirement for the coreceptors GAS1, CDO, and BOC in SHH pathway function. *Dev Cell* *20*, 775-787. 10.1016/j.devcel.2011.04.018.
32. Cardozo, M.J., Sanchez-Arrones, L., Sandonis, A., Sanchez-Camacho, C., Gestri, G., Wilson, S.W., Guerrero, I., and Bovolenta, P. (2014). Cdon acts as a Hedgehog decoy receptor during proximal-distal patterning of the optic vesicle. *Nat Commun* *5*, 4272. 10.1038/ncomms5272.
33. Beachy, P.A., Hymowitz, S.G., Lazarus, R.A., Leahy, D.J., and Siebold, C. (2010). Interactions between Hedgehog proteins and their binding partners come into view. *Genes Dev* *24*, 2001-2012. 10.1101/gad.1951710.
34. Kenney, A.M., Cole, M.D., and Rowitch, D.H. (2003). Nmyc upregulation by sonic hedgehog signaling promotes proliferation in developing cerebellar granule neuron precursors. *Development* *130*, 15-28. 10.1242/dev.00182.
35. Kenney, A.M., and Rowitch, D.H. (2000). Sonic hedgehog promotes G(1) cyclin expression and sustained cell cycle progression in mammalian neuronal precursors. *Mol Cell Biol* *20*, 9055-9067. 10.1128/MCB.20.23.9055-9067.2000.
36. Lee, E.Y., Ji, H., Ouyang, Z., Zhou, B., Ma, W., Vokes, S.A., McMahon, A.P., Wong, W.H., and Scott, M.P. (2010). Hedgehog pathway-regulated gene networks in cerebellum development and tumorigenesis. *Proc Natl Acad Sci U S A* *107*, 9736-9741. 10.1073/pnas.1004602107.
37. Knoepfler, P.S., Cheng, P.F., and Eisenman, R.N. (2002). N-myc is essential during neurogenesis for the rapid expansion of progenitor cell populations and the inhibition of neuronal differentiation. *Genes Dev* *16*, 2699-2712. 10.1101/gad.1021202.
38. Pogoriler, J., Millen, K., Utset, M., and Du, W. (2006). Loss of cyclin D1 impairs cerebellar development and suppresses medulloblastoma formation. *Development* *133*, 3929-3937. 10.1242/dev.02556.
39. Oliver, T.G., Grasfeder, L.L., Carroll, A.L., Kaiser, C., Gillingham, C.L., Lin, S.M., Wickramasinghe, R., Scott, M.P., and Wechsler-Reya, R.J. (2003). Transcriptional profiling of the Sonic hedgehog response: a critical role for N-myc in proliferation of neuronal precursors. *Proc Natl Acad Sci U S A* *100*, 7331-7336. 10.1073/pnas.0832317100.
40. Yam, P.T., and Charron, F. (2013). Signaling mechanisms of non-conventional axon guidance cues: the Shh, BMP and Wnt morphogens. *Curr Opin Neurobiol* *23*, 965-973. 10.1016/j.conb.2013.09.002.
41. Flora, A., Klisch, T.J., Schuster, G., and Zoghbi, H.Y. (2009). Deletion of Atoh1 disrupts Sonic Hedgehog signaling in the developing cerebellum and prevents medulloblastoma. *Science* *326*, 1424-1427. 10.1126/science.1181453.
42. Goodrich, L.V., Milenkovic, L., Higgins, K.M., and Scott, M.P. (1997). Altered neural cell fates and medulloblastoma in mouse patched mutants. *Science* *277*, 1109-1113. 10.1126/science.277.5329.1109.

43. Hallahan, A.R., Pritchard, J.I., Hansen, S., Benson, M., Stoeck, J., Hatton, B.A., Russell, T.L., Ellenbogen, R.G., Bernstein, I.D., Beachy, P.A., and Olson, J.M. (2004). The SmoA1 mouse model reveals that notch signaling is critical for the growth and survival of sonic hedgehog-induced medulloblastomas. *Cancer Res* *64*, 7794-7800. 10.1158/0008-5472.CAN-04-1813.
44. Yang, Z.J., Ellis, T., Markant, S.L., Read, T.A., Kessler, J.D., Bourbonoulas, M., Schuller, U., Machold, R., Fishell, G., Rowitch, D.H., et al. (2008). Medulloblastoma can be initiated by deletion of Patched in lineage-restricted progenitors or stem cells. *Cancer Cell* *14*, 135-145. 10.1016/j.ccr.2008.07.003.
45. Schuller, U., Heine, V.M., Mao, J., Kho, A.T., Dillon, A.K., Han, Y.G., Huillard, E., Sun, T., Ligon, A.H., Qian, Y., et al. (2008). Acquisition of granule neuron precursor identity is a critical determinant of progenitor cell competence to form Shh-induced medulloblastoma. *Cancer Cell* *14*, 123-134. 10.1016/j.ccr.2008.07.005.
46. Oliver, T.G., Read, T.A., Kessler, J.D., Mehmeti, A., Wells, J.F., Huynh, T.T., Lin, S.M., and Wechsler-Reya, R.J. (2005). Loss of patched and disruption of granule cell development in a pre-neoplastic stage of medulloblastoma. *Development* *132*, 2425-2439. 10.1242/dev.01793.
47. Smith, K.S., Bihannic, L., Gudenas, B.L., Haldipur, P., Tao, R., Gao, Q., Li, Y., Aldinger, K.A., Iskusnykh, I.Y., Chizhikov, V.V., et al. (2022). Unified rhombic lip origins of group 3 and group 4 medulloblastoma. *Nature* *609*, 1012-1020. 10.1038/s41586-022-05208-9.
48. Swartling, F.J., Savov, V., Persson, A.I., Chen, J., Hackett, C.S., Northcott, P.A., Grimmer, M.R., Lau, J., Chesler, L., Perry, A., et al. (2012). Distinct neural stem cell populations give rise to disparate brain tumors in response to N-MYC. *Cancer Cell* *21*, 601-613. 10.1016/j.ccr.2012.04.012.
49. Gibson, P., Tong, Y., Robinson, G., Thompson, M.C., Currle, D.S., Eden, C., Kranenburg, T.A., Hogg, T., Poppleton, H., Martin, J., et al. (2010). Subtypes of medulloblastoma have distinct developmental origins. *Nature* *468*, 1095-1099. 10.1038/nature09587.
50. Wefers, A.K., Warmuth-Metz, M., Poschl, J., von Bueren, A.O., Monoranu, C.M., Seelos, K., Peraud, A., Tonn, J.C., Koch, A., Pietsch, T., et al. (2014). Subgroup-specific localization of human medulloblastoma based on pre-operative MRI. *Acta Neuropathol* *127*, 931-933. 10.1007/s00401-014-1271-5.
51. Mille, F., Tamayo-Orrego, L., Levesque, M., Remke, M., Korshunov, A., Cardin, J., Bouchard, N., Izzi, L., Kool, M., Northcott, P.A., et al. (2014). The Shh receptor Boc promotes progression of early medulloblastoma to advanced tumors. *Dev Cell* *31*, 34-47. 10.1016/j.devcel.2014.08.010.
52. Tamayo-Orrego, L., Gallo, D., Racicot, F., Bemmo, A., Mohan, S., Ho, B., Salameh, S., Hoang, T., Jackson, A.P., Brown, G.W., and Charron, F. (2020). Sonic hedgehog accelerates DNA replication to cause replication stress promoting cancer initiation in medulloblastoma. *Nat Cancer* *1*, 840-854. 10.1038/s43018-020-0094-7.
53. Kimura, H., Stephen, D., Joyner, A., and Curran, T. (2005). Gli1 is important for medulloblastoma formation in Ptc1^{+/-} mice. *Oncogene* *24*, 4026-4036. 10.1038/sj.onc.1208567.
54. Gershon, T.R., Crowther, A.J., Tikunov, A., Garcia, I., Annis, R., Yuan, H., Miller, C.R., Macdonald, J., Olson, J., and Deshmukh, M. (2013). Hexokinase-2-mediated aerobic

- glycolysis is integral to cerebellar neurogenesis and pathogenesis of medulloblastoma. *Cancer Metab* 1, 2. 10.1186/2049-3002-1-2.
55. Fernandez, C., Tatard, V.M., Bertrand, N., and Dahmane, N. (2010). Differential modulation of Sonic-hedgehog-induced cerebellar granule cell precursor proliferation by the IGF signaling network. *Dev Neurosci* 32, 59-70. 10.1159/000274458.
 56. Tanori, M., Santone, M., Mancuso, M., Pasquali, E., Leonardi, S., Di Majo, V., Rebessi, S., Saran, A., and Pazzaglia, S. (2010). Developmental and oncogenic effects of insulin-like growth factor-I in Ptc1+/- mouse cerebellum. *Mol Cancer* 9, 53. 10.1186/1476-4598-9-53.
 57. Corcoran, R.B., Bachar Raveh, T., Barakat, M.T., Lee, E.Y., and Scott, M.P. (2008). Insulin-like growth factor 2 is required for progression to advanced medulloblastoma in patched1 heterozygous mice. *Cancer Res* 68, 8788-8795. 10.1158/0008-5472.CAN-08-2135.
 58. Quail, D.F., and Joyce, J.A. (2017). The Microenvironmental Landscape of Brain Tumors. *Cancer Cell* 31, 326-341. 10.1016/j.ccell.2017.02.009.
 59. Wang, Y., Rattner, A., Zhou, Y., Williams, J., Smallwood, P.M., and Nathans, J. (2012). Norrin/Frizzled4 signaling in retinal vascular development and blood brain barrier plasticity. *Cell* 151, 1332-1344. 10.1016/j.cell.2012.10.042.
 60. Xu, Q., Wang, Y., Dabdoub, A., Smallwood, P.M., Williams, J., Woods, C., Kelley, M.W., Jiang, L., Tasman, W., Zhang, K., and Nathans, J. (2004). Vascular development in the retina and inner ear: control by Norrin and Frizzled-4, a high-affinity ligand-receptor pair. *Cell* 116, 883-895. 10.1016/s0092-8674(04)00216-8.
 61. Zhou, Y., Wang, Y., Tischfield, M., Williams, J., Smallwood, P.M., Rattner, A., Taketo, M.M., and Nathans, J. (2014). Canonical WNT signaling components in vascular development and barrier formation. *J Clin Invest* 124, 3825-3846. 10.1172/JCI76431.
 62. Phoenix, T.N., Patmore, D.M., Boop, S., Boulos, N., Jacus, M.O., Patel, Y.T., Roussel, M.F., Finkelstein, D., Goumnerova, L., Perreault, S., et al. (2016). Medulloblastoma Genotype Dictates Blood Brain Barrier Phenotype. *Cancer Cell* 29, 508-522. 10.1016/j.ccell.2016.03.002.
 63. Bassett, E.A., Tokarew, N., Allemanno, E.A., Mazerolle, C., Morin, K., Mears, A.J., McNeill, B., Ringuette, R., Campbell, C., Smiley, S., et al. (2016). Norrin/Frizzled4 signalling in the preneoplastic niche blocks medulloblastoma initiation. *Elife* 5. 10.7554/eLife.16764.
 64. Taylor, M.D., Northcott, P.A., Korshunov, A., Remke, M., Cho, Y.J., Clifford, S.C., Eberhart, C.G., Parsons, D.W., Rutkowski, S., Gajjar, A., et al. (2012). Molecular subgroups of medulloblastoma: the current consensus. *Acta Neuropathol* 123, 465-472. 10.1007/s00401-011-0922-z.
 65. Cho, Y.J., Tsherniak, A., Tamayo, P., Santagata, S., Ligon, A., Greulich, H., Berhoukim, R., Amani, V., Goumnerova, L., Eberhart, C.G., et al. (2011). Integrative genomic analysis of medulloblastoma identifies a molecular subgroup that drives poor clinical outcome. *J Clin Oncol* 29, 1424-1430. 10.1200/JCO.2010.28.5148.
 66. Diede, S.J., Guenthoer, J., Geng, L.N., Mahoney, S.E., Marotta, M., Olson, J.M., Tanaka, H., and Tapscott, S.J. (2010). DNA methylation of developmental genes in pediatric medulloblastomas identified by denaturation analysis of methylation differences. *Proc Natl Acad Sci U S A* 107, 234-239. 10.1073/pnas.0907606106.

67. Jones, D.T., Jager, N., Kool, M., Zichner, T., Hutter, B., Sultan, M., Cho, Y.J., Pugh, T.J., Hovestadt, V., Stutz, A.M., et al. (2012). Dissecting the genomic complexity underlying medulloblastoma. *Nature* 488, 100-105. 10.1038/nature11284.
68. Northcott, P.A., Shih, D.J., Peacock, J., Garzia, L., Morrissy, A.S., Zichner, T., Stutz, A.M., Korshunov, A., Reimand, J., Schumacher, S.E., et al. (2012). Subgroup-specific structural variation across 1,000 medulloblastoma genomes. *Nature* 488, 49-56. 10.1038/nature11327.
69. Parsons, D.W., Li, M., Zhang, X., Jones, S., Leary, R.J., Lin, J.C., Boca, S.M., Carter, H., Samayoa, J., Bettegowda, C., et al. (2011). The genetic landscape of the childhood cancer medulloblastoma. *Science* 331, 435-439. 10.1126/science.1198056.
70. Pugh, T.J., Weeraratne, S.D., Archer, T.C., Pomeranz Krummel, D.A., Auclair, D., Bochicchio, J., Carneiro, M.O., Carter, S.L., Cibulskis, K., Erlich, R.L., et al. (2012). Medulloblastoma exome sequencing uncovers subtype-specific somatic mutations. *Nature* 488, 106-110. 10.1038/nature11329.
71. Robinson, G., Parker, M., Kranenburg, T.A., Lu, C., Chen, X., Ding, L., Phoenix, T.N., Hedlund, E., Wei, L., Zhu, X., et al. (2012). Novel mutations target distinct subgroups of medulloblastoma. *Nature* 488, 43-48. 10.1038/nature11213.
72. Cavalli, F.M.G., Remke, M., Rampasek, L., Peacock, J., Shih, D.J.H., Luu, B., Garzia, L., Torchia, J., Nor, C., Morrissy, A.S., et al. (2017). Intertumoral Heterogeneity within Medulloblastoma Subgroups. *Cancer Cell* 31, 737-754 e736. 10.1016/j.ccell.2017.05.005.
73. Schwalbe, E.C., Lindsey, J.C., Nakjang, S., Crosier, S., Smith, A.J., Hicks, D., Rafiee, G., Hill, R.M., Iliasova, A., Stone, T., et al. (2017). Novel molecular subgroups for clinical classification and outcome prediction in childhood medulloblastoma: a cohort study. *Lancet Oncol* 18, 958-971. 10.1016/S1470-2045(17)30243-7.
74. Sharma, T., Schwalbe, E.C., Williamson, D., Sill, M., Hovestadt, V., Mynarek, M., Rutkowski, S., Robinson, G.W., Gajjar, A., Cavalli, F., et al. (2019). Second-generation molecular subgrouping of medulloblastoma: an international meta-analysis of Group 3 and Group 4 subtypes. *Acta Neuropathol* 138, 309-326. 10.1007/s00401-019-02020-0.
75. Northcott, P.A., Hielscher, T., Dubuc, A., Mack, S., Shih, D., Remke, M., Al-Halabi, H., Albrecht, S., Jabado, N., Eberhart, C.G., et al. (2011). Pediatric and adult sonic hedgehog medulloblastomas are clinically and molecularly distinct. *Acta Neuropathol* 122, 231-240. 10.1007/s00401-011-0846-7.
76. Northcott, P.A., Korshunov, A., Pfister, S.M., and Taylor, M.D. (2012). The clinical implications of medulloblastoma subgroups. *Nat Rev Neurol* 8, 340-351. 10.1038/nrneurol.2012.78.
77. Bale, S.J., Falk, R.T., and Rogers, G.R. (1998). Patching together the genetics of Gorlin syndrome. *J Cutan Med Surg* 3, 31-34. 10.1177/120347549800300109.
78. Taylor, M.D., Mainprize, T.G., and Rutka, J.T. (2000). Molecular insight into medulloblastoma and central nervous system primitive neuroectodermal tumor biology from hereditary syndromes: a review. *Neurosurgery* 47, 888-901. 10.1097/00006123-200010000-00020.
79. Pastorino, L., Ghiorzo, P., Nasti, S., Battistuzzi, L., Cusano, R., Marzocchi, C., Garre, M.L., Clementi, M., and Scarra, G.B. (2009). Identification of a SUFU germline mutation in a

- family with Gorlin syndrome. *Am J Med Genet A* 149A, 1539-1543. 10.1002/ajmg.a.32944.
80. Taylor, M.D., Liu, L., Raffel, C., Hui, C.C., Mainprize, T.G., Zhang, X., Agatep, R., Chiappa, S., Gao, L., Lowrance, A., et al. (2002). Mutations in *SUFU* predispose to medulloblastoma. *Nat Genet* 31, 306-310. 10.1038/ng916.
 81. Rausch, T., Jones, D.T., Zapatka, M., Stutz, A.M., Zichner, T., Weischenfeldt, J., Jager, N., Remke, M., Shih, D., Northcott, P.A., et al. (2012). Genome sequencing of pediatric medulloblastoma links catastrophic DNA rearrangements with TP53 mutations. *Cell* 148, 59-71. 10.1016/j.cell.2011.12.013.
 82. Kool, M., Jones, D.T., Jager, N., Northcott, P.A., Pugh, T.J., Hovestadt, V., Piro, R.M., Esparza, L.A., Markant, S.L., Remke, M., et al. (2014). Genome sequencing of SHH medulloblastoma predicts genotype-related response to smoothed inhibition. *Cancer Cell* 25, 393-405. 10.1016/j.ccr.2014.02.004.
 83. Waszak, S.M., Northcott, P.A., Buchhalter, I., Robinson, G.W., Sutter, C., Groebner, S., Grund, K.B., Brugieres, L., Jones, D.T.W., Pajtler, K.W., et al. (2018). Spectrum and prevalence of genetic predisposition in medulloblastoma: a retrospective genetic study and prospective validation in a clinical trial cohort. *Lancet Oncol* 19, 785-798. 10.1016/S1470-2045(18)30242-0.
 84. Skowron, P., Farooq, H., Cavalli, F.M.G., Morrissy, A.S., Ly, M., Hendrikse, L.D., Wang, E.Y., Djambazian, H., Zhu, H., Mungall, K.L., et al. (2021). The transcriptional landscape of Shh medulloblastoma. *Nat Commun* 12, 1749. 10.1038/s41467-021-21883-0.
 85. Kool, M., Korshunov, A., Remke, M., Jones, D.T., Schlanstein, M., Northcott, P.A., Cho, Y.J., Koster, J., Schouten-van Meeteren, A., van Vuurden, D., et al. (2012). Molecular subgroups of medulloblastoma: an international meta-analysis of transcriptome, genetic aberrations, and clinical data of WNT, SHH, Group 3, and Group 4 medulloblastomas. *Acta Neuropathol* 123, 473-484. 10.1007/s00401-012-0958-8.
 86. Rutkowski, S., Bode, U., Deinlein, F., Ottensmeier, H., Warmuth-Metz, M., Soerensen, N., Graf, N., Emser, A., Pietsch, T., Wolff, J.E., et al. (2005). Treatment of early childhood medulloblastoma by postoperative chemotherapy alone. *N Engl J Med* 352, 978-986. 10.1056/NEJMoa042176.
 87. Martin, A.M., Raabe, E., Eberhart, C., and Cohen, K.J. (2014). Management of pediatric and adult patients with medulloblastoma. *Curr Treat Options Oncol* 15, 581-594. 10.1007/s11864-014-0306-4.
 88. Romer, J.T., Kimura, H., Magdaleno, S., Sasai, K., Fuller, C., Baines, H., Connelly, M., Stewart, C.F., Gould, S., Rubin, L.L., and Curran, T. (2004). Suppression of the Shh pathway using a small molecule inhibitor eliminates medulloblastoma in *Ptc1(+/-)p53(-/-)* mice. *Cancer Cell* 6, 229-240. 10.1016/j.ccr.2004.08.019.
 89. Rudin, C.M. (2012). Vismodegib. *Clin Cancer Res* 18, 3218-3222. 10.1158/1078-0432.CCR-12-0568.
 90. Goranci-Buzhala, G., Gabriel, E., Mariappan, A., and Gopalakrishnan, J. (2017). Losers of Primary Cilia Gain the Benefit of Survival. *Cancer Discov* 7, 1374-1375. 10.1158/2159-8290.CD-17-1085.
 91. Zhao, X., Pak, E., Ornell, K.J., Pazyra-Murphy, M.F., MacKenzie, E.L., Chadwick, E.J., Ponomaryov, T., Kelleher, J.F., and Segal, R.A. (2017). A Transposon Screen Identifies Loss

- of Primary Cilia as a Mechanism of Resistance to SMO Inhibitors. *Cancer Discov* 7, 1436-1449. 10.1158/2159-8290.CD-17-0281.
92. Hovestadt, V., Ayrault, O., Swartling, F.J., Robinson, G.W., Pfister, S.M., and Northcott, P.A. (2020). Medulloblastomics revisited: biological and clinical insights from thousands of patients. *Nat Rev Cancer* 20, 42-56. 10.1038/s41568-019-0223-8.
 93. Gajjar, A.J., and Robinson, G.W. (2014). Medulloblastoma-translating discoveries from the bench to the bedside. *Nat Rev Clin Oncol* 11, 714-722. 10.1038/nrclinonc.2014.181.
 94. Hamilton, S.R., Liu, B., Parsons, R.E., Papadopoulos, N., Jen, J., Powell, S.M., Krush, A.J., Berk, T., Cohen, Z., Tetu, B., and et al. (1995). The molecular basis of Turcot's syndrome. *N Engl J Med* 332, 839-847. 10.1056/NEJM199503303321302.
 95. Zurawel, R.H., Chiappa, S.A., Allen, C., and Raffel, C. (1998). Sporadic medulloblastomas contain oncogenic beta-catenin mutations. *Cancer Res* 58, 896-899.
 96. Northcott, P.A., Buchhalter, I., Morrissy, A.S., Hovestadt, V., Weischenfeldt, J., Ehrenberger, T., Grobner, S., Segura-Wang, M., Zichner, T., Rudneva, V.A., et al. (2017). The whole-genome landscape of medulloblastoma subtypes. *Nature* 547, 311-317. 10.1038/nature22973.
 97. Ellison, D.W., Onilude, O.E., Lindsey, J.C., Lusher, M.E., Weston, C.L., Taylor, R.E., Pearson, A.D., Clifford, S.C., and United Kingdom Children's Cancer Study Group Brain Tumour, C. (2005). beta-Catenin status predicts a favorable outcome in childhood medulloblastoma: the United Kingdom Children's Cancer Study Group Brain Tumour Committee. *J Clin Oncol* 23, 7951-7957. 10.1200/JCO.2005.01.5479.
 98. Wang, X., Ramaswamy, V., Remke, M., Mack, S.C., Dubuc, A.M., Northcott, P.A., and Taylor, M.D. (2013). Intertumoral and intratumoral heterogeneity as a barrier for effective treatment of medulloblastoma. *Neurosurgery* 60 *Suppl* 1, 57-63. 10.1227/01.neu.0000430318.01821.6f.
 99. Ivanov, D.P., Coyle, B., Walker, D.A., and Grabowska, A.M. (2016). In vitro models of medulloblastoma: Choosing the right tool for the job. *J Biotechnol* 236, 10-25. 10.1016/j.jbiotec.2016.07.028.
 100. Northcott, P.A., Lee, C., Zichner, T., Stutz, A.M., Erkek, S., Kawauchi, D., Shih, D.J., Hovestadt, V., Zapatka, M., Sturm, D., et al. (2014). Enhancer hijacking activates GF11 family oncogenes in medulloblastoma. *Nature* 511, 428-434. 10.1038/nature13379.
 101. Morfouace, M., Shelat, A., Jacus, M., Freeman, B.B., 3rd, Turner, D., Robinson, S., Zindy, F., Wang, Y.D., Finkelstein, D., Ayrault, O., et al. (2014). Pemetrexed and gemcitabine as combination therapy for the treatment of Group3 medulloblastoma. *Cancer Cell* 25, 516-529. 10.1016/j.ccr.2014.02.009.
 102. Bandopadhyay, P., Bergthold, G., Nguyen, B., Schubert, S., Gholamin, S., Tang, Y., Bolin, S., Schumacher, S.E., Zeid, R., Masoud, S., et al. (2014). BET bromodomain inhibition of MYC-amplified medulloblastoma. *Clin Cancer Res* 20, 912-925. 10.1158/1078-0432.CCR-13-2281.
 103. Furchert, S.E., Lanvers-Kaminsky, C., Juurgens, H., Jung, M., Loidl, A., and Fruhwald, M.C. (2007). Inhibitors of histone deacetylases as potential therapeutic tools for high-risk embryonal tumors of the nervous system of childhood. *Int J Cancer* 120, 1787-1794. 10.1002/ijc.22401.

104. Korshunov, A., Remke, M., Kool, M., Hielscher, T., Northcott, P.A., Williamson, D., Pfaff, E., Witt, H., Jones, D.T., Ryzhova, M., et al. (2012). Biological and clinical heterogeneity of MYCN-amplified medulloblastoma. *Acta Neuropathol* 123, 515-527. 10.1007/s00401-011-0918-8.
105. El Doussouki, M., Gajjar, A., and Chamdine, O. (2019). Molecular genetics of medulloblastoma in children: diagnostic, therapeutic and prognostic implications. *Futur Neurol* 14. ARTN FNL8 10.2217/fnl-2018-0030.
106. Wu, X., Northcott, P.A., Croul, S., and Taylor, M.D. (2011). Mouse models of medulloblastoma. *Chin J Cancer* 30, 442-449. 10.5732/cjc.011.10040.
107. Roussel, M.F., and Stripay, J.L. (2020). Modeling pediatric medulloblastoma. *Brain Pathol* 30, 703-712. 10.1111/bpa.12803.
108. Wetmore, C., Eberhart, D.E., and Curran, T. (2000). The normal patched allele is expressed in medulloblastomas from mice with heterozygous germ-line mutation of patched. *Cancer Res* 60, 2239-2246.
109. Wetmore, C., Eberhart, D.E., and Curran, T. (2001). Loss of p53 but not ARF accelerates medulloblastoma in mice heterozygous for patched. *Cancer Res* 61, 513-516.
110. Xie, J., Murone, M., Luoh, S.M., Ryan, A., Gu, Q., Zhang, C., Bonifas, J.M., Lam, C.W., Hynes, M., Goddard, A., et al. (1998). Activating Smoothed mutations in sporadic basal-cell carcinoma. *Nature* 391, 90-92. 10.1038/34201.
111. Dey, J., Ditzler, S., Knoblauch, S.E., Hatton, B.A., Schelter, J.M., Cleary, M.A., Mecham, B., Rorke-Adams, L.B., and Olson, J.M. (2012). A distinct Smoothed mutation causes severe cerebellar developmental defects and medulloblastoma in a novel transgenic mouse model. *Mol Cell Biol* 32, 4104-4115. 10.1128/MCB.00862-12.
112. Hatton, B.A., Villavicencio, E.H., Tsuchiya, K.D., Pritchard, J.I., Ditzler, S., Pullar, B., Hansen, S., Knoblauch, S.E., Lee, D., Eberhart, C.G., et al. (2008). The Smo/Smo model: hedgehog-induced medulloblastoma with 90% incidence and leptomeningeal spread. *Cancer Res* 68, 1768-1776. 10.1158/0008-5472.CAN-07-5092.
113. Mao, J., Ligon, K.L., Rakhlin, E.Y., Thayer, S.P., Bronson, R.T., Rowitch, D., and McMahon, A.P. (2006). A novel somatic mouse model to survey tumorigenic potential applied to the Hedgehog pathway. *Cancer Res* 66, 10171-10178. 10.1158/0008-5472.CAN-06-0657.
114. Gorlin, R.J. (1987). Nevoid basal-cell carcinoma syndrome. *Medicine (Baltimore)* 66, 98-113. 10.1097/00005792-198703000-00002.
115. Johnson, R.L., Rothman, A.L., Xie, J., Goodrich, L.V., Bare, J.W., Bonifas, J.M., Quinn, A.G., Myers, R.M., Cox, D.R., Epstein, E.H., Jr., and Scott, M.P. (1996). Human homolog of patched, a candidate gene for the basal cell nevus syndrome. *Science* 272, 1668-1671. 10.1126/science.272.5268.1668.
116. Northcott, P.A., Jones, D.T., Kool, M., Robinson, G.W., Gilbertson, R.J., Cho, Y.J., Pomeroy, S.L., Korshunov, A., Lichter, P., Taylor, M.D., and Pfister, S.M. (2012). Medulloblastomics: the end of the beginning. *Nat Rev Cancer* 12, 818-834. 10.1038/nrc3410.
117. Tostar, U., Malm, C.J., Meis-Kindblom, J.M., Kindblom, L.G., Toftgard, R., and Unden, A.B. (2006). Deregulation of the hedgehog signalling pathway: a possible role for the PTCH and SUFU genes in human rhabdomyoma and rhabdomyosarcoma development. *J Pathol* 208, 17-25. 10.1002/path.1882.

118. Pazzaglia, S., Tanori, M., Mancuso, M., Gessi, M., Pasquali, E., Leonardi, S., Oliva, M.A., Rebessi, S., Di Majo, V., Covelli, V., et al. (2006). Two-hit model for progression of medulloblastoma preneoplasia in Patched heterozygous mice. *Oncogene* 25, 5575-5580. 10.1038/sj.onc.1209544.
119. Ishida, Y., Takabatake, T., Kakinuma, S., Doi, K., Yamauchi, K., Kaminishi, M., Kito, S., Ohta, Y., Amasaki, Y., Moritake, H., et al. (2010). Genomic and gene expression signatures of radiation in medulloblastomas after low-dose irradiation in Ptch1 heterozygous mice. *Carcinogenesis* 31, 1694-1701. 10.1093/carcin/bgq145.
120. Tamayo-Orrego, L., Wu, C.L., Bouchard, N., Khedher, A., Swikert, S.M., Remke, M., Skowron, P., Taylor, M.D., and Charron, F. (2016). Evasion of Cell Senescence Leads to Medulloblastoma Progression. *Cell Rep* 14, 2925-2937. 10.1016/j.celrep.2016.02.061.
121. Tamayo-Orrego, L., Swikert, S.M., and Charron, F. (2016). Evasion of cell senescence in SHH medulloblastoma. *Cell Cycle* 15, 2102-2107. 10.1080/15384101.2016.1189044.
122. Isken, O., and Maquat, L.E. (2007). Quality control of eukaryotic mRNA: safeguarding cells from abnormal mRNA function. *Genes Dev* 21, 1833-1856. 10.1101/gad.1566807.
123. Kurosaki, T., Popp, M.W., and Maquat, L.E. (2019). Quality and quantity control of gene expression by nonsense-mediated mRNA decay. *Nat Rev Mol Cell Biol* 20, 406-420. 10.1038/s41580-019-0126-2.
124. Hug, N., Longman, D., and Caceres, J.F. (2016). Mechanism and regulation of the nonsense-mediated decay pathway. *Nucleic Acids Res* 44, 1483-1495. 10.1093/nar/gkw010.
125. Behm-Ansmant, I., and Izaurralde, E. (2006). Quality control of gene expression: a stepwise assembly pathway for the surveillance complex that triggers nonsense-mediated mRNA decay. *Genes Dev* 20, 391-398. 10.1101/gad.1407606.
126. Nicholson, P., Yepiskoposyan, H., Metze, S., Zamudio Orozco, R., Kleinschmidt, N., and Muhlemann, O. (2010). Nonsense-mediated mRNA decay in human cells: mechanistic insights, functions beyond quality control and the double-life of NMD factors. *Cell Mol Life Sci* 67, 677-700. 10.1007/s00018-009-0177-1.
127. Kashima, I., Yamashita, A., Izumi, N., Kataoka, N., Morishita, R., Hoshino, S., Ohno, M., Dreyfuss, G., and Ohno, S. (2006). Binding of a novel SMG-1-Upf1-eRF1-eRF3 complex (SURF) to the exon junction complex triggers Upf1 phosphorylation and nonsense-mediated mRNA decay. *Genes Dev* 20, 355-367. 10.1101/gad.1389006.
128. Melero, R., Uchiyama, A., Castano, R., Kataoka, N., Kurosawa, H., Ohno, S., Yamashita, A., and Llorca, O. (2014). Structures of SMG1-UPFs complexes: SMG1 contributes to regulate UPF2-dependent activation of UPF1 in NMD. *Structure* 22, 1105-1119. 10.1016/j.str.2014.05.015.
129. Deniaud, A., Karuppasamy, M., Bock, T., Masiulis, S., Huard, K., Garzoni, F., Kerschgens, K., Hentze, M.W., Kulozik, A.E., Beck, M., et al. (2015). A network of SMG-8, SMG-9 and SMG-1 C-terminal insertion domain regulates UPF1 substrate recruitment and phosphorylation. *Nucleic Acids Res* 43, 7600-7611. 10.1093/nar/gkv668.
130. Nicholson, P., Gkratsou, A., Josi, C., Colombo, M., and Muhlemann, O. (2018). Dissecting the functions of SMG5, SMG7, and PNRC2 in nonsense-mediated mRNA decay of human cells. *RNA* 24, 557-573. 10.1261/rna.063719.117.

131. Fukuhara, N., Ebert, J., Unterholzner, L., Lindner, D., Izaurralde, E., and Conti, E. (2005). SMG7 is a 14-3-3-like adaptor in the nonsense-mediated mRNA decay pathway. *Mol Cell* *17*, 537-547. 10.1016/j.molcel.2005.01.010.
132. Unterholzner, L., and Izaurralde, E. (2004). SMG7 acts as a molecular link between mRNA surveillance and mRNA decay. *Mol Cell* *16*, 587-596. 10.1016/j.molcel.2004.10.013.
133. Huntzinger, E., Kashima, I., Fauser, M., Sauliere, J., and Izaurralde, E. (2008). SMG6 is the catalytic endonuclease that cleaves mRNAs containing nonsense codons in metazoan. *RNA* *14*, 2609-2617. 10.1261/rna.1386208.
134. Eberle, A.B., Lykke-Andersen, S., Muhlemann, O., and Jensen, T.H. (2009). SMG6 promotes endonucleolytic cleavage of nonsense mRNA in human cells. *Nat Struct Mol Biol* *16*, 49-55. 10.1038/nsmb.1530.
135. Schmidt, S.A., Foley, P.L., Jeong, D.H., Rymarquis, L.A., Doyle, F., Tenenbaum, S.A., Belasco, J.G., and Green, P.J. (2015). Identification of SMG6 cleavage sites and a preferred RNA cleavage motif by global analysis of endogenous NMD targets in human cells. *Nucleic Acids Res* *43*, 309-323. 10.1093/nar/gku1258.
136. Anders, K.R., Grimson, A., and Anderson, P. (2003). SMG-5, required for *C.elegans* nonsense-mediated mRNA decay, associates with SMG-2 and protein phosphatase 2A. *EMBO J* *22*, 641-650. 10.1093/emboj/cdg056.
137. Chiu, S.Y., Serin, G., Ohara, O., and Maquat, L.E. (2003). Characterization of human Smg5/7a: a protein with similarities to *Caenorhabditis elegans* SMG5 and SMG7 that functions in the dephosphorylation of Upf1. *RNA* *9*, 77-87. 10.1261/rna.2137903.
138. Page, M.F., Carr, B., Anders, K.R., Grimson, A., and Anderson, P. (1999). SMG-2 is a phosphorylated protein required for mRNA surveillance in *Caenorhabditis elegans* and related to Upf1p of yeast. *Mol Cell Biol* *19*, 5943-5951. 10.1128/MCB.19.9.5943.
139. Gehring, N.H., Kunz, J.B., Neu-Yilik, G., Breit, S., Viegas, M.H., Hentze, M.W., and Kulozik, A.E. (2005). Exon-junction complex components specify distinct routes of nonsense-mediated mRNA decay with differential cofactor requirements. *Mol Cell* *20*, 65-75. 10.1016/j.molcel.2005.08.012.
140. Metze, S., Herzog, V.A., Ruepp, M.D., and Muhlemann, O. (2013). Comparison of EJC-enhanced and EJC-independent NMD in human cells reveals two partially redundant degradation pathways. *RNA* *19*, 1432-1448. 10.1261/rna.038893.113.
141. Ivanov, A., Mikhailova, T., Eliseev, B., Yeramala, L., Sokolova, E., Susorov, D., Shuvalov, A., Schaffitzel, C., and Alkalaeva, E. (2016). PABP enhances release factor recruitment and stop codon recognition during translation termination. *Nucleic Acids Res* *44*, 7766-7776. 10.1093/nar/gkw635.
142. Kurosaki, T., and Maquat, L.E. (2013). Rules that govern UPF1 binding to mRNA 3' UTRs. *Proc Natl Acad Sci U S A* *110*, 3357-3362. 10.1073/pnas.1219908110.
143. Ivanov, P.V., Gehring, N.H., Kunz, J.B., Hentze, M.W., and Kulozik, A.E. (2008). Interactions between UPF1, eRFs, PABP and the exon junction complex suggest an integrated model for mammalian NMD pathways. *EMBO J* *27*, 736-747. 10.1038/emboj.2008.17.
144. Peixeiro, I., Inacio, A., Barbosa, C., Silva, A.L., Liebhaber, S.A., and Romao, L. (2012). Interaction of PABPC1 with the translation initiation complex is critical to the NMD resistance of AUG-proximal nonsense mutations. *Nucleic Acids Res* *40*, 1160-1173. 10.1093/nar/gkr820.

145. Silva, A.L., Ribeiro, P., Inacio, A., Liebhaber, S.A., and Romao, L. (2008). Proximity of the poly(A)-binding protein to a premature termination codon inhibits mammalian nonsense-mediated mRNA decay. *RNA* *14*, 563-576. 10.1261/rna.815108.
146. Singh, G., Rebbapragada, I., and Lykke-Andersen, J. (2008). A competition between stimulators and antagonists of Upf complex recruitment governs human nonsense-mediated mRNA decay. *PLoS Biol* *6*, e111. 10.1371/journal.pbio.0060111.
147. Kurosaki, T., Li, W., Hoque, M., Popp, M.W., Ermolenko, D.N., Tian, B., and Maquat, L.E. (2014). A post-translational regulatory switch on UPF1 controls targeted mRNA degradation. *Genes Dev* *28*, 1900-1916. 10.1101/gad.245506.114.
148. Imamachi, N., Salam, K.A., Suzuki, Y., and Akimitsu, N. (2017). A GC-rich sequence feature in the 3' UTR directs UPF1-dependent mRNA decay in mammalian cells. *Genome Res* *27*, 407-418. 10.1101/gr.206060.116.
149. Leeds, P., Wood, J.M., Lee, B.S., and Culbertson, M.R. (1992). Gene products that promote mRNA turnover in *Saccharomyces cerevisiae*. *Mol Cell Biol* *12*, 2165-2177. 10.1128/mcb.12.5.2165-2177.1992.
150. Lykke-Andersen, J., Shu, M.D., and Steitz, J.A. (2000). Human Upf proteins target an mRNA for nonsense-mediated decay when bound downstream of a termination codon. *Cell* *103*, 1121-1131. 10.1016/s0092-8674(00)00214-2.
151. Gatfield, D., Unterholzner, L., Ciccarelli, F.D., Bork, P., and Izaurralde, E. (2003). Nonsense-mediated mRNA decay in *Drosophila*: at the intersection of the yeast and mammalian pathways. *EMBO J* *22*, 3960-3970. 10.1093/emboj/cdg371.
152. Franks, T.M., Singh, G., and Lykke-Andersen, J. (2010). Upf1 ATPase-dependent mRNP disassembly is required for completion of nonsense-mediated mRNA decay. *Cell* *143*, 938-950. 10.1016/j.cell.2010.11.043.
153. Yamashita, A., Ohnishi, T., Kashima, I., Taya, Y., and Ohno, S. (2001). Human SMG-1, a novel phosphatidylinositol 3-kinase-related protein kinase, associates with components of the mRNA surveillance complex and is involved in the regulation of nonsense-mediated mRNA decay. *Genes Dev* *15*, 2215-2228. 10.1101/gad.913001.
154. Okada-Katsuhata, Y., Yamashita, A., Kutsuzawa, K., Izumi, N., Hirahara, F., and Ohno, S. (2012). N- and C-terminal Upf1 phosphorylations create binding platforms for SMG-6 and SMG-5:SMG-7 during NMD. *Nucleic Acids Res* *40*, 1251-1266. 10.1093/nar/gkr791.
155. Chamieh, H., Ballut, L., Bonneau, F., and Le Hir, H. (2008). NMD factors UPF2 and UPF3 bridge UPF1 to the exon junction complex and stimulate its RNA helicase activity. *Nat Struct Mol Biol* *15*, 85-93. 10.1038/nsmb1330.
156. Fiorini, F., Boudvillain, M., and Le Hir, H. (2013). Tight intramolecular regulation of the human Upf1 helicase by its N- and C-terminal domains. *Nucleic Acids Res* *41*, 2404-2415. 10.1093/nar/gks1320.
157. Kadlec, J., Guilligay, D., Ravelli, R.B., and Cusack, S. (2006). Crystal structure of the UPF2-interacting domain of nonsense-mediated mRNA decay factor UPF1. *RNA* *12*, 1817-1824. 10.1261/rna.177606.
158. Chakrabarti, S., Jayachandran, U., Bonneau, F., Fiorini, F., Basquin, C., Domcke, S., Le Hir, H., and Conti, E. (2011). Molecular mechanisms for the RNA-dependent ATPase activity of Upf1 and its regulation by Upf2. *Mol Cell* *41*, 693-703. 10.1016/j.molcel.2011.02.010.

159. Kim, Y.K., and Maquat, L.E. (2019). UPFfront and center in RNA decay: UPF1 in nonsense-mediated mRNA decay and beyond. *RNA* 25, 407-422. 10.1261/rna.070136.118.
160. Mendell, J.T., Sharifi, N.A., Meyers, J.L., Martinez-Murillo, F., and Dietz, H.C. (2004). Nonsense surveillance regulates expression of diverse classes of mammalian transcripts and mutates genomic noise. *Nat Genet* 36, 1073-1078. 10.1038/ng1429.
161. Lopez-Perrote, A., Castano, R., Melero, R., Zamarro, T., Kurosawa, H., Ohnishi, T., Uchiyama, A., Aoyagi, K., Buchwald, G., Kataoka, N., et al. (2016). Human nonsense-mediated mRNA decay factor UPF2 interacts directly with eRF3 and the SURF complex. *Nucleic Acids Res* 44, 1909-1923. 10.1093/nar/gkv1527.
162. Culbertson, M.R., and Leeds, P.F. (2003). Looking at mRNA decay pathways through the window of molecular evolution. *Curr Opin Genet Dev* 13, 207-214. 10.1016/s0959-437x(03)00014-5.
163. Serin, G., Gersappe, A., Black, J.D., Aronoff, R., and Maquat, L.E. (2001). Identification and characterization of human orthologues to *Saccharomyces cerevisiae* Upf2 protein and Upf3 protein (*Caenorhabditis elegans* SMG-4). *Mol Cell Biol* 21, 209-223. 10.1128/MCB.21.1.209-223.2001.
164. Shum, E.Y., Jones, S.H., Shao, A., Chousal, J.N., Krause, M.D., Chan, W.K., Lou, C.H., Espinoza, J.L., Song, H.W., Phan, M.H., et al. (2016). The Antagonistic Gene Paralogs Upf3a and Upf3b Govern Nonsense-Mediated RNA Decay. *Cell* 165, 382-395. 10.1016/j.cell.2016.02.046.
165. Neu-Yilik, G., Raimondeau, E., Eliseev, B., Yeramala, L., Amthor, B., Deniaud, A., Huard, K., Kerschgens, K., Hentze, M.W., Schaffitzel, C., and Kulozik, A.E. (2017). Dual function of UPF3B in early and late translation termination. *EMBO J* 36, 2968-2986. 10.15252/embj.201797079.
166. Chan, W.K., Bhalla, A.D., Le Hir, H., Nguyen, L.S., Huang, L., Gecz, J., and Wilkinson, M.F. (2009). A UPF3-mediated regulatory switch that maintains RNA surveillance. *Nat Struct Mol Biol* 16, 747-753. 10.1038/nsmb.1612.
167. Denning, G., Jamieson, L., Maquat, L.E., Thompson, E.A., and Fields, A.P. (2001). Cloning of a novel phosphatidylinositol kinase-related kinase: characterization of the human SMG-1 RNA surveillance protein. *J Biol Chem* 276, 22709-22714. 10.1074/jbc.C100144200.
168. Arias-Palomo, E., Yamashita, A., Fernandez, I.S., Nunez-Ramirez, R., Bamba, Y., Izumi, N., Ohno, S., and Llorca, O. (2011). The nonsense-mediated mRNA decay SMG-1 kinase is regulated by large-scale conformational changes controlled by SMG-8. *Genes Dev* 25, 153-164. 10.1101/gad.606911.
169. Fernandez, I.S., Yamashita, A., Arias-Palomo, E., Bamba, Y., Bartolome, R.A., Canales, M.A., Teixido, J., Ohno, S., and Llorca, O. (2011). Characterization of SMG-9, an essential component of the nonsense-mediated mRNA decay SMG1C complex. *Nucleic Acids Res* 39, 347-358. 10.1093/nar/gkq749.
170. Yamashita, A., Izumi, N., Kashima, I., Ohnishi, T., Saari, B., Katsuhata, Y., Muramatsu, R., Morita, T., Iwamatsu, A., Hachiya, T., et al. (2009). SMG-8 and SMG-9, two novel subunits of the SMG-1 complex, regulate remodeling of the mRNA surveillance complex during nonsense-mediated mRNA decay. *Genes Dev* 23, 1091-1105. 10.1101/gad.1767209.

171. Zhu, L., Li, L., Qi, Y., Yu, Z., and Xu, Y. (2019). Cryo-EM structure of SMG1-SMG8-SMG9 complex. *Cell Res* 29, 1027-1034. 10.1038/s41422-019-0255-3.
172. Li, L., Lingaraju, M., Basquin, C., Basquin, J., and Conti, E. (2017). Structure of a SMG8-SMG9 complex identifies a G-domain heterodimer in the NMD effector proteins. *RNA* 23, 1028-1034. 10.1261/rna.061200.117.
173. Durand, S., Franks, T.M., and Lykke-Andersen, J. (2016). Hyperphosphorylation amplifies UPF1 activity to resolve stalls in nonsense-mediated mRNA decay. *Nat Commun* 7, 12434. 10.1038/ncomms12434.
174. Brumbaugh, K.M., Otterness, D.M., Geisen, C., Oliveira, V., Brognard, J., Li, X., Lejeune, F., Tibbetts, R.S., Maquat, L.E., and Abraham, R.T. (2004). The mRNA surveillance protein hSMG-1 functions in genotoxic stress response pathways in mammalian cells. *Mol Cell* 14, 585-598. 10.1016/j.molcel.2004.05.005.
175. Azzalin, C.M., Reichenbach, P., Khoriantseva, L., Giulotto, E., and Lingner, J. (2007). Telomeric repeat containing RNA and RNA surveillance factors at mammalian chromosome ends. *Science* 318, 798-801. 10.1126/science.1147182.
176. Gehen, S.C., Staversky, R.J., Bambara, R.A., Keng, P.C., and O'Reilly, M.A. (2008). hSMG-1 and ATM sequentially and independently regulate the G1 checkpoint during oxidative stress. *Oncogene* 27, 4065-4074. 10.1038/onc.2008.48.
177. McIlwain, D.R., Pan, Q., Reilly, P.T., Elia, A.J., McCracken, S., Wakeham, A.C., Itie-Youten, A., Blencowe, B.J., and Mak, T.W. (2010). Smg1 is required for embryogenesis and regulates diverse genes via alternative splicing coupled to nonsense-mediated mRNA decay. *Proc Natl Acad Sci U S A* 107, 12186-12191. 10.1073/pnas.1007336107.
178. Ballut, L., Marchadier, B., Baguet, A., Tomasetto, C., Seraphin, B., and Le Hir, H. (2005). The exon junction core complex is locked onto RNA by inhibition of eIF4AIII ATPase activity. *Nat Struct Mol Biol* 12, 861-869. 10.1038/nsmb990.
179. Andersen, C.B., Ballut, L., Johansen, J.S., Chamieh, H., Nielsen, K.H., Oliveira, C.L., Pedersen, J.S., Seraphin, B., Le Hir, H., and Andersen, G.R. (2006). Structure of the exon junction core complex with a trapped DEAD-box ATPase bound to RNA. *Science* 313, 1968-1972. 10.1126/science.1131981.
180. Isken, O., Kim, Y.K., Hosoda, N., Mayeur, G.L., Hershey, J.W., and Maquat, L.E. (2008). Upf1 phosphorylation triggers translational repression during nonsense-mediated mRNA decay. *Cell* 133, 314-327. 10.1016/j.cell.2008.02.030.
181. Ohnishi, T., Yamashita, A., Kashima, I., Schell, T., Anders, K.R., Grimson, A., Hachiya, T., Hentze, M.W., Anderson, P., and Ohno, S. (2003). Phosphorylation of hUPF1 induces formation of mRNA surveillance complexes containing hSMG-5 and hSMG-7. *Mol Cell* 12, 1187-1200. 10.1016/s1097-2765(03)00443-x.
182. Schmid, M., and Jensen, T.H. (2008). The exosome: a multipurpose RNA-decay machine. *Trends Biochem Sci* 33, 501-510. 10.1016/j.tibs.2008.07.003.
183. Kurosaki, T., Miyoshi, K., Myers, J.R., and Maquat, L.E. (2018). NMD-degradome sequencing reveals ribosome-bound intermediates with 3'-end non-templated nucleotides. *Nat Struct Mol Biol* 25, 940-950. 10.1038/s41594-018-0132-7.
184. Malecki, M., Viegas, S.C., Carneiro, T., Golik, P., Dressaire, C., Ferreira, M.G., and Arraiano, C.M. (2013). The exoribonuclease Dis3L2 defines a novel eukaryotic RNA degradation pathway. *EMBO J* 32, 1842-1854. 10.1038/emboj.2013.63.

185. Lejeune, F., Li, X., and Maquat, L.E. (2003). Nonsense-mediated mRNA decay in mammalian cells involves decapping, deadenylating, and exonucleolytic activities. *Mol Cell* 12, 675-687. 10.1016/s1097-2765(03)00349-6.
186. Loh, B., Jonas, S., and Izaurralde, E. (2013). The SMG5-SMG7 heterodimer directly recruits the CCR4-NOT deadenylase complex to mRNAs containing nonsense codons via interaction with POP2. *Genes Dev* 27, 2125-2138. 10.1101/gad.226951.113.
187. Yamashita, A., Chang, T.C., Yamashita, Y., Zhu, W., Zhong, Z., Chen, C.Y., and Shyu, A.B. (2005). Concerted action of poly(A) nucleases and decapping enzyme in mammalian mRNA turnover. *Nat Struct Mol Biol* 12, 1054-1063. 10.1038/nsmb1016.
188. Cho, H., Kim, K.M., and Kim, Y.K. (2009). Human proline-rich nuclear receptor coregulatory protein 2 mediates an interaction between mRNA surveillance machinery and decapping complex. *Mol Cell* 33, 75-86. 10.1016/j.molcel.2008.11.022.
189. Cho, H., Han, S., Choe, J., Park, S.G., Choi, S.S., and Kim, Y.K. (2013). SMG5-PNRC2 is functionally dominant compared with SMG5-SMG7 in mammalian nonsense-mediated mRNA decay. *Nucleic Acids Res* 41, 1319-1328. 10.1093/nar/gks1222.
190. Chan, W.K., Huang, L., Gudikote, J.P., Chang, Y.F., Imam, J.S., MacLean, J.A., 2nd, and Wilkinson, M.F. (2007). An alternative branch of the nonsense-mediated decay pathway. *EMBO J* 26, 1820-1830. 10.1038/sj.emboj.7601628.
191. Huang, L., Lou, C.H., Chan, W., Shum, E.Y., Shao, A., Stone, E., Karam, R., Song, H.W., and Wilkinson, M.F. (2011). RNA homeostasis governed by cell type-specific and branched feedback loops acting on NMD. *Mol Cell* 43, 950-961. 10.1016/j.molcel.2011.06.031.
192. Yepiskoposyan, H., Aeschmann, F., Nilsson, D., Okoniewski, M., and Muhlemann, O. (2011). Autoregulation of the nonsense-mediated mRNA decay pathway in human cells. *RNA* 17, 2108-2118. 10.1261/rna.030247.111.
193. Hogg, J.R. (2011). This message was inspected by Upf1: 3'UTR length sensing in mRNA quality control. *Cell Cycle* 10, 372-373. 10.4161/cc.10.3.14735.
194. Hogg, J.R., and Goff, S.P. (2010). Upf1 senses 3'UTR length to potentiate mRNA decay. *Cell* 143, 379-389. 10.1016/j.cell.2010.10.005.
195. Hwang, J., Sato, H., Tang, Y., Matsuda, D., and Maquat, L.E. (2010). UPF1 association with the cap-binding protein, CBP80, promotes nonsense-mediated mRNA decay at two distinct steps. *Mol Cell* 39, 396-409. 10.1016/j.molcel.2010.07.004.
196. Hsu Ia, W., Hsu, M., Li, C., Chuang, T.W., Lin, R.I., and Tarn, W.Y. (2005). Phosphorylation of Y14 modulates its interaction with proteins involved in mRNA metabolism and influences its methylation. *J Biol Chem* 280, 34507-34512. 10.1074/jbc.M507658200.
197. Trembley, J.H., Tatsumi, S., Sakashita, E., Loyer, P., Slaughter, C.A., Suzuki, H., Endo, H., Kidd, V.J., and Mayeda, A. (2005). Activation of pre-mRNA splicing by human RNPS1 is regulated by CK2 phosphorylation. *Mol Cell Biol* 25, 1446-1457. 10.1128/MCB.25.4.1446-1457.2005.
198. Ryu, I., Won, Y.S., Ha, H., Kim, E., Park, Y., Kim, M.K., Kwon, D.H., Choe, J., Song, H.K., Jung, H., and Kim, Y.K. (2019). eIF4A3 Phosphorylation by CDKs Affects NMD during the Cell Cycle. *Cell Rep* 26, 2126-2139 e2129. 10.1016/j.celrep.2019.01.101.
199. Bartel, D.P. (2009). MicroRNAs: target recognition and regulatory functions. *Cell* 136, 215-233. 10.1016/j.cell.2009.01.002.

200. Bruno, I.G., Karam, R., Huang, L., Bhardwaj, A., Lou, C.H., Shum, E.Y., Song, H.W., Corbett, M.A., Gifford, W.D., Gecz, J., et al. (2011). Identification of a microRNA that activates gene expression by repressing nonsense-mediated RNA decay. *Mol Cell* 42, 500-510. 10.1016/j.molcel.2011.04.018.
201. Lou, C.H., Shao, A., Shum, E.Y., Espinoza, J.L., Huang, L., Karam, R., and Wilkinson, M.F. (2014). Posttranscriptional control of the stem cell and neurogenic programs by the nonsense-mediated RNA decay pathway. *Cell Rep* 6, 748-764. 10.1016/j.celrep.2014.01.028.
202. Frischmeyer-Guerrero, P.A., Montgomery, R.A., Warren, D.S., Cooke, S.K., Lutz, J., Sonnenday, C.J., Guerrero, A.L., and Dietz, H.C. (2011). Perturbation of thymocyte development in nonsense-mediated decay (NMD)-deficient mice. *Proc Natl Acad Sci U S A* 108, 10638-10643. 10.1073/pnas.1019352108.
203. Hoshino, S., Imai, M., Kobayashi, T., Uchida, N., and Katada, T. (1999). The eukaryotic polypeptide chain releasing factor (eRF3/GSPT) carrying the translation termination signal to the 3'-Poly(A) tail of mRNA. Direct association of erf3/GSPT with polyadenylate-binding protein. *J Biol Chem* 274, 16677-16680. 10.1074/jbc.274.24.16677.
204. Uchida, N., Hoshino, S., Imataka, H., Sonenberg, N., and Katada, T. (2002). A novel role of the mammalian GSPT/eRF3 associating with poly(A)-binding protein in Cap/Poly(A)-dependent translation. *J Biol Chem* 277, 50286-50292. 10.1074/jbc.M203029200.
205. Amrani, N., Ghosh, S., Mangus, D.A., and Jacobson, A. (2008). Translation factors promote the formation of two states of the closed-loop mRNP. *Nature* 453, 1276-1280. 10.1038/nature06974.
206. Wells, S.E., Hillner, P.E., Vale, R.D., and Sachs, A.B. (1998). Circularization of mRNA by eukaryotic translation initiation factors. *Mol Cell* 2, 135-140. 10.1016/s1097-2765(00)80122-7.
207. Eberle, A.B., Stalder, L., Mathys, H., Orozco, R.Z., and Muhlemann, O. (2008). Posttranscriptional gene regulation by spatial rearrangement of the 3' untranslated region. *PLoS Biol* 6, e92. 10.1371/journal.pbio.0060092.
208. Fatscher, T., Boehm, V., Weiche, B., and Gehring, N.H. (2014). The interaction of cytoplasmic poly(A)-binding protein with eukaryotic initiation factor 4G suppresses nonsense-mediated mRNA decay. *RNA* 20, 1579-1592. 10.1261/rna.044933.114.
209. Amrani, N., Ganesan, R., Kervestin, S., Mangus, D.A., Ghosh, S., and Jacobson, A. (2004). A faux 3'-UTR promotes aberrant termination and triggers nonsense-mediated mRNA decay. *Nature* 432, 112-118. 10.1038/nature03060.
210. Behm-Ansmant, I., Gatfield, D., Rehwinkel, J., Hilgers, V., and Izaurralde, E. (2007). A conserved role for cytoplasmic poly(A)-binding protein 1 (PABPC1) in nonsense-mediated mRNA decay. *EMBO J* 26, 1591-1601. 10.1038/sj.emboj.7601588.
211. Lykke-Andersen, S., and Jensen, T.H. (2015). Nonsense-mediated mRNA decay: an intricate machinery that shapes transcriptomes. *Nat Rev Mol Cell Biol* 16, 665-677. 10.1038/nrm4063.
212. Baker, K.E., and Parker, R. (2004). Nonsense-mediated mRNA decay: terminating erroneous gene expression. *Curr Opin Cell Biol* 16, 293-299. 10.1016/j.ceb.2004.03.003.
213. Nicholson, P., and Muhlemann, O. (2010). Cutting the nonsense: the degradation of PTC-containing mRNAs. *Biochem Soc Trans* 38, 1615-1620. 10.1042/BST0381615.

214. He, F., and Jacobson, A. (2015). Nonsense-Mediated mRNA Decay: Degradation of Defective Transcripts Is Only Part of the Story. *Annu Rev Genet* 49, 339-366. 10.1146/annurev-genet-112414-054639.
215. Karousis, E.D., and Muhlemann, O. (2019). Nonsense-Mediated mRNA Decay Begins Where Translation Ends. *Cold Spring Harb Perspect Biol* 11. 10.1101/cshperspect.a032862.
216. Buhler, M., Steiner, S., Mohn, F., Paillusson, A., and Muhlemann, O. (2006). EJC-independent degradation of nonsense immunoglobulin-mu mRNA depends on 3' UTR length. *Nat Struct Mol Biol* 13, 462-464. 10.1038/nsmb1081.
217. Nagy, E., and Maquat, L.E. (1998). A rule for termination-codon position within intron-containing genes: when nonsense affects RNA abundance. *Trends Biochem Sci* 23, 198-199. 10.1016/s0968-0004(98)01208-0.
218. Peccarelli, M., and Kebaara, B.W. (2014). Regulation of natural mRNAs by the nonsense-mediated mRNA decay pathway. *Eukaryot Cell* 13, 1126-1135. 10.1128/EC.00090-14.
219. Li, T., Shi, Y., Wang, P., Guachalla, L.M., Sun, B., Joerss, T., Chen, Y.S., Groth, M., Krueger, A., Platzer, M., et al. (2015). Smg6/Est1 licenses embryonic stem cell differentiation via nonsense-mediated mRNA decay. *EMBO J* 34, 1630-1647. 10.15252/embj.201489947.
220. Lou, C.H., Chousal, J., Goetz, A., Shum, E.Y., Brafman, D., Liao, X., Mora-Castilla, S., Ramaiah, M., Cook-Andersen, H., Laurent, L., and Wilkinson, M.F. (2016). Nonsense-Mediated RNA Decay Influences Human Embryonic Stem Cell Fate. *Stem Cell Reports* 6, 844-857. 10.1016/j.stemcr.2016.05.008.
221. Colak, D., Ji, S.J., Porse, B.T., and Jaffrey, S.R. (2013). Regulation of axon guidance by compartmentalized nonsense-mediated mRNA decay. *Cell* 153, 1252-1265. 10.1016/j.cell.2013.04.056.
222. Eom, T., Zhang, C., Wang, H., Lay, K., Fak, J., Noebels, J.L., and Darnell, R.B. (2013). NOVA-dependent regulation of cryptic NMD exons controls synaptic protein levels after seizure. *Elife* 2, e00178. 10.7554/eLife.00178.
223. Gardner, L.B. (2008). Hypoxic inhibition of nonsense-mediated RNA decay regulates gene expression and the integrated stress response. *Mol Cell Biol* 28, 3729-3741. 10.1128/MCB.02284-07.
224. Nelson, J.O., Moore, K.A., Chapin, A., Hollien, J., and Metzstein, M.M. (2016). Degradation of Gadd45 mRNA by nonsense-mediated decay is essential for viability. *Elife* 5. 10.7554/eLife.12876.
225. Nickless, A., Bailis, J.M., and You, Z. (2017). Control of gene expression through the nonsense-mediated RNA decay pathway. *Cell Biosci* 7, 26. 10.1186/s13578-017-0153-7.
226. Wittkopp, N., Huntzinger, E., Weiler, C., Sauliere, J., Schmidt, S., Sonawane, M., and Izaurralde, E. (2009). Nonsense-mediated mRNA decay effectors are essential for zebrafish embryonic development and survival. *Mol Cell Biol* 29, 3517-3528. 10.1128/MCB.00177-09.
227. Medghalchi, S.M., Frischmeyer, P.A., Mendell, J.T., Kelly, A.G., Lawler, A.M., and Dietz, H.C. (2001). Rent1, a trans-effector of nonsense-mediated mRNA decay, is essential for mammalian embryonic viability. *Hum Mol Genet* 10, 99-105. 10.1093/hmg/10.2.99.
228. Weischenfeldt, J., Damgaard, I., Bryder, D., Theilgaard-Monch, K., Thoren, L.A., Nielsen, F.C., Jacobsen, S.E., Nerlov, C., and Porse, B.T. (2008). NMD is essential for hematopoietic

- stem and progenitor cells and for eliminating by-products of programmed DNA rearrangements. *Genes Dev* 22, 1381-1396. 10.1101/gad.468808.
229. Thoren, L.A., Norgaard, G.A., Weischenfeldt, J., Waage, J., Jakobsen, J.S., Damgaard, I., Bergstrom, F.C., Blom, A.M., Borup, R., Bisgaard, H.C., and Porse, B.T. (2010). UPF2 is a critical regulator of liver development, function and regeneration. *PLoS One* 5, e11650. 10.1371/journal.pone.0011650.
 230. Bao, J., Tang, C., Yuan, S., Porse, B.T., and Yan, W. (2015). UPF2, a nonsense-mediated mRNA decay factor, is required for prepubertal Sertoli cell development and male fertility by ensuring fidelity of the transcriptome. *Development* 142, 352-362. 10.1242/dev.115642.
 231. Graveley, B.R. (2001). Alternative splicing: increasing diversity in the proteomic world. *Trends Genet* 17, 100-107. 10.1016/s0168-9525(00)02176-4.
 232. Nilsen, T.W., and Graveley, B.R. (2010). Expansion of the eukaryotic proteome by alternative splicing. *Nature* 463, 457-463. 10.1038/nature08909.
 233. Kelemen, O., Convertini, P., Zhang, Z., Wen, Y., Shen, M., Falaleeva, M., and Stamm, S. (2013). Function of alternative splicing. *Gene* 514, 1-30. 10.1016/j.gene.2012.07.083.
 234. Lewis, B.P., Green, R.E., and Brenner, S.E. (2003). Evidence for the widespread coupling of alternative splicing and nonsense-mediated mRNA decay in humans. *Proc Natl Acad Sci U S A* 100, 189-192. 10.1073/pnas.0136770100.
 235. Chang, Y.F., Imam, J.S., and Wilkinson, M.F. (2007). The nonsense-mediated decay RNA surveillance pathway. *Annu Rev Biochem* 76, 51-74. 10.1146/annurev.biochem.76.050106.093909.
 236. Lareau, L.F., Brooks, A.N., Soergel, D.A., Meng, Q., and Brenner, S.E. (2007). The coupling of alternative splicing and nonsense-mediated mRNA decay. *Adv Exp Med Biol* 623, 190-211. 10.1007/978-0-387-77374-2_12.
 237. Garcia-Moreno, J.F., and Romao, L. (2020). Perspective in Alternative Splicing Coupled to Nonsense-Mediated mRNA Decay. *Int J Mol Sci* 21. 10.3390/ijms21249424.
 238. Lareau, L.F., Inada, M., Green, R.E., Wengrod, J.C., and Brenner, S.E. (2007). Unproductive splicing of SR genes associated with highly conserved and ultraconserved DNA elements. *Nature* 446, 926-929. 10.1038/nature05676.
 239. Jumaa, H., and Nielsen, P.J. (1997). The splicing factor SRp20 modifies splicing of its own mRNA and ASF/SF2 antagonizes this regulation. *EMBO J* 16, 5077-5085. 10.1093/emboj/16.16.5077.
 240. Lejeune, F., Cavaloc, Y., and Stevenin, J. (2001). Alternative splicing of intron 3 of the serine/arginine-rich protein 9G8 gene. Identification of flanking exonic splicing enhancers and involvement of 9G8 as a trans-acting factor. *J Biol Chem* 276, 7850-7858. 10.1074/jbc.M009510200.
 241. Ni, J.Z., Grate, L., Donohue, J.P., Preston, C., Nobida, N., O'Brien, G., Shiue, L., Clark, T.A., Blume, J.E., and Ares, M., Jr. (2007). Ultraconserved elements are associated with homeostatic control of splicing regulators by alternative splicing and nonsense-mediated decay. *Genes Dev* 21, 708-718. 10.1101/gad.1525507.
 242. Yan, Q., Weyn-Vanhentenryck, S.M., Wu, J., Sloan, S.A., Zhang, Y., Chen, K., Wu, J.Q., Barres, B.A., and Zhang, C. (2015). Systematic discovery of regulated and conserved

- alternative exons in the mammalian brain reveals NMD modulating chromatin regulators. *Proc Natl Acad Sci U S A* *112*, 3445-3450. 10.1073/pnas.1502849112.
243. Hamid, F.M., and Makeyev, E.V. (2014). Regulation of mRNA abundance by polypyrimidine tract-binding protein-controlled alternate 5' splice site choice. *PLoS Genet* *10*, e1004771. 10.1371/journal.pgen.1004771.
244. Longman, D., Hug, N., Keith, M., Anastasaki, C., Patton, E.E., Grimes, G., and Caceres, J.F. (2013). DHX34 and NBAS form part of an autoregulatory NMD circuit that regulates endogenous RNA targets in human cells, zebrafish and *Caenorhabditis elegans*. *Nucleic Acids Res* *41*, 8319-8331. 10.1093/nar/gkt585.
245. Drechsel, G., Kahles, A., Kesarwani, A.K., Stauffer, E., Behr, J., Drewe, P., Ratsch, G., and Wachter, A. (2013). Nonsense-mediated decay of alternative precursor mRNA splicing variants is a major determinant of the Arabidopsis steady state transcriptome. *Plant Cell* *25*, 3726-3742. 10.1105/tpc.113.115485.
246. Kawashima, T., Douglass, S., Gabunilas, J., Pellegrini, M., and Chanfreau, G.F. (2014). Widespread use of non-productive alternative splice sites in *Saccharomyces cerevisiae*. *PLoS Genet* *10*, e1004249. 10.1371/journal.pgen.1004249.
247. Karousis, E.D., Nasif, S., and Muhlemann, O. (2016). Nonsense-mediated mRNA decay: novel mechanistic insights and biological impact. *Wiley Interdiscip Rev RNA* *7*, 661-682. 10.1002/wrna.1357.
248. Gardner, L.B. (2010). Nonsense-mediated RNA decay regulation by cellular stress: implications for tumorigenesis. *Mol Cancer Res* *8*, 295-308. 10.1158/1541-7786.MCR-09-0502.
249. Wang, D., Wengrod, J., and Gardner, L.B. (2011). Overexpression of the c-myc oncogene inhibits nonsense-mediated RNA decay in B lymphocytes. *J Biol Chem* *286*, 40038-40043. 10.1074/jbc.M111.266361.
250. Harding, H.P., Zhang, Y., Zeng, H., Novoa, I., Lu, P.D., Calton, M., Sadri, N., Yun, C., Popko, B., Paules, R., et al. (2003). An integrated stress response regulates amino acid metabolism and resistance to oxidative stress. *Mol Cell* *11*, 619-633. 10.1016/s1097-2765(03)00105-9.
251. Ron, D., and Walter, P. (2007). Signal integration in the endoplasmic reticulum unfolded protein response. *Nat Rev Mol Cell Biol* *8*, 519-529. 10.1038/nrm2199.
252. Belgrader, P., Cheng, J., and Maquat, L.E. (1993). Evidence to implicate translation by ribosomes in the mechanism by which nonsense codons reduce the nuclear level of human triosephosphate isomerase mRNA. *Proc Natl Acad Sci U S A* *90*, 482-486. 10.1073/pnas.90.2.482.
253. Li, S., Leonard, D., and Wilkinson, M.F. (1997). T cell receptor (TCR) mini-gene mRNA expression regulated by nonsense codons: a nuclear-associated translation-like mechanism. *J Exp Med* *185*, 985-992. 10.1084/jem.185.6.985.
254. Martin, L., and Gardner, L.B. (2015). Stress-induced inhibition of nonsense-mediated RNA decay regulates intracellular cystine transport and intracellular glutathione through regulation of the cystine/glutamate exchanger SLC7A11. *Oncogene* *34*, 4211-4218. 10.1038/onc.2014.352.

255. Karam, R., Lou, C.H., Kroeger, H., Huang, L., Lin, J.H., and Wilkinson, M.F. (2015). The unfolded protein response is shaped by the NMD pathway. *EMBO Rep* 16, 599-609. 10.15252/embr.201439696.
256. Oren, Y.S., McClure, M.L., Rowe, S.M., Sorscher, E.J., Bester, A.C., Manor, M., Kerem, E., Rivlin, J., Zahdeh, F., Mann, M., et al. (2014). The unfolded protein response affects readthrough of premature termination codons. *EMBO Mol Med* 6, 685-701. 10.1002/emmm.201303347.
257. Vattam, K.M., and Wek, R.C. (2004). Reinitiation involving upstream ORFs regulates ATF4 mRNA translation in mammalian cells. *Proc Natl Acad Sci U S A* 101, 11269-11274. 10.1073/pnas.0400541101.
258. Mourtada-Maarabouni, M., and Williams, G.T. (2013). Growth arrest on inhibition of nonsense-mediated decay is mediated by noncoding RNA GAS5. *Biomed Res Int* 2013, 358015. 10.1155/2013/358015.
259. Smith, C.M., and Steitz, J.A. (1998). Classification of gas5 as a multi-small-nucleolar-RNA (snoRNA) host gene and a member of the 5'-terminal oligopyrimidine gene family reveals common features of snoRNA host genes. *Mol Cell Biol* 18, 6897-6909. 10.1128/MCB.18.12.6897.
260. Ideue, T., Sasaki, Y.T., Hagiwara, M., and Hirose, T. (2007). Introns play an essential role in splicing-dependent formation of the exon junction complex. *Genes Dev* 21, 1993-1998. 10.1101/gad.1557907.
261. Jolly, L.A., Homan, C.C., Jacob, R., Barry, S., and Gecz, J. (2013). The UPF3B gene, implicated in intellectual disability, autism, ADHD and childhood onset schizophrenia regulates neural progenitor cell behaviour and neuronal outgrowth. *Hum Mol Genet* 22, 4673-4687. 10.1093/hmg/ddt315.
262. Huang, L., Shum, E.Y., Jones, S.H., Lou, C.H., Chousal, J., Kim, H., Roberts, A.J., Jolly, L.A., Espinoza, J.L., Skarbrevik, D.M., et al. (2018). A Upf3b-mutant mouse model with behavioral and neurogenesis defects. *Mol Psychiatry* 23, 1773-1786. 10.1038/mp.2017.173.
263. Farris, S., Lewandowski, G., Cox, C.D., and Steward, O. (2014). Selective localization of arc mRNA in dendrites involves activity- and translation-dependent mRNA degradation. *J Neurosci* 34, 4481-4493. 10.1523/JNEUROSCI.4944-13.2014.
264. Nguyen, L.S., Kim, H.G., Rosenfeld, J.A., Shen, Y., Gusella, J.F., Lacassie, Y., Layman, L.C., Shaffer, L.G., and Gecz, J. (2013). Contribution of copy number variants involving nonsense-mediated mRNA decay pathway genes to neuro-developmental disorders. *Hum Mol Genet* 22, 1816-1825. 10.1093/hmg/ddt035.
265. Tarpey, P.S., Raymond, F.L., Nguyen, L.S., Rodriguez, J., Hackett, A., Vandeleur, L., Smith, R., Shoubridge, C., Edkins, S., Stevens, C., et al. (2007). Mutations in UPF3B, a member of the nonsense-mediated mRNA decay complex, cause syndromic and nonsyndromic mental retardation. *Nat Genet* 39, 1127-1133. 10.1038/ng2100.
266. Johnson, J.L., Stoica, L., Liu, Y., Zhu, P.J., Bhattacharya, A., Buffington, S.A., Huq, R., Eissa, N.T., Larsson, O., Porse, B.T., et al. (2019). Inhibition of Upf2-Dependent Nonsense-Mediated Decay Leads to Behavioral and Neurophysiological Abnormalities by Activating the Immune Response. *Neuron*. 10.1016/j.neuron.2019.08.027.

267. Shaheen, R., Anazi, S., Ben-Omran, T., Seidahmed, M.Z., Caddle, L.B., Palmer, K., Ali, R., Alshidi, T., Hagos, S., Goodwin, L., et al. (2016). Mutations in SMG9, Encoding an Essential Component of Nonsense-Mediated Decay Machinery, Cause a Multiple Congenital Anomaly Syndrome in Humans and Mice. *Am J Hum Genet* *98*, 643-652. 10.1016/j.ajhg.2016.02.010.
268. Johnson, J.L., Stoica, L., Liu, Y., Zhu, P.J., Bhattacharya, A., Buffington, S.A., Huq, R., Eissa, N.T., Larsson, O., Porse, B.T., et al. (2019). Inhibition of Upf2-Dependent Nonsense-Mediated Decay Leads to Behavioral and Neurophysiological Abnormalities by Activating the Immune Response. *Neuron* *104*, 665-679 e668. 10.1016/j.neuron.2019.08.027.
269. Mao, H., Pilaz, L.J., McMahan, J.J., Golzio, C., Wu, D., Shi, L., Katsanis, N., and Silver, D.L. (2015). Rbm8a haploinsufficiency disrupts embryonic cortical development resulting in microcephaly. *J Neurosci* *35*, 7003-7018. 10.1523/JNEUROSCI.0018-15.2015.
270. Silver, D.L., Watkins-Chow, D.E., Schreck, K.C., Pierfelice, T.J., Larson, D.M., Burnett, A.J., Liaw, H.J., Myung, K., Walsh, C.A., Gaiano, N., and Pavan, W.J. (2010). The exon junction complex component Magoh controls brain size by regulating neural stem cell division. *Nat Neurosci* *13*, 551-558. 10.1038/nn.2527.
271. Mao, H., McMahan, J.J., Tsai, Y.H., Wang, Z., and Silver, D.L. (2016). Haploinsufficiency for Core Exon Junction Complex Components Disrupts Embryonic Neurogenesis and Causes p53-Mediated Microcephaly. *PLoS Genet* *12*, e1006282. 10.1371/journal.pgen.1006282.
272. Boehm, V., and Gehring, N.H. (2016). Exon Junction Complexes: Supervising the Gene Expression Assembly Line. *Trends Genet* *32*, 724-735. 10.1016/j.tig.2016.09.003.
273. Woodward, L.A., Mabin, J.W., Gangras, P., and Singh, G. (2017). The exon junction complex: a lifelong guardian of mRNA fate. *Wiley Interdiscip Rev RNA* *8*. 10.1002/wrna.1411.
274. Zou, D., McSweeney, C., Sebastian, A., Reynolds, D.J., Dong, F., Zhou, Y., Deng, D., Wang, Y., Liu, L., Zhu, J., et al. (2015). A critical role of RBM8a in proliferation and differentiation of embryonic neural progenitors. *Neural Dev* *10*, 18. 10.1186/s13064-015-0045-7.
275. Lynch, S.A., Nguyen, L.S., Ng, L.Y., Waldron, M., McDonald, D., and Gecz, J. (2012). Broadening the phenotype associated with mutations in UPF3B: two further cases with renal dysplasia and variable developmental delay. *Eur J Med Genet* *55*, 476-479. 10.1016/j.ejmg.2012.03.010.
276. Gubanov, E., Brown, B., Ivanov, S.V., Helleday, T., Mills, G.B., Yarbrough, W.G., and Issaeva, N. (2012). Downregulation of SMG-1 in HPV-positive head and neck squamous cell carcinoma due to promoter hypermethylation correlates with improved survival. *Clin Cancer Res* *18*, 1257-1267. 10.1158/1078-0432.CCR-11-2058.
277. Roberts, T.L., Ho, U., Luff, J., Lee, C.S., Apte, S.H., MacDonald, K.P., Raggat, L.J., Pettit, A.R., Morrow, C.A., Waters, M.J., et al. (2013). Smg1 haploinsufficiency predisposes to tumor formation and inflammation. *Proc Natl Acad Sci U S A* *110*, E285-294. 10.1073/pnas.1215696110.
278. Du, Y., Lu, F., Li, P., Ye, J., Ji, M., Ma, D., and Ji, C. (2014). SMG1 acts as a novel potential tumor suppressor with epigenetic inactivation in acute myeloid leukemia. *Int J Mol Sci* *15*, 17065-17076. 10.3390/ijms150917065.
279. Anczukow, O., Ware, M.D., Buisson, M., Zetoune, A.B., Stoppa-Lyonnet, D., Sinilnikova, O.M., and Mazoyer, S. (2008). Does the nonsense-mediated mRNA decay mechanism

- prevent the synthesis of truncated BRCA1, CHK2, and p53 proteins? *Hum Mutat* 29, 65-73. 10.1002/humu.20590.
280. Perrin-Vidoz, L., Sinilnikova, O.M., Stoppa-Lyonnet, D., Lenoir, G.M., and Mazoyer, S. (2002). The nonsense-mediated mRNA decay pathway triggers degradation of most BRCA1 mRNAs bearing premature termination codons. *Hum Mol Genet* 11, 2805-2814. 10.1093/hmg/11.23.2805.
281. Pinyol, M., Bea, S., Pla, L., Ribrag, V., Bosq, J., Rosenwald, A., Campo, E., and Jares, P. (2007). Inactivation of RB1 in mantle-cell lymphoma detected by nonsense-mediated mRNA decay pathway inhibition and microarray analysis. *Blood* 109, 5422-5429. 10.1182/blood-2006-11-057208.
282. Reddy, J.C., Morris, J.C., Wang, J., English, M.A., Haber, D.A., Shi, Y., and Licht, J.D. (1995). WT1-mediated transcriptional activation is inhibited by dominant negative mutant proteins. *J Biol Chem* 270, 10878-10884. 10.1074/jbc.270.18.10878.
283. Hu, Z., Yau, C., and Ahmed, A.A. (2017). A pan-cancer genome-wide analysis reveals tumour dependencies by induction of nonsense-mediated decay. *Nat Commun* 8, 15943. 10.1038/ncomms15943.
284. Wang, D., Zavadil, J., Martin, L., Parisi, F., Friedman, E., Levy, D., Harding, H., Ron, D., and Gardner, L.B. (2011). Inhibition of nonsense-mediated RNA decay by the tumor microenvironment promotes tumorigenesis. *Mol Cell Biol* 31, 3670-3680. 10.1128/MCB.05704-11.
285. Wengrod, J., Martin, L., Wang, D., Frischmeyer-Guerrerio, P., Dietz, H.C., and Gardner, L.B. (2013). Inhibition of nonsense-mediated RNA decay activates autophagy. *Mol Cell Biol* 33, 2128-2135. 10.1128/MCB.00174-13.
286. Liu, C., Karam, R., Zhou, Y., Su, F., Ji, Y., Li, G., Xu, G., Lu, L., Wang, C., Song, M., et al. (2014). The UPF1 RNA surveillance gene is commonly mutated in pancreatic adenocarcinoma. *Nat Med* 20, 596-598. 10.1038/nm.3548.
287. Lu, J., Plank, T.D., Su, F., Shi, X., Liu, C., Ji, Y., Li, S., Huynh, A., Shi, C., Zhu, B., et al. (2016). The nonsense-mediated RNA decay pathway is disrupted in inflammatory myofibroblastic tumors. *J Clin Invest* 126, 3058-3062. 10.1172/JCI86508.
288. Jeong, J., Mao, J., Tenzen, T., Kottmann, A.H., and McMahon, A.P. (2004). Hedgehog signaling in the neural crest cells regulates the patterning and growth of facial primordia. *Genes Dev* 18, 937-951. 10.1101/gad.1190304.
289. Matei, V., Pauley, S., Kaing, S., Rowitch, D., Beisel, K.W., Morris, K., Feng, F., Jones, K., Lee, J., and Fritzsche, B. (2005). Smaller inner ear sensory epithelia in Neurog 1 null mice are related to earlier hair cell cycle exit. *Dev Dyn* 234, 633-650. 10.1002/dvdy.20551.
290. Zhang, J., Sun, X., Qian, Y., and Maquat, L.E. (1998). Intron function in the nonsense-mediated decay of beta-globin mRNA: indications that pre-mRNA splicing in the nucleus can influence mRNA translation in the cytoplasm. *RNA* 4, 801-815. 10.1017/s1355838298971849.
291. Kurosaki, T., Hoque, M., and Maquat, L.E. (2018). Identifying Cellular Nonsense-Mediated mRNA Decay (NMD) Targets: Immunoprecipitation of Phosphorylated UPF1 Followed by RNA Sequencing (p-UPF1 RIP-Seq). *Methods Mol Biol* 1720, 175-186. 10.1007/978-1-4939-7540-2_13.

292. Xiao, W., Sun, Y., Xu, J., Zhang, N., and Dong, L. (2022). uORF-Mediated Translational Regulation of ATF4 Serves as an Evolutionarily Conserved Mechanism Contributing to Non-Small-Cell Lung Cancer (NSCLC) and Stress Response. *J Mol Evol* 90, 375-388. 10.1007/s00239-022-10068-y.
293. Ait Ghezala, H., Jolles, B., Salhi, S., Castrillo, K., Carpentier, W., Cagnard, N., Bruhat, A., Fafournoux, P., and Jean-Jean, O. (2012). Translation termination efficiency modulates ATF4 response by regulating ATF4 mRNA translation at 5' short ORFs. *Nucleic Acids Res* 40, 9557-9570. 10.1093/nar/gks762.
294. Baird, T.D., Cheng, K.C., Chen, Y.C., Buehler, E., Martin, S.E., Inglese, J., and Hogg, J.R. (2018). ICE1 promotes the link between splicing and nonsense-mediated mRNA decay. *Elife* 7. 10.7554/eLife.33178.
295. Tani, H., Torimura, M., and Akimitsu, N. (2013). The RNA degradation pathway regulates the function of GAS5 a non-coding RNA in mammalian cells. *PLoS One* 8, e55684. 10.1371/journal.pone.0055684.
296. Echols, J., Siddiqui, A., Dai, Y., Havasi, V., Sun, R., Kaczmarczyk, A., and Keeling, K.M. (2020). A regulated NMD mouse model supports NMD inhibition as a viable therapeutic option to treat genetic diseases. *Dis Model Mech* 13. 10.1242/dmm.044891.
297. Li, L., Geng, Y., Feng, R., Zhu, Q., Miao, B., Cao, J., and Fei, S. (2017). The Human RNA Surveillance Factor UPF1 Modulates Gastric Cancer Progression by Targeting Long Non-Coding RNA MALAT1. *Cell Physiol Biochem* 42, 2194-2206. 10.1159/000479994.
298. Miyashita, S., Owa, T., Seto, Y., Yamashita, M., Aida, S., Sone, M., Ichijo, K., Nishioka, T., Kaibuchi, K., Kawaguchi, Y., et al. (2021). Cyclin D1 controls development of cerebellar granule cell progenitors through phosphorylation and stabilization of ATOH1. *EMBO J* 40, e105712. 10.15252/embj.2020105712.
299. Duman-Scheel, M., Weng, L., Xin, S., and Du, W. (2002). Hedgehog regulates cell growth and proliferation by inducing Cyclin D and Cyclin E. *Nature* 417, 299-304. 10.1038/417299a.
300. Consalez, G.G., Goldowitz, D., Casoni, F., and Hawkes, R. (2020). Origins, Development, and Compartmentation of the Granule Cells of the Cerebellum. *Front Neural Circuits* 14, 611841. 10.3389/fncir.2020.611841.
301. Hsieh, M.C., Lai, C.Y., Yeh, C.M., Yang, P.S., Cheng, J.K., Wang, H.H., Lin, K.H., Nie, S.T., Lin, T.B., and Peng, H.Y. (2023). Phosphorylated upstream frameshift 1-dependent nonsense-mediated mu opioid receptor mRNA decay in the spinal cord contributes to the development of neuropathic allodynia-like behavior in rats. *Anesthesiology*. 10.1097/ALN.0000000000004550.
302. Chang, J.C., and Kan, Y.W. (1979). beta 0 thalassemia, a nonsense mutation in man. *Proc Natl Acad Sci U S A* 76, 2886-2889. 10.1073/pnas.76.6.2886.
303. Lim, S., Mullins, J.J., Chen, C.M., Gross, K.W., and Maquat, L.E. (1989). Novel metabolism of several beta zero-thalassemic beta-globin mRNAs in the erythroid tissues of transgenic mice. *EMBO J* 8, 2613-2619. 10.1002/j.1460-2075.1989.tb08401.x.
304. Carter, M.S., Doskow, J., Morris, P., Li, S., Nhim, R.P., Sandstedt, S., and Wilkinson, M.F. (1995). A regulatory mechanism that detects premature nonsense codons in T-cell receptor transcripts in vivo is reversed by protein synthesis inhibitors in vitro. *J Biol Chem* 270, 28995-29003. 10.1074/jbc.270.48.28995.

305. Trcek, T., Sato, H., Singer, R.H., and Maquat, L.E. (2013). Temporal and spatial characterization of nonsense-mediated mRNA decay. *Genes Dev* 27, 541-551. 10.1101/gad.209635.112.
306. Haystead, T.A., Sim, A.T., Carling, D., Honnor, R.C., Tsukitani, Y., Cohen, P., and Hardie, D.G. (1989). Effects of the tumour promoter okadaic acid on intracellular protein phosphorylation and metabolism. *Nature* 337, 78-81. 10.1038/337078a0.
307. Wang, G., Jiang, B., Jia, C., Chai, B., and Liang, A. (2013). MicroRNA 125 represses nonsense-mediated mRNA decay by regulating SMG1 expression. *Biochem Biophys Res Commun* 435, 16-20. 10.1016/j.bbrc.2013.03.129.
308. Chang, L., Li, C., Guo, T., Wang, H., Ma, W., Yuan, Y., Liu, Q., Ye, Q., and Liu, Z. (2016). The human RNA surveillance factor UPF1 regulates tumorigenesis by targeting Smad7 in hepatocellular carcinoma. *J Exp Clin Cancer Res* 35, 8. 10.1186/s13046-016-0286-2.
309. Cao, L., Qi, L., Zhang, L., Song, W., Yu, Y., Xu, C., Li, L., Guo, Y., Yang, L., Liu, C., et al. (2017). Human nonsense-mediated RNA decay regulates EMT by targeting the TGF- β signaling pathway in lung adenocarcinoma. *Cancer Lett* 403, 246-259. 10.1016/j.canlet.2017.06.021.
310. Li, F., Yi, Y., Miao, Y., Long, W., Long, T., Chen, S., Cheng, W., Zou, C., Zheng, Y., Wu, X., et al. (2019). N(6)-Methyladenosine Modulates Nonsense-Mediated mRNA Decay in Human Glioblastoma. *Cancer Res* 79, 5785-5798. 10.1158/0008-5472.CAN-18-2868.
311. Hurt, J.A., Robertson, A.D., and Burge, C.B. (2013). Global analyses of UPF1 binding and function reveal expanded scope of nonsense-mediated mRNA decay. *Genome Res* 23, 1636-1650. 10.1101/gr.157354.113.
312. Zund, D., Gruber, A.R., Zavolan, M., and Muhlemann, O. (2013). Translation-dependent displacement of UPF1 from coding sequences causes its enrichment in 3' UTRs. *Nat Struct Mol Biol* 20, 936-943. 10.1038/nsmb.2635.
313. Kebaara, B.W., and Atkin, A.L. (2009). Long 3'-UTRs target wild-type mRNAs for nonsense-mediated mRNA decay in *Saccharomyces cerevisiae*. *Nucleic Acids Res* 37, 2771-2778. 10.1093/nar/gkp146.
314. Peterson, K.A., Nishi, Y., Ma, W., Vedenko, A., Shokri, L., Zhang, X., McFarlane, M., Baizabal, J.M., Junker, J.P., van Oudenaarden, A., et al. (2012). Neural-specific Sox2 input and differential Gli-binding affinity provide context and positional information in Shh-directed neural patterning. *Genes Dev* 26, 2802-2816. 10.1101/gad.207142.112.
315. Sirkisoon, S.R., Carpenter, R.L., Rimkus, T., Anderson, A., Harrison, A., Lange, A.M., Jin, G., Watabe, K., and Lo, H.W. (2018). Interaction between STAT3 and GLI1/tGLI1 oncogenic transcription factors promotes the aggressiveness of triple-negative breast cancers and HER2-enriched breast cancer. *Oncogene* 37, 2502-2514. 10.1038/s41388-018-0132-4.
316. Yuan, L., Zhang, H., Liu, J., Malhotra, A., Dey, A., Yu, B., Jella, K.K., McSwain, L.F., Schniederjan, M.J., and MacDonald, T.J. (2022). STAT3 is required for Smo-dependent signaling and mediates Smo-targeted treatment resistance and tumorigenesis in Shh medulloblastoma. *Mol Oncol* 16, 1009-1025. 10.1002/1878-0261.13097.
317. Cheng, Y., Liao, S., Xu, G., Hu, J., Guo, D., Du, F., Contreras, A., Cai, K.Q., Peri, S., Wang, Y., et al. (2020). NeuroD1 Dictates Tumor Cell Differentiation in Medulloblastoma. *Cell Rep* 31, 107782. 10.1016/j.celrep.2020.107782.

318. Bao, X., Huang, Y., Xu, W., and Xiong, G. (2020). Functions and Clinical Significance of UPF3a Expression in Human Colorectal Cancer. *Cancer Manag Res* 12, 4271-4281. 10.2147/CMAR.S244486.
319. Ye, J., Kumanova, M., Hart, L.S., Sloane, K., Zhang, H., De Panis, D.N., Bobrovnikova-Marjon, E., Diehl, J.A., Ron, D., and Koumenis, C. (2010). The GCN2-ATF4 pathway is critical for tumour cell survival and proliferation in response to nutrient deprivation. *EMBO J* 29, 2082-2096. 10.1038/emboj.2010.81.
320. Li, Y., Wu, M., Zhang, L., Wan, L., Li, H., Zhang, L., Sun, G., Huang, W., Zhang, J., Su, F., et al. (2022). Nonsense-mediated mRNA decay inhibition synergizes with MDM2 inhibition to suppress TP53 wild-type cancer cells in p53 isoform-dependent manner. *Cell Death Discov* 8, 402. 10.1038/s41420-022-01190-3.
321. Bokhari, A., Jonchere, V., Lagrange, A., Bertrand, R., Svrcek, M., Marisa, L., Buhard, O., Greene, M., Demidova, A., Jia, J., et al. (2018). Targeting nonsense-mediated mRNA decay in colorectal cancers with microsatellite instability. *Oncogenesis* 7, 70. 10.1038/s41389-018-0079-x.
322. Azzalin, C.M., and Lingner, J. (2006). The human RNA surveillance factor UPF1 is required for S phase progression and genome stability. *Curr Biol* 16, 433-439. 10.1016/j.cub.2006.01.018.
323. Nie, C., Zhou, X.A., Zhou, J., Liu, Z., Gu, Y., Liu, W., Zhan, J., Li, S., Xiong, Y., Zhou, M., et al. (2023). A transcription-independent mechanism determines rapid periodic fluctuations of BRCA1 expression. *EMBO J* 42, e111951. 10.15252/embj.2022111951.
324. Frappart, P.O., Lee, Y., Lamont, J., and McKinnon, P.J. (2007). BRCA2 is required for neurogenesis and suppression of medulloblastoma. *EMBO J* 26, 2732-2742. 10.1038/sj.emboj.7601703.
325. Madabhushi, R., Gao, F., Pfenning, A.R., Pan, L., Yamakawa, S., Seo, J., Rueda, R., Phan, T.X., Yamakawa, H., Pao, P.C., et al. (2015). Activity-Induced DNA Breaks Govern the Expression of Neuronal Early-Response Genes. *Cell* 161, 1592-1605. 10.1016/j.cell.2015.05.032.
326. Wei, P.C., Chang, A.N., Kao, J., Du, Z., Meyers, R.M., Alt, F.W., and Schwer, B. (2016). Long Neural Genes Harbor Recurrent DNA Break Clusters in Neural Stem/Progenitor Cells. *Cell* 164, 644-655. 10.1016/j.cell.2015.12.039.
327. Nickless, A., Cheruiyot, A., Flanagan, K.C., Piwnica-Worms, D., Stewart, S.A., and You, Z. (2017). p38 MAPK inhibits nonsense-mediated RNA decay in response to persistent DNA damage in noncycling cells. *J Biol Chem* 292, 15266-15276. 10.1074/jbc.M117.787846.
328. Xu, W., Bao, P., Jiang, X., Wang, H., Qin, M., Wang, R., Wang, T., Yang, Y., Lorenzini, I., Liao, L., et al. (2019). Reactivation of nonsense-mediated mRNA decay protects against C9orf72 dipeptide-repeat neurotoxicity. *Brain* 142, 1349-1364. 10.1093/brain/awz070.
329. Darakhshan, S., and Pour, A.B. (2015). Tranilast: a review of its therapeutic applications. *Pharmacol Res* 91, 15-28. 10.1016/j.phrs.2014.10.009.
330. Sanchez, G., Bondy-Chorney, E., Laframboise, J., Paris, G., Didillon, A., Jasmin, B.J., and Cote, J. (2016). A novel role for CARM1 in promoting nonsense-mediated mRNA decay: potential implications for spinal muscular atrophy. *Nucleic Acids Res* 44, 2661-2676. 10.1093/nar/gkv1334.

331. Tano, V., Jans, D.A., and Bogoyevitch, M.A. (2019). Oligonucleotide-directed STAT3 alternative splicing switch drives anti-tumorigenic outcomes in MCF10 human breast cancer cells. *Biochem Biophys Res Commun* 513, 1076-1082. 10.1016/j.bbrc.2019.04.054.
332. Liang, X.H., Nichols, J.G., Hsu, C.W., Vickers, T.A., and Crooke, S.T. (2019). mRNA levels can be reduced by antisense oligonucleotides via no-go decay pathway. *Nucleic Acids Res* 47, 6900-6916. 10.1093/nar/gkz500.
333. Jackson, K.L., Dayton, R.D., Orchard, E.A., Ju, S., Ringe, D., Petsko, G.A., Maquat, L.E., and Klein, R.L. (2015). Preservation of forelimb function by UPF1 gene therapy in a rat model of TDP-43-induced motor paralysis. *Gene Ther* 22, 20-28. 10.1038/gt.2014.101.
334. Jia, J., Furlan, A., Gonzalez-Hilarion, S., Leroy, C., Gruenert, D.C., Tulasne, D., and Lejeune, F. (2015). Caspases shutdown nonsense-mediated mRNA decay during apoptosis. *Cell Death Differ* 22, 1754-1763. 10.1038/cdd.2015.18.
335. Popp, M.W., and Maquat, L.E. (2015). Attenuation of nonsense-mediated mRNA decay facilitates the response to chemotherapeutics. *Nat Commun* 6, 6632. 10.1038/ncomms7632.
336. Goetz, A.E., and Wilkinson, M. (2017). Stress and the nonsense-mediated RNA decay pathway. *Cell Mol Life Sci* 74, 3509-3531. 10.1007/s00018-017-2537-6.